UNIVERSITY OF CALIFORNIA
RIVERSIDE

In-Use Emissions From Heavy Duty Off-Road Equipment and On-Road Vehicles

A Dissertation submitted in partial satisfaction
of the requirements for the degree of

Doctor of Philosophy

in

Chemical and Environmental Engineering

by

Hanwei Zhu

March 2023

Dissertation Committee:

Dr. David R. Cocker III, Co-Chairperson
Dr. Mark D. Durbin, Co-Chairperson
Dr. Georgios Karavalakis
Dr. Don R. Collins

The Dissertation of Hanwei Zhu is approved:

_____

_____

_____

Committee Co-Chairperson

_____

Committee Co-Chairperson

University of California, Riverside

Acknowledgements

I would like to thank many individuals for making this dissertation possible. I would like to thank my advisor Dr. David R. Cocker and Dr. Thomas D. Durbin for their support throughout the PhD program. I would like to thank Dr. Georgios Karavalakis and Dr. Kent Johnson for training me throughout my PhD program. I would like to thank Dr. Don R. Collins for his guidance during my PhD program. I would like to thank Dr. Wayne Miller and Dr. Heejung Jung for their guidance.

I would also like to thank Mr. Dan Hartnett for his continued help and support with the entire emissions field testing. I am also very grateful to Mr. Mark Villela, Mr. Daniel Gomez for their help with all the field study tests.

I thank Dr. Jiacheng Yang and Dr. Yu Jiang for all their recommendations to join the Emissions and Fuels Research group and thanks for their help and support. Thanks to staff member Dr. Chengguo Li and Dr. George Scora for his help and support. I would also like to thank former and current graduate students, Dr. Tanfeng Cao, Dr. Cavan McCaffery, Dr. Zisimos Toumasatos, Mr. Chas Frederickson, Mr. Tianbo Tang, Mr. Tianyi Ma, Ms. Grace Johnson, and all the undergraduate students for all of their help.

I would like to recognize the funding sources including California Energy Commission (CEC), California Air Resources Board (CARB), Cummins Westport, Inc, South Coast Air Quality Management District (SCAQMD), Southern California Gas Company (SoCalGas), Caltrans for the projects that made this dissertation possible.

The text of Chapter 2 of this dissertation, in part or in full, is reprinted from SAE Technical Paper, No. 2022-01-0577; Zhu, Hanwei, George Scora, Georgios Karavalakis, Kent Johnson, Robert Russell, and Tom Durbin. Real World Emissions from Tier 4F Off-Road

Construction Equipment, Copyright (2022), with permission from SAE. The text of Chapter 3 of this dissertation, in part or in full, is reprinted from Fuel, Volume 277; Zhu, Hanwei, Cavan McCaffery, Jiacheng Yang, Chengguo Li, Georgios Karavalakis, Kent C. Johnson, and Thomas D. Durbin. Characterizing emission rates of regulated and unregulated pollutants from two ultra-low NOx CNG heavy-duty vehicles, Pages 118-192, Copyright (2018), with permission from Elsevier.

Dedication

I dedicate this work to my parents Xinhong Guo and Baoxian Zhu, for their love, encouragement, and support all through my life.

ABSTRACT OF THE DISSERTATION

In-Use Emissions From Heavy Duty Off-Road Equipment and On-Road Vehicles

by

Hanwei Zhu

Doctor of Philosophy, Graduate Program in Chemical and Environmental Engineering
University of California, Riverside, March 2023
Dr. David R. Cocker III, Co-Chairperson
Dr. Thomas D. Durbin, Co-Chairperson

This dissertation provides investigation and evaluation of new engine technologies and aftertreatment systems on reducing emissions of critical pollutants on in-use heavy-duty vehicles or off-road equipment under real-world operation conditions. Real-world driving emissions have become a key factor to understand or identify high-emitting events under real-world driving conditions.

This dissertation evaluated emissions from in-use heavy-duty on-road vehicles, off-road equipment under a variety of different conditions. This dissertation characterized NOx and PM emissions for 10 pieces of Tier 4 final construction equipment including 3 excavators, 3 wheel loaders, 2 crawler tractors and 2 backhoe/loaders. The duty cycles included a pre-defined combined sequence of a cold-start phase, trenching, backfilling, travelling, and idling. The information obtained in this study provides a more accurate dataset for emissions inventory development, and for designing or optimizing emissions

models such as NONROAD or OFFROAD, which are currently utilized for estimating off-road emissions.

The dissertation also discussed gaseous and particulate emissions from a fleet of 14 heavy-duty vehicles. The test matrix includes vehicles from vocations including transit buses, school buses, refuse trucks, delivery trucks, and goods movement trucks fueled with a combination of alternative fuels, conventional and alternative diesel fuels. This thesis evaluated the impact, issues, improvement, and benefits of the current technologies for heavy-duty vehicles.

This thesis also measured and characterized NOx emissions from five heavy-duty diesel and natural gas goods movement vehicles with different engine technologies under real-world conditions. All five vehicles were tested on-road under four pre-defined goods movement routes in SCAB, representing grocery distribution, port-drayage operation, and highway driving with and without elevation change. NOx emissions were measured using a mobile emissions laboratory.

Understanding emissions from ultra-low NOx CNG vehicles is important as CNG vehicles/engines are capable of meeting more stringent emission standards. This dissertation in detail evaluated and characterized two near-zero NOx stoichiometric ultra-low natural gas engines in different vocations. This demonstration of this engine technology was done in a goods movement vehicle and a yard tractor. Both vocations represent a major source of NOx emissions and other pollutants within the heavy-duty vehicle population.

Table of Contents

List of Figures

List of Tables

Acronyms and Abbreviations

ARB	Air Resources Board
bhp	brake horsepower
bhp-hr	brake horsepower – hour
CAFEE	West Virginia University Center for Alternative Fuels Engines and Emissions Laboratory
CARB	California Air Resources Board
CBD	Central Business District
CE-CERT	College of Engineering-Center for Environmental Research and Technology (University of California, Riverside)
CFR	Code of Federal Regulations
CH_4	methane
CI	compression-ignition
CO	carbon monoxide
CO_2	carbon dioxide
CPC	condensation particle counter
CS	Catalytic Stripper
CVS	constant volume sampling
DEF	diesel emissions fluid
DI	direct injection
DOC	diesel oxidation catalyst
DPF	diesel particulate filter
Dp	particle diameter
DTP	Drayage Truck Port
EC	elemental carbon
ECM	engine control module
EGR	exhaust gas recirculation
EFs	emission factors
EMFAC	EMission FACtors inventory model
EPA	United States Environmental Protection Agency
FID	flame ionization detector
FTP	Federal Test Procedure
g/mi	grams per mile
HDDE	heavy-duty diesel engine
HDDV	heavy-duty diesel vehicle
lbs.	pounds
ICCT	International Council on Clean Transportation
LD	Light-duty
MAW	Moving Averaging Window
MEL	CE-CERT's Mobile Emissions Laboratory
MIL	Malfunction Indicator Light
mpg	miles per gallon
mph	Miles per Hour
m/s^2	meters per second squared

MSS.....Micro Soot Sensor
MY .....Model Year
NDIR.....non-dispersive infrared detector
nm .....nanometer
NMHC.....non-methane hydrocarbons
NO.....Nitric Oxide
NO_2 .....Nitrogen Dioxide
NO_x .....oxides of nitrogen
NTE.....Not to Exceed
O_2 .....Oxygen
OBD .....On-Board Diagnostics
OC.....Organic carbon
OEM.....Original Equipment Manufacturer
PEMS .....portable emissions measurement systems
PM.....particulate matter
PN .....particle number
PSD .....Particle Size Distributions
RDE.....real driving emissions
DF .....dilution factor
SI.....spark-ignition
SCAQMD .....South Coast Air Quality Management District
SCR.....Selective Catalytic Reduction
SET .....Supplemental Emissions Test
TEM .....Transmission Electron Microscopy
THC.....total hydrocarbons
UCR .....University of California, Riverside
UDDS.....Urban Dynamometer Driving Schedule
ULSD .....ultralow sulfur diesel
USEPA.....United States Environmental Protection Agency

1. Introduction

Internal combustion engine (ICE) has enabled many key areas for human beings, including providing power source of the vehicles, generating electricity and mechanical power in many applications. There are two main types of ICEs: spark-ignition (SI) engines and compression ignition (CI) engines. Compression-ignition engines, also known as diesel engines, were developed over a century ago and have been steadily improved as new technologies have become available, and as more demanding to meet regulation requirement (Heywood, 2018). Spark-ignition engines are commonly used on light-duty passenger cars, small electric generators, etc. Diesel engines are typically used for stationary applications such as power/electricity generation, and for mobile applications such as heavy-duty trucks, off-road equipment, and marines.

Both SI and diesel engines are one of the major sources of air pollutants. In spark-ignition and diesel engine exhaust, air pollutants that are of concern include oxides of nitrogen (nitric oxide, NO, and nitrogen dioxide, NO_2 -combined known as NOx), hydrocarbon (HC), carbon monoxide (CO), particulate matter (PM), and carbon dioxide (CO_2). Both engine types represent one of the significant contributors to ambient NOx and PM emissions. Greenhouse gases (GHG) emissions of concern from SI and diesel engine are CO_2, CH_4, and nitrous oxide (N_2O).

The formation of NOx during the combustion process is because of high temperatures and pressures. NOx is a regulated criteria pollutant, which can have an adverse effect on human health. NOx is also an important precursor for the formation of

ozone with the presence of volatile organic compounds (VOCs) and sunlight (Seinfeld and Pandis, 2006). Engine-our NOx emission levels for diesel engines are typically higher than those for spark-ignition engines due to higher in-cylinder combustion temperatures and limited methods to control them.

PM is another pollutant of great concern due to it being harmful to human health. In 2019, particulate matter with a diameter less than 2.5 μm ($PM_{2.5}$) represents the largest environmental risk factor human health (Murray et al., 2020). Exposure to $PM_{2.5}$ increases the risk of chronic disease, such as lung cancer and cardiopulmonary disease. Excessive $PM_{2.5}$ in the air can reduce visibility. Compared to fine particles ($PM_{2.5}$), smaller particles such as ultrafine particles with a diameter less than 100nm have more surface area and would cause more pulmonary inflammation and stay longer in the lung (Schraufnagel, 2020).

Greenhouse gas emissions have been of great importance due to global climate change. Starting from 2017, U.S. EPA has regulated GHG emissions from medium- or heavy- duty vehicles based on the vocations of the engine (EPA, 2011). In 2020, transportation sector accounts for 27% greenhouse gas emissions, representing the largest source of GHG emissions (EPA, 2022). CO_2 emissions come mostly from burning fossil fuels in the combustion process, which represent the largest contributor of GHG emissions (EPA, 2020).

In the United States (U.S.), heavy-duty diesel vehicles (HDDVs) and heavy-duty diesel engines (HDDEs) are the largest sources of NOx emissions in transportation sector (EPA, 2008). On-road heavy duty vehicles contribute 31 percent of all statewide emissions

in the transportation sector, which represent the largest single source category of NOx emissions.

U.S. EPA has also imposed more stringent emissions standards for light-duty or heavy-duty vehicles to regulate PM mass emissions. Same for off-road sector, the U.S. national emission inventory also indicates that off-road diesel equipment is the third-largest source for NOx emissions and the second largest source for PM with a diameter smaller than 2.5 μm (PM2.5) emissions, representing 14.5% and 24.3% of total mobile source emissions, respectively (EPA, 2008).

A series of regulations have been set by worldwide government agencies, such as U.S. EPA on NOx and PM over the past couple decades. The implementation of NOx emission standards started in 1974, and more stringent emission standards in recent years in 2007 and 2010, which require NOx emissions reduction to 0.2 g/bhp-hr. To meet the standards, more advanced engine technologies and exhaust aftertreatment systems were developed such as selective catalytic reduction (SCR) and exhaust gas recirculation (EGR) to meet the NOx 2010 standard as well as diesel particulate filter (DPF) to meet the PM 2007 standard.

The United States Environmental Protection Agency (U.S. EPA) has set a series of regulations to archive progressive reductions in NOx and PM emissions from HDDTs over the last forty years. The NOx emission standards were implemented starting in 1974 and were last made more stringent in 2007 and 2010. Those rules have required that emissions of NOx be reduced from an estimated unregulated emission level of 16 g/bhp-hr to 0.20 g/bhp-hr. The combination of selective catalytic reduction (SCR) and exhaust gas recirculation (EGR), along with other engine design changes, were used to meet the NOx

2010 standard. Recently, the California Air Resources Board (CARB) adopted optional low NOx standards, which targeted an additional order of magnitude reduction in NOx emissions (from 0.2 to 0.02 g/bhp-hr) for the model year of 2015 and newer HDDTs. Regulations of PM emissions have remained static since 2007, when the PM was reduced from 0.1 to 0.01 g/bhp-hr. The diesel engines were equipped with DPFs to remove particles to meet the 2007 PM standards.

This dissertation provides investigation and evaluation of new engine technologies and aftertreatment systems on reducing emissions of critical pollutants on in-use heavy-duty vehicles or equipment under real-world operation conditions. Real-world driving emissions have become a key factor to understand or identify high-emitting events under real-world driving conditions.

1.1. Real-World NOx and PM Emissions From Off-Road Construction

The U.S. national emission inventory indicates that off-road diesel equipment is the third-largest source for NOx emissions and the second largest source for PM with a diameter smaller than 2.5 μm (PM2.5) emissions, representing 14.5% and 24.3% of total mobile source emissions, respectively (EPA, 2008). Developing emissions factors and emissions inventories for off-road equipment has inherently been more challenging than for on-road vehicles. The current Tier 4 final emissions standards for off-road diesel engines have pushed the implementation of diesel particulate filters (DPFs) to meet PM standards, and SCR systems to meet NOx standards, though their implementation is still not universal. While there are extensive data on the effectiveness of DPF and SCR systems over certification test cycles run on an engine-dynamometer, real world data from modern diesel engines with these aftertreatment systems in off-road applications are scarce (Misra et al.,

2013; Quiros et al., 2016). Data on SCR performance also show some variation depending on the type of vehicle tested and its operational cycle. Of importance has been the finding that for on-road engines operating under low load conditions where exhaust temperatures are lower, the SCR system has a lower NOx emissions reduction efficiency than under high load conditions (Jiang et al., 2018; Misra et al., 2013). While it is expected that a similar phenomenon would be found for off-road engines, it is still not known the extent to which these conditions occur in real-world conditions.

1.2. Regulated and Unregulated Emissions From Two Ultra-Low NOx CNG Heavy-Duty Vehicles

Although the 2010 certification standards were designed to reduce NOx emissions, the in-use NOx emissions are actually much higher than certification standards for certain fleets (Monks et al., 2015; Quiros et al., 2016; Thiruvengadam et al., 2015). The magnitude is largely dependent on the duty cycle (Dixit et al., 2017). Since engines are certified at moderate to high engine loads, low load duty cycles can show different emission rates (Misra et al., 2017). For diesel engines, low load duty cycles have a significant impact on NOx emissions. Cold-start emissions can be several times higher than the certification standard, and much higher than the corresponding hot-start emissions (Herner et al., 2009; Velders et al., 2011). The main cause for the high NOx emissions is low selective catalytic reduction (SCR) inlet temperatures resulting from low power operation (Bishop et al., 2013; Misra et al., 2013; Thiruvengadam et al., 2016). Stoichiometric natural gas engines equipped with three-way catalysts (TWCs) are not subjected to the limitations posed by the use of SCR systems, resulting in in-use emissions that are more comparable to the emission certification levels. Previous studies have shown NOx emissions benefits with

heavy-duty CNG vehicles equipped with TWCs (Misra et al., 2017; Thiruvengadam et al., 2015).

New engine designs and alternative fuels are expected to play a major role in controlling NOx emissions and subsequently improving air quality. Several studies have shown the pathway for ultra-low NOx emissions from stoichiometric compressed natural gas (CNG) engines, capable of achieving sub 0.02 g/bhp-hr of NOx emissions(Sharp et al., 2017a; Sharp et al., 2017b). The use of natural gas has significantly increased in many fleets, such as refuse trucks, buses, delivery trucks, and yard tractors commonly used in on-terminal container movement (Fontaras et al., 2012; Karavalakis et al., 2013; Thiruvengadam et al., 2016). Natural gas is a clean-burning alternative fuel known for its soot-free combustion due to its lower carbon fraction compared to any other fossil fuel (Hesterberg et al., 2008; Korakianitis et al., 2011). Natural gas has a high octane number (up to 130) and relatively higher knock resistance compared to gasoline, which enables the use of higher compression ratio engines that provide better efficiency (Korakianitis et al., 2011; Thiruvengadam et al., 2018). Legacy natural gas engines were built on a diesel engine block retrofitted with a spark ignition platform and operated with lean-burn combustion and an oxidation catalyst that served to control carbon monoxide (CO) and nonmethane hydrocarbon (NMHC) emissions. Legacy lean-burn natural gas engines produced comparable levels of NOx emissions to diesel vehicles without SCR systems (Korakianitis et al., 2011). Current natural engines operate with spark ignited stoichiometric combustion with exhaust gas recirculation (EGR) and three-way catalysts (TWCs) to control NOx, CO, and total hydrocarbon (THC) emissions. The simultaneous reductions in CO and NOx emissions in the TWC are favored from oxygen deficient

exhaust conditions occurring during stoichiometric combustion (DeFoort et al., 2004). Studies have shown important reductions in NOx and THC emissions with stoichiometric natural gas engines compared to lean burn engines (Einewall et al., 2005; Hajbabaei et al., 2013; Yoon et al., 2013). Both Hajbabaei et al. and Yoon et al. showed that NOx emissions from stoichiometric natural gas engines equipped with a TWC were over 90% lower compared to lean-burn natural gas engines but showed higher CO emissions. Other studies have also shown that stoichiometric combustion is the most effective technology in reducing gaseous toxic pollutants, such as aldehydes and polycyclic aromatic hydrocarbons (Yoon et al., 2014). Recent investigations have reported dramatic NOx reductions with ultra-low NOx heavy-duty vehicles, even well below the 0.02 g/bhp-hr standard (Li et al., 2019).

1.3. NOx Emissions From In-Use Heavy-Duty Vehicles-200 Vehicle Study Chassis

As part of efforts to reduce emissions from on-road heavy-duty engines, more stringent U.S. EPA emissions standards of 0.20 g/bhp-hr NOx were introduced for 2010 and newer on-road heavy-duty engines. Since then, the heavy-duty vehicle population has included vehicles with more advanced engines and technologies, such as Selective Catalyst Reduction (SCR) for diesel vehicles. SCR utilizes ammonia that is hydrolyzed from an aqueous urea solution as a reactant to convert NOx into nitrogen and water (Guan et al., 2014). Although SCR catalysts provide good NOx emissions reductions under certain conditions, the conversion efficiency is highly dependent on the catalyst materials and conditions, urea injection timing and volume, etc. Many studies have shown elevated NOx emissions when the SCR inlet temperature is below 250 °C under various driving conditions (Tan et al., 2019). Studies have also shown that NOx emissions under real-world

conditions can significantly differ from those under more controlled laboratory conditions using an engine or chassis dynamometer. Real-world conditions, such as frequent stop-go events, extended idling, and low load/speed operation can have a large impact on SCR efficiency and tailpipe NOx emissions (Grigoratos et al., 2019; Kotz et al., 2016; Mendoza-Villafuerte et al., 2017). Studies have also found higher NOx emissions during cold start operation when the SCR catalyst is well below its light-off temperature (Weilenmann et al., 2009; Weilenmann et al., 2005).

Natural gas engines are another technology that can meet not only the 0.2 g/bhp-hr NOx standard, but also an optional 0.02 g/bhp-hr NOx standard, which is 90% below 2010 certification standard. Current natural engines technologies utilized spark-ignited, stoichiometric combustion with a three-way catalysts (TWC) aftertreatment system, as well as exhaust gas recirculation (EGR) to control NOx emissions. Several chassis dynamometer studies have demonstrated that late-model, stoichiometric, compressed natural gas (CNG) engines can achieve emissions at or below 0.02 g/bhp-hr NOx levels under a variety of conditions (Li et al., 2019; Zhu et al., 2020). Data from vehicles equipped with 0.2 and 0.02 g/bhp-hr CNG engines is still relatively limited in terms of the number of vehicles and testing over a wide range of mileages, so it is uncertain how effective these engines are over a wide range of applications and over the full useful vehicle lifespan. Additional data is also needed for emissions inventory models that are used for policy development.

Aside from NOx emissions, NH_3 and N_2O emissions are also pollutants of concern. NH_3 is considered to be a precursor to secondary inorganic aerosol formation (Liu et al., 2015). N_2O is an important greenhouse gas (GHG), which has a lifetime of about 121 years

in the atmosphere and a GWP of 298 based on a 100-year time horizon (Seyboth, 2013). Both NH_3 and N_2O are generally formed through reactions over the surfaces of the catalyst. A number of studies have demonstrated the formation of NH_3 over the surfaces of TWCs or other catalytic surfaces (Bae et al., 2022; Wang et al., 2015). Relatively high NH_3 emissions have been observed from heavy-duty CNG vehicles with TWCs in several studies (Thiruvengadam et al., 2016). For SCR-equipped diesel vehicles, overdosing of urea can also lead to "ammonia slip" that can in turn lead to elevated tailpipe NH_3 emissions. In spark-ignited engines, elevated N_2O emissions have been observed primarily during the initial warm-up period of the catalyst between temperatures of 300 °C to 500 °C. The formation of N_2O emissions under higher temperatures is minimal unless deterioration of the catalyst happens. Over the SCR catalyst, N_2O emissions form preliminarily due to both ammonia oxidation and decomposition of ammonium nitrate particles (Thiruvengadam et al., 2016). While the potential importance of NH_3 and N_2O emissions from heavy-duty vehicles is recognized, data for these two pollutants is still limited from heavy-duty vehicles, particularly over a wide range of operating conditions, and for vehicles with different mileages.

1.4. Particulate Matter Emissions From In-Use Heavy-Duty Vehicles-200 Vehicle Study Chassis

Regulators and policy makers worldwide have been implementing regulations that will control the PM emissions. Particle emission standards worldwide are generally based on the PM mass emissions. In the United States (U.S.), the Environmental Protect Agency (EPA) has imposed more stringent emissions standards for light-duty or heavy-duty vehicles to regulate PM mass emissions in the recent years. More advanced emissions

control systems such as diesel particulate filters (DPFs) for diesel vehicles and alternative fuels such as compressed natural gas, have been playing an important role in meeting PM mass standards. However, these advanced systems may be limited in reducing particle number emissions. Many recent studies have found that both DPF-equipped diesel vehicles and compressed natural gas vehicles emit more particle number emissions for the ultra-fine particles than larger size particles (Toumasatos et al., 2021). The European Union (EU) introduced solid particle number (SPN) emissions standards for diesel light-duty vehicles in 2011, which utilized the Particle Measurement Program (PMP) method to measure SPN with a cut size of 23 nm (Giechaskiel et al., 2017). There are still questions about the methodology of measuring "real" particle number emissions, however, due to different sampling artifacts (i.e. the sampling system, sampling location, instrument measurement accuracy, and particle loss rates) that may lead to significantly different results. The U.S. has also been considering total particle number emissions as key factor of PN regulation. Therefore, it is important to show total particle number emissions with different cut sizes to compare the PM and PN emissions standards and provide insights on setting the appropriate cut size for PN emissions.

Greenhouse gas emissions have become more and more important due to global climate change. Carbon-dioxide (CO_2), nitrous oxide (N_2O) and methane (CH_4) are combustion products or catalyst artifacts from diesel or natural gas engines that need to be considered. Starting from 2017, U.S. EPA has regulated GHG emissions from medium- or heavy- duty vehicles based on the vocations of the engine (EPA, 2011). In 2020, the transportation sector accounted for 27% of total greenhouse gas emissions, representing the largest source of GHG emissions in the transportation sector (EPA, 2020). CO_2

emissions come mostly from burning fossil fuels such as diesel or natural gas in the combustion process, which represent the largest contributor of GHG emissions (EPA, 2008). CH_4 emissions in the transportation sector mainly come from natural gas vehicles, since the major component of natural gas fuel is CH_4. N_2O emissions are mostly observed during the cold start operation for spark-ignited engines. N_2O emissions are also commonly seen for TWC-equipped vehicles where N_2O is a byproduct of catalyst reactions.

The chemical and toxicological properties of emissions from vehicles with more advanced technologies are also a concern. Many studies have been investigating the impact of advanced engine/aftertreatment technologies or fuel composition on emissions components with high toxicity(Li et al., 2021; Yoon et al., 2013). Yoon et al. showed stochiometric combustion with a three-way catalyst can be effective for reducing particulate compounds. Another recent study showed that renewable natural gas (RNG) may also be a strategy that could lead to reductions in the toxicity of the emissions.

1.5. Real World NOx Emissions From In-Use Heavy-Duty Goods Movement Vehicles-200 Vehicle Study On-Road

Studies have shown that the reduction efficiencies of NOx emissions from SCR-equipped engines vary significantly under real-world conditions due to patterns of operation that are different from laboratory testing, such as more frequent stop-go driving, extended idling and more low load/speed events (Haugen and Bishop, 2018; McCaffery et al., 2021; Misra et al., 2017; Preble et al., 2019; Tan et al., 2019).

Other engine technologies and alternative fuels could also play an important role in reducing NOx emissions. Natural gas engines technology can meet the NOx emission standard of 0.2 g/bhp-hr, with recent advancements in natural gas engine technology being

capable of meeting the optional 0.02 g/bhp-hr NOx emission standard, which is 90% below the 2010 certification standard. Several recent studies have shown that late-model, stoichiometric compressed ignition engines can achieve emissions at or below the 0.02 g/bhp-hr NOx levels under various conditions during chassis dynamometer and portable emissions measurement system (PEMS) testing (Li et al., 2019; McCaffery et al., 2021; Zhu et al., 2020). However, in-use emissions data under real-world operations is still limited compared to that for diesel vehicles, so there is still uncertainty about how effective these engines are over a wide range of applications, over a variety of driving operations, and over the vehicle's full lifetime.

Controlling NOx emissions for on-road heavy-duty vehicles under real-world driving conditions is challenging. In the U.S, heavy-duty engines are typically certified using an engine dynamometer over two main test cycles, the transient Federal Test Procedure (FTP) and the Supplement Emissions Test (SET). In-use compliance testing is also conducted that covers operation during not-to exceed (NTE) events, which are characterized by operation in the NTE zone, with the engine load above 30% and SCR operational temperatures greater than 250°C, as well as other requirements, for a period 30 continuous seconds, as specified in 40 CFR 86.1370-2007. A number of studies, however, have shown that only a small fraction of in-use operation occurs under conditions meeting the conditions for an NTE event (Badshah et al., 2019; McCaffery et al., 2021; Posada et al., 2020; Tan et al., 2019). As such, the U.S. EPA and the California Air resources Board (CARB) are in the process of setting forward and implementing new methodologies for in-use compliance testing. It is still important in the near term, however, to understand how vehicles will perform under these different types of operation on a wide scale.

1.6. **Outline of Dissertation**

Chapter 2 presents NOx and PM emissions for 10 pieces of Tier 4 final construction equipment including 3 excavators, 3 wheel loaders, 2 crawler tractors and 2 backhoe/loaders. The duty cycles included a pre-defined combined sequence of a cold-start phase, trenching, backfilling, travelling, and idling. This information will be useful for developing emissions inventory models, understanding the differences between certification levels and real-world emissions, and in understanding the effectiveness of advanced aftertreatment systems for off-road applications.

The results indicate that for all types of equipment, the highest NOx emissions were seen for the cold start phase due to exhaust temperatures being below the activation temperatures for the SCR system. NOx emissions for the trench and backfill modes were generally close to or below the in-use compliance emission rate, except for a few pieces of equipment that had higher NOx emissions due to cooler aftertreatment systems. Compared to the previous studies, the Tier 4 final equipment showed an average reduction of 91% for NOx emissions. This indicates a significant benefit could be achieved for NOx emissions by deploying Tier 4 final advanced technology, such as SCR, from an emission reduction perspective.

For Chapter 3, a goods movement vehicle equipped with the ISX12N 400 near-zero natural gas engine and a yard tractor equipped with the B6.7N 240 near-zero natural engine were evaluated over different test cycles on a heavy-duty chassis dynamometer. Both heavy-duty vehicles were operated stoichiometrically and equipped with a three-way catalyst (TWC). Experiments emphasized nitrogen oxide (NOx) emissions, greenhouse gases (GHGs), and particulate emissions. Results showed substantially low levels of NOx

emissions of both vehicles and dramatic reductions of up to 90% compared to the 2010 certification standard.

Chapter 4 and chapter 5 discuss gaseous and particulate emissions from a fleet of 14 heavy-duty vehicles of different vocations (school bus, transit bus, refuse hauler, delivery vehicle, and goods movement vehicle), fuels (diesel, hydrogenated vegetable oil [HVO]/renewable diesel (RD), and CNG), engine types, and aftertreatment controls (SCR or TWC), and over different drive cycles using a chassis dynamometer. Each vehicle selected for chassis dynamometer testing was tested over several driving cycles. All vehicles were tested over the Urban Dynamometer Driving Schedule (UDDS), allowing the UDDS test results to serve as a cross-vocational comparison point for all vehicles. Additionally, each vehicle was tested over one or more vocational cycles. The vocational test cycles were assigned based on the vehicle vocation. Delivery and goods movement vehicles were also tested with HHDDT cruise cycles.

Chapter 4 showed that the UDDS NOx emissions varied depending on the vocation and the technology with average NOx emissions across all vehicles ranged from 0.003 to 6.16 g/bhp-hr. NOx emissions for vocational cycle and HHDDT cruise cycles showed some variances compared with the UDDS cycle but in the same range.NH_3 and N_2O emissions are also pollutants of concern for air quality and global warming, which originates from the catalyst reaction. N_2O emissions from SCR equipped diesel vehicles originate from the catalyst reaction involving NH_3 and NOx emissions as well as the decomposition of nitrite particles.

Chapter 5 showed PM emissions were below the 10 mg/bhp-hr certification for all vehicles over both cold and hot start cycles. Total particle number emissions for most of

the CNG vehicles were above the European particle number limit, although the Euro limit is only for solid particles. This indicates that more efforts need to be made to reduce particle number emissions from natural gas vehicles to the emission certification levels. Most DPF-equipped diesel vehicles showed particle number emissions below the standard. CO_2 emissions are the main contributor to GHG emissions for all vehicles.

Chapter 6 measured and characterized NOx emissions from five heavy-duty diesel and natural gas goods movement vehicles with different engine technologies. All five vehicles were tested on-road under four pre-defined goods movement routes in SCAB, representing grocery distribution, port-drayage operation, and highway driving with and without elevation change. NOx emissions were measured using a mobile emissions laboratory. NOx emissions varied depending on the vehicle and the route. The newly proposed three-bin MAW method was utilized to show the NOx emissions across various modes of operation conditions, including idle, low load, and medium/high load.

1.7. **References**

Badshah H, Posada F, Muncrief R. Current State of NO_x Emissions from In-Use Heavy-Duty Diesel Vehicles in the United States. 2019.

Bae WB, Byun SW, Hazlett M, Jung C, Kim CH, Kang SB. Emission of NH3 and N2O during NO reduction over commercial aged three-way catalyst (TWC): Role of individual reductants in simulated exhausts. Chemical Engineering Journal Advances 2022; 9: 100222.

Bishop GA, Schuchmann BG, Stedman DH. Heavy-duty truck emissions in the South Coast Air Basin of California. Environmental science & technology 2013; 47: 9523-9529.

DeFoort M, Olsen D, Willson B. The effect of air-fuel ratio control strategies on nitrogen compound formation in three-way catalysts. International Journal of Engine Research 2004; 5: 115-122.

Dixit P, Miller JW, Cocker III DR, Oshinuga A, Jiang Y, Durbin TD, et al. Differences between emissions measured in urban driving and certification testing of heavy-duty diesel engines. Atmospheric Environment 2017; 166: 276-285.

Einewall P, Tunestål P, Johansson B. Lean burn natural gas operation vs. stoichiometric operation with EGR and a three way catalyst. SAE technical paper 2005: 0250.

EPA, 2008. National Emissions Inventory (NEI). https://www.epa.gov/air-emissions-inventories/2008-national-emissions-inventory-nei-data, accessed Nov 2022.

EPA, Inventory of U.S. Greenhouse Gas Emissions and Sinks: 1990-2020, published 2022, https://www.epa.gov/ghgemissions/inventory-us-greenhouse-gas-emissions-and-sinks-1990-2020, Accessed Nov 2022.

EPA, Office of Transportation and Air Quality, 2011. Final Rulemaking to establish greenhouse gas emissions standards and fuel efficiency standards for medium- and heavy-duty engines and vehicles, https://www3.epa.gov/otaq/climate/documents/420r11901.pdf, Accessed Nov 2022.

EPA, 2020, Overview of Greenhouse Gases.https://www.epa.gov/ghgemissions/overview-greenhouse-gases#carbon-dioxide, Accessed Nov 2022.

EPA, 2008, NONROAD2008 Model, https://www.epa.gov/moves/nonroad-technical reports# 2008a, Accessed Sep 2022.

Fontaras G, Martini G, Manfredi U, Marotta A, Krasenbrink A, Maffioletti F, et al. Assessment of on-road emissions of four Euro V diesel and CNG waste collection trucks for supporting air-quality improvement initiatives in the city of Milan. Science of the total environment 2012; 426: 65-72.

Giechaskiel B, Vanhanen J, Väkevä M, Martini G. Investigation of vehicle exhaust sub-23 nm particle emissions. Aerosol Science and Technology 2017; 51: 626-641.

Grigoratos T, Fontaras G, Giechaskiel B, Zacharof N. Real world emissions performance of heavy-duty Euro VI diesel vehicles. Atmospheric environment 2019; 201: 348-359.

Guan B, Zhan R, Lin H, Huang Z. Review of state of the art technologies of selective catalytic reduction of NOx from diesel engine exhaust. Applied Thermal Engineering 2014; 66: 395-414.

Hajbabaei M, Karavalakis G, Johnson KC, Lee L, Durbin TD. Impact of natural gas fuel composition on criteria, toxic, and particle emissions from transit buses equipped with lean burn and stoichiometric engines. Energy 2013; 62: 425-434.

Haugen MJ, Bishop GA. Long-term fuel-specific NO x and particle emission trends for in-use heavy-duty vehicles in california. Environmental science & technology 2018; 52: 6070-6076.

Herner JD, Hu S, Robertson WH, Huai T, Collins JF, Dwyer H, et al. Effect of advanced aftertreatment for PM and NO x control on heavy-duty diesel truck emissions. Environmental science & technology 2009; 43: 5928-5933.

Hesterberg TW, Lapin CA, Bunn WB. A comparison of emissions from vehicles fueled with diesel or compressed natural gas. Environmental science & technology 2008; 42: 6437-6445.

Heywood JB. Internal combustion engine fundamentals: McGraw-Hill Education, 2018.

Jiang Y, Yang J, Cocker III D, Karavalakis G, Johnson KC, Durbin TD. Characterizing emission rates of regulated pollutants from model year 2012+ heavy-duty diesel vehicles equipped with DPF and SCR systems. Science of The Total Environment 2018; 619: 765-771.

Karavalakis G, Hajbabaei M, Durbin TD, Johnson KC, Zheng Z, Miller WJ. The effect of natural gas composition on the regulated emissions, gaseous toxic pollutants, and ultrafine particle number emissions from a refuse hauler vehicle. Energy 2013; 50: 280-291.

Korakianitis T, Namasivayam A, Crookes R. Natural-gas fueled spark-ignition (SI) and compression-ignition (CI) engine performance and emissions. Progress in energy and combustion science 2011; 37: 89-112.

Kotz AJ, Kittelson DB, Northrop WF. Lagrangian hotspots of in-use NOx emissions from transit buses. Environmental Science & Technology 2016; 50: 5750-5756.

Li C, Han Y, Jiang Y, Yang J, Karavalakis G, Durbin TD, et al. Emissions from advanced ultra-low-NOx heavy-duty natural gas vehicles. 2019.

Li Y, Xue J, Peppers J, Kado NY, Vogel CF, Alaimo CP, et al. Chemical and toxicological properties of emissions from a Light-Duty compressed natural gas vehicle fueled with renewable natural gas. Environmental science & technology 2021; 55: 2820-2830.

Liu T, Wang X, Deng W, Zhang Y, Chu B, Ding X, et al. Role of ammonia in forming secondary aerosols from gasoline vehicle exhaust. Science China Chemistry 2015; 58: 1377-1384.

McCaffery C, Zhu H, Tang T, Li C, Karavalakis G, Cao S, et al. Real-world NOx emissions from heavy-duty diesel, natural gas, and diesel hybrid electric vehicles of different vocations on California roadways. Science of The Total Environment 2021; 784: 147224.

Mendoza-Villafuerte P, Suarez-Bertoa R, Giechaskiel B, Riccobono F, Bulgheroni C, Astorga C, et al. NOx, NH3, N2O and PN real driving emissions from a Euro VI heavy-duty vehicle. Impact of regulatory on-road test conditions on emissions. Science of The Total Environment 2017; 609: 546-555.

Misra C, Collins JF, Herner JD, Sax T, Krishnamurthy M, Sobieralski W, et al. In-use NO x emissions from model year 2010 and 2011 heavy-duty diesel engines equipped with aftertreatment devices. Environmental science & technology 2013; 47: 7892-7898.

Misra C, Ruehl C, Collins J, Chernich D, Herner J. In-use NOx emissions from diesel and liquefied natural gas refuse trucks equipped with SCR and TWC, respectively. Environmental science & technology 2017; 51: 6981-6989.

Monks PS, Archibald A, Colette A, Cooper O, Coyle M, Derwent R, et al. Tropospheric ozone and its precursors from the urban to the global scale from air quality to short-lived climate forcer. Atmospheric Chemistry and Physics 2015; 15: 8889-8973.

Murray CJ, Aravkin AY, Zheng P, Abbafati C, Abbas KM, Abbasi-Kangevari M, et al. Global burden of 87 risk factors in 204 countries and territories, 1990–2019: a systematic analysis for the Global Burden of Disease Study 2019. The Lancet 2020; 396: 1223-1249.

Posada F, Badshah H, Rodriguez F. In-use NOx emissions and compliance evaluation for modern heavy-duty vehicles in Europe and the United States. 2020.

Preble CV, Harley RA, Kirchstetter TW. Control technology-driven changes to in-use heavy-duty diesel truck emissions of nitrogenous species and related environmental impacts. Environmental science & technology 2019; 53: 14568-14576.

Quiros DC, Thiruvengadam A, Pradhan S, Besch M, Thiruvengadam P, Demirgok B, et al. Real-world emissions from modern heavy-duty diesel, natural gas, and hybrid diesel trucks operating along major California freight corridors. Emission Control Science and Technology 2016; 2: 156-172.

Schraufnagel DE. The health effects of ultrafine particles. Experimental & molecular medicine 2020; 52: 311-317.

Seinfeld J, Pandis S. Atmospheric chemistry and physics: from air pollution to climate change. Atmospheric chemistry and physics: from air pollution to climate change. 2006.

Seyboth K. Intergovernmental panel on climate change (IPCC). Encyclopedia of Energy, Natural Resource, and Environmental Economics 2013.

Sharp C, Webb CC, Neely G, Carter M, Yoon S, Henry C. Achieving ultra low NOx emissions levels with a 2017 heavy-duty on-highway TC diesel engine and an advanced technology emissions system-thermal management strategies. SAE International Journal of Engines 2017a; 10: 1697-1712.

Sharp C, Webb CC, Yoon S, Carter M, Henry C. Achieving ultra low NOx emissions levels with a 2017 heavy-duty on-highway TC diesel engine-comparison of advanced technology approaches. SAE International Journal of Engines 2017b; 10: 1722-1735.

Tan Y, Henderick P, Yoon S, Herner J, Montes T, Boriboonsomsin K, et al. On-board sensor-based NO x emissions from heavy-duty diesel vehicles. Environmental science & technology 2019; 53: 5504-5511.

Thiruvengadam A, Besch M, Carder D, Oshinuga A, Pasek R, Hogo H, et al. Unregulated greenhouse gas and ammonia emissions from current technology heavy-duty vehicles. Journal of the Air & Waste Management Association 2016; 66: 1045-1060.

Thiruvengadam A, Besch M, Padmanaban V, Pradhan S, Demirgok B. Natural gas vehicles in heavy-duty transportation-A review. Energy Policy 2018; 122: 253-259.

Thiruvengadam A, Besch MC, Thiruvengadam P, Pradhan S, Carder D, Kappanna H, et al. Emission rates of regulated pollutants from current technology heavy-duty diesel and natural gas goods movement vehicles. Environmental science & technology 2015; 49: 5236-5244.

Toumasatos Z, Kontses A, Doulgeris S, Samaras Z, Ntziachristos L. Particle emissions measurements on CNG vehicles focusing on Sub-23nm. Aerosol Science and Technology 2021; 55: 182-193.

Velders GJ, Geilenkirchen GP, de Lange R. Higher than expected NOx emission from trucks may affect attainability of NO2 limit values in the Netherlands. Atmospheric environment 2011; 45: 3025-3033.

Wang J, Chen H, Hu Z, Yao M, Li Y. A review on the Pd-based three-way catalyst. Catalysis Reviews 2015; 57: 79-144.

Weilenmann M, Favez J-Y, Alvarez R. Cold-start emissions of modern passenger cars at different low ambient temperatures and their evolution over vehicle legislation categories. Atmospheric environment 2009; 43: 2419-2429.

Weilenmann M, Soltic P, Saxer C, Forss A-M, Heeb N. Regulated and nonregulated diesel and gasoline cold start emissions at different temperatures. Atmospheric environment 2005; 39: 2433-2441.

Yoon S, Collins J, Thiruvengadam A, Gautam M, Herner J, Ayala A. Criteria pollutant and greenhouse gas emissions from CNG transit buses equipped with three-way catalysts compared to lean-burn engines and oxidation catalyst technologies. Journal of the Air & Waste Management Association 2013; 63: 926-933.

Yoon S, Hu S, Kado NY, Thiruvengadam A, Collins JF, Gautam M, et al. Chemical and toxicological properties of emissions from CNG transit buses equipped with three-way catalysts compared to lean-burn engines and oxidation catalyst technologies. Atmospheric Environment 2014; 83: 220-228.

Zhu H, McCaffery C, Yang J, Li C, Karavalakis G, Johnson KC, et al. Characterizing emission rates of regulated and unregulated pollutants from two ultra-low NOx CNG heavy-duty vehicles. Fuel 2020; 277: 118192.

2. Real World Emissions From Tier 4F Off-Road Construction Equipment

2.1. Abstract

The primary purpose of this study was to obtain gas-phase and particular matter (PM) emissions from newer Tier 4 final off-road construction equipment using a Portable Emissions Measurement System (PEMS). This information can be used to provide accurate estimates of emissions from off-road construction equipment under real-world scenarios. Emission measurements were made for 10 pieces of Tier 4 final construction equipment including 3 excavators, 3 wheel loaders, 2 crawler tractors and 2 backhoe/loaders. The duty cycles included a pre-defined combined sequence of a cold-start phase, trenching, backfilling, travelling, and idling. For all types of equipment, the highest emissions were seen for the cold start phase, which showed NOx emissions levels ranging from 3.4 to 6.3 g/bhp-hr, from 15.8 to 26.1 g/kg-fuel and from 107 to 249 g/hour, with an average exhaust temperature around 100℃.The next highest emissions were found for the travel mode. NOx emissions from the idle period ranged from 12.8 to 50 g/hour. NOx emissions from all equipment categories over trench and backfill modes show a range from 0.07 to 0.69 g/bhp-hr, from 0.4 to 3.7 g/kg-fuel, and from 11.4 to 34.2 g/hour. NOx emissions over trench and backfill work modes were generally close to or below the in-use compliance emission rate (1.5 times engine certified emissions rate) except for a few pieces of equipment that showed higher emissions due to less effective aftertreatment systems or lower exhaust temperatures. PM emissions ranged from 0.1 to 13 mg/bhp-hr, which is below the standard of 20 mg/bhp-hr for Tier 4 final off-road equipment. The

backhoe/loader category shows the highest emissions because both pieces of equipment in this category lacked a DPF to reduce PM emissions.

2.2. **Introduction**

Controlling pollutant emissions from mobile sources has been a key topic worldwide over the past several decades. Off-road equipment is considered one of the most significant sources of nitrogen oxides (NOx) and particulate matter (PM) both nationally within the United States (U.S.) and within California (EPA, 2017; CARB, 2020). The U.S. national emission inventory indicates that off-road diesel equipment is the third-largest source for NOx emissions and the second largest source for PM with a diameter smaller than 2.5 μm (PM2.5) emissions, representing 14.5% and 24.3% of total mobile source emissions, respectively (EPA, 2008). In California, emissions from the off-road sector represent 15% of NOx and 20% of PM2.5 emissions from mobile sources in 2020 (CARB, 2017; 2020). Although emission standards have been made increasingly more stringent over the past decade, there is still some lag between the implementation of the standards for off-road equipment compared to similar standards for on-road vehicles. Off-road engines also have a relatively longer lifespan than on-road vehicle engines. Those factors suggest that the contributions of emissions from off-road equipment will continue to increase relative to that of on-road vehicle emissions. This makes the control of emissions from off-road equipment one of the more critical areas in terms of reducing emissions and protecting public health.

Developing emissions factors and emissions inventories for off-road equipment has inherently been more challenging than for on-road vehicles. The estimation of emissions factors for off-road equipment can be obtained from non-road vehicle emission models,

such as NONROAD developed by the US EPA (EPA, 2008) (Marshall et al., 2012; Rasdorf et al., 2012), and the OFFROAD model developed by the California Air Resource Broad (CARB) (CARB, 2017)(Lewis et al., 2012b; Rasdorf et al., 2010; Shao, 2016). However, these emissions factor values from the models are usually derived from engine dynamometer tests that may not necessarily be representative of engine operation under real-world conditions due to different activities modes, varied operations, different machine types, and engine deterioration (Cao et al., 2018; Lewis et al., 2009a; Lewis et al., 2019; Lewis et al., 2009b; Shao, 2016; Tan et al., 2021). Although newer engines are now certified on a combination of steady-state and transient engine dynamometer test cycles, in general, the certification of off-road engines is still not designed to represent the full range of in-use operations that the engines might be operated over under real-world conditions.

Although some studies have measured emissions from in-use off-road equipment, the available data for off-road equipment is still considerably more limited compared to on-road mobiles sources. Many previous studies measured emissions from off-road equipment using portable emissions measurement systems (PEMS). Frey et al., (Frey et al., 2008a; Frey et al., 2008b; Frey et al., 2010) and Lewis et al., (Lewis et al., 2009a; Lewis et al., 2019; Lewis et al., 2011; Lewis et al., 2009b) measured emissions from a number of pieces of Tier 1 and 2 construction equipment using PEMS, and also developed an emissions model to estimate the emissions impact of the whole category. Abolhasani et al. measured three excavators certified to Tier 1 standards using PEMS and found the importance of accounting for inter-cycle variability in real-world, in-use emissions to develop more accurate emission inventories (Abolhasani et al., 2008). Fu et al. measured gaseous and PM emissions of twelve excavators and eight wheel loaders and found the greater the

accumulated working hours, the higher their HC and NO emissions factor were(Fu et al., 2012). Cao et al. evaluated in-use emission factors from twenty-seven pieces of construction equipment including four backhoes, six-wheel loaders, four excavators, two scrapers, six bulldozers, and four graders (Cao et al., 2018). This study covered a wide range of equipment types, and both Tier 2 and Tier 3 certified equipment. Cao et al. also characterized emissions from three hybrid excavators and four conventional excavators with PEMS over duty cycles designed from real-world activity data. They found utilizing hybrid technology can provide potential benefits in CO_2 emissions reductions but can also lead to increases in PM emissions(Cao et al., 2016). Desouza et al. measured NO_X, CO_2, and PM exhaust emissions from a total of 30 construction machines certified to Euro Stage III to Stage IV in London using PEMS over real world conditions and illustrated the importance of selective catalytic reduction (SCR) in reaching and maintaining low NOx emission standards (Desouza et al., 2020).

The current Tier 4 final emissions standards for off-road diesel engines have pushed the implementation of diesel particulate filters (DPFs) to meet PM standards, and SCR systems to meet NOx standards, though their implementation is still not universal. While there are extensive data on the effectiveness of DPF and SCR systems over certification test cycles run on an engine-dynamometer, real world data from modern diesel engines with these aftertreatment systems in off-road applications are scarce (Misra et al., 2013; Miller et al., 2013; CARB, 2014; Quiros et al., 2017). Data on SCR performance also show some variation depending on the type of vehicle tested and its operational cycle. Of importance has been the finding that for on-road engines operating under low load conditions where exhaust temperatures are lower, the SCR system has a lower NOx emissions reduction

efficiency than under high load conditions (Jiang et al., 2018; Misra et al., 2013). While it is expected that a similar phenomenon would be found for off-road engines, it is still not known the extent to which these conditions occur in real-world conditions.

The primary purpose of this research is to obtain NOx and PM emissions from Tier 4 final off-road construction equipment using PEMS under real-world scenarios. This study included 10 pieces of construction equipment, including excavators, wheel loaders, crawler dozers, and backhoes/loaders. The information obtained in this study provides a more accurate dataset for emissions inventory development, and for designing or optimizing emissions models such as NONROAD or OFFROAD, which are currently utilized for estimating off-road emissions. NOx emissions analysis was also provided in this study to understand the differences between engine certification standard values and real-world emissions rates. Finally, these results show how advanced aftertreatment systems perform over real-world conditions.

2.3. **Materials and Methods**

2.3.1. **Test Matrix**

Emission Measurements were made for 10 pieces of Tier 4 final equipment, which included 3 excavators, 3 wheel loaders, 2 backhoe/loaders, and 2 crawler tractors. The basic specifications for the off-road equipment tested are summarized in Table 2.1. Detailed information about the engines is presented in Table 2.3. The equipment types are denoted as EX for excavator, WL for wheel loader, CD for crawler dozer and BH/L for backhoe/loader, followed by the equipment numbers. The engines ranged from model year 2014 to 2017, in rated horsepower from 115 to 397 horsepower (hp), and in hours of operation from 91 to 3,652 hours. Of the ten engines, eight were equipped with DPF-SCR

aftertreatment systems, while the other two were equipped with only an SCR aftertreatment system. The equipment was all tested with retail ultra-low sulfur diesel (ULSD) with a sulfur content of less than 15 ppm. All the equipment was rented from local companies and operated in test lots at the rental agency's sites. The equipment was operated by experienced operators.

Table 2.1 Equipment tested using PEMS

Type	Make	Model Year	Size (liters)	Power (HP)	Odometer Reading (Hours)	Aftertreatment Device
EX_#1	CAT	2015	7.0	204	2063	DPF-SCR
EX_#2	CAT	2016	9.3	318	1615	DPF-SCR
EX_#3	Hitachi	2017	5.2	172	350	DPF-SCR
WL_#1	CAT	2015	7.0	188	2057	DPF-SCR
WL_#2	JD	2017	9.0	365	359	DPF-SCR
WL_#3	JD	2014	13.5	397	97	DPF-SCR
CD_#1	JD	2014	13.5	397	1996	DPF-SCR
CD_#2	CAT	2015	15.2	357	3654	DPF-SCR
BH/L_#1	CAT	2015	4.4	115	1601	SCR
BH/L_#2	JD	2017	4.5	126	695	SCR

2.3.2. **Work Mode**

The equipment was tested over different conditions, designed to represent the different types of operation the equipment performs in the field. A summary of the work modes descriptions is provided in Table 2.2. The primary physical work consisted of trenching, backfilling, idling, and general equipment movement between locations. The

cold-start, travel, and idle modes for the different pieces of equipment were similar between the different pieces of equipment, but the trenching and backfilling modes were different for each equipment category based on its typical operation. Here, the terms “Trench” and “Backfill” were used to universally represent “Digging” and “Refilling” type of work, respectively. For the trenching and backfilling operations, the equipment was subjected to different loads (classified as light, medium, and heavy) based on how full the bucket was or the amount of dirt being pushed around. It was hard to distinguish between different workload activities visually or through analysis of the dataset, therefore the data for light, medium, and heavy load was combined within each of the primary operation categories.

Table 2.2 Mode Names and Description

Mode Name	Description
Cold-Start	Start engine and idle for 5 min.
Idle	Idle between each trench or backfill for 60 seconds
Travel	For Excavator and Crawler Dozer, traveling from parking area to test lot. For Wheel Loader and Backhoe/Loader, driving around test lots in addition.
Trench	Dig a trench and empty the bucket. For Crawler Dozer, using the ripper rip the soil instead.
Backfill	Backfilling each trench

2.3.3. **PEMS Descriptions**

Gas-phase emissions were measured with a CFR1065 compliant SEMTECH DS PEMS. This PEMS measures pollutant concentrations in the raw exhaust using a non-dispersive ultra-violent (NDUV) analyzer to measure NOx, and a non-dispersive infrared

(NDIR) analyzer to measure carbon monoxide (CO) and carbon dioxide (CO_2). The SEMTECH DS system also records information broadcast by the Engine Control Module (ECM).

PM emissions were measured with an AVL Micro Soot Sensor (MSS) with a gravimetric filter box. The MSS measures soot concentration (solid particles) on a second-by-second basis using the photo-acoustic principle. The gravimetric filter box adjusts the soot measurement using a combination of time resolved soot values and integrated volatile organic compounds (VOC) values to calculate an equivalent total PM mass. The accumulated soot signal from the MSS is compared with the total mass on the filter. The ratio of the difference is multiplied by the soot real-time signal to estimate the total PM.

A 5-inch SEMTECH exhaust flow meter (EFM) was used to measure real-time exhaust flow, which is multiplied by the exhaust concentrations on a second-by-second basis to obtain mass emission results. The EFM was placed in line with the engine tailpipe. Other important test parameters collected included location data from a Global Positioning System (GPS), ambient temperature, pressure, and humidity. All the equipment tested had ECM data available.

2.3.4. **PEMS Installation**

Due to the complexity of measuring real-world off-road emissions, each piece of equipment required a unique installation approach. A custom steel frame instrument package with the gas-phase PEMS, PM PEMS, data logging equipment, batteries, a battery charger, and other necessary operating auxiliary items was used to mount all of instruments on the equipment in a single package. The custom frame with the instruments was lifted by a forklift or a crane, placed on the roof of the equipment to be tested, and fastened down

with straps. Vibration isolation mounts installed onto the steel frame and a six-inch-thick high-density foam pad between the frame and the equipment were utilized to provide vibrational dampening. The routing of the exhaust pipes to the EFM, connecting the PEMS to the ECM, and installing the auxiliary generator for power was done after this. Weather shielding was used to protect the PEMS package from direct sunlight.

2.4. **Results**

2.4.1. **NOx Emissions**

NOx emissions for the different equipment types over different modes are presented in Figure 2.1 Averaged NOx emissions profile in units of g/kg-fuel and g/hour and averaged exhaust temperature profile by modes and equipment types. in units of g/bhp-hr, g/kg-fuel and g/hour. The values are the averages for pieces of equipment in each category, and the error bars represent the standard deviation of the average within that category. The corresponding average exhaust temperature from each category is also included in the figure. The units of grams of pollutant per horsepower-hour (or per kilowatt-hour) of work provide a comparison with the certification standard. However, g/bhp-hr unit are less precise compared to fuel-based or time-based units because work values are not easily attained through the ECM logger for some off-road equipment.

For all types of equipment, the highest emissions were seen for the cold-start phase, which showed NOx emissions levels ranging from 3.4 to 6.3 g/bhp-hr, from 15.8 to 26.1 g/kg-fuel, and from 107 to 249 g/hour. The average exhaust temperature from the cold-start phase was around 100°C. NOx emissions are expected to be higher for cold-start conditions than hot-running operation due to the SCR system being below its effective operating range, resulting in a reduced NOx conversion efficiency during cold-starts. The next

highest emissions were found for the travel mode with a range from 0.41 to 3.7 g/bhp-hr, from 2.3 to 6.7 g/kg-fuel, and from 46 to 112 g/hour. It should be noted that both cold-starts and travel activity, representing movement of the equipment between the parking area and working site, and thus only represent a small fraction of the daily operation.

NOx emissions from all equipment categories for trench and backfill operation showed a range from 0.07 to 0.69 g/bhp-hr, from 0.4 to 3.7 g/kg-fuel, and from 11.4 to 34.2 g/hour. It is noted that backhoe/loader category showed average emissions rate higher than the current certification standard of 0.30 g/bhp-hr for off-road Tier 4 final equipment, ranging from 0.61 to 0.69 g/bhp-hr, from 3.4 to 3.7 g/kg-fuel, and from 30 to 33 g/hour. However, the variance between equipment within this category was large due to higher emissions from BH/L_#1, which was equipped with a smaller displacement engine and a less efficient aftertreatment system. A more detailed analysis for BH/L_#1 is provided in the next section. Emissions for the excavator and crawler dozer categories, on the other hand, showed emissions lower than the certification standard, ranging from 0.07 to 0.16 g/bhp-hr, from 0.42 to 0.87 g/kg-fuel, and from 11.4 to 18.3 g/hour. Emissions from the wheel loader category were close to the certification standard ranging from 0.22 to 0.35 g/bhp-hr.

Idle emissions from heavy-duty diesel engines have been a key subject for regulatory agencies. For example, California has adopted measures that could limit the idling of long-haul trucks equipped with and without sleeper cabs and buses to no more than 5 minutes (Khan et al., 2009) (CARB, 2004). Idle emissions have been underestimated for heavy-duty vehicles, especially for off-road equipment, due to a large fraction of idle activities under real-world conditions (Lewis et al., 2012a). Idle emissions are generally expressed

in unit of g/hour instead of on a load-specific basis because the load percent obtained from the ECM logger during the idle period is very low and is less accurate. NOx emissions from idle period ranged from 12.8 to 50 g/hour.

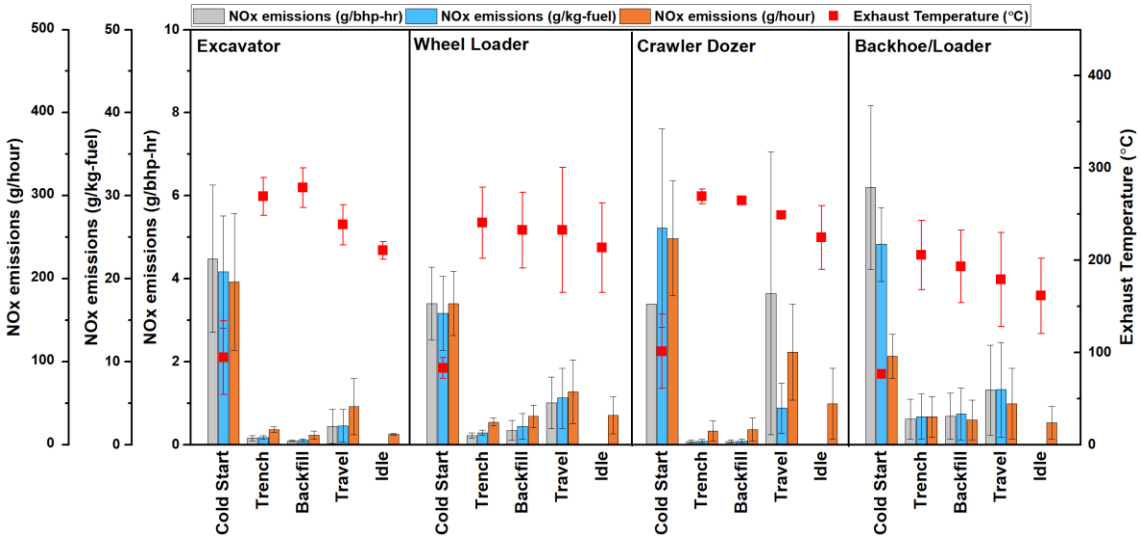

Figure 2.1 Averaged NOx emissions profile in units of g/kg-fuel and g/hour and averaged exhaust temperature profile by modes and equipment types.

2.4.2. In-Use Compliance Emissions vs. Real World Emissions

Figure 2.2 Averaged NOx emissions profile in units of g/bhp-hr, averaged exhaust temperature, and certification standard profile by modes and equipment types. shows NOx emissions on a g/bhp-hr basis, as well as average exhaust temperature for each piece of equipment for the trench and backfill work mode operations. These operational modes are examined in greater detail because they are the primary activities for off-road construction equipment. The certification standard for each engine is listed in Table 2.4 and estimated in-use compliance levels are also given in the Figure 2.2 Averaged NOx emissions profile in units of g/bhp-hr, averaged exhaust temperature, and certification standard profile by modes and equipment types. The in-use compliance level is based on 1.5 times the certified

standard, which is the criteria used for in-use compliance testing for heavy-duty on-road engines and is also included for comparison purposes.

NOx emissions for the trench and backfill work modes were generally close or below the estimated in-use compliance emission rate (1.5 times engine certified emissions rate), except for the trench mode for EX_#3, and the backfill modes for WL_#1, WL_#2 and BH/L_#1. Real-world emission rates from these four pieces of equipment were higher than the engine certified standard by an approximate average factor of 5 and higher than the estimated in-use compliance rate by an approximate average factor of 3. The exhaust temperatures averaged above 250℃, except for the WL_#1 and BH/L_#1 which showed an average exhaust temperature below 200℃. Lower exhaust temperatures indicate relatively cooler aftertreatment systems, therefore lower NOx conversion efficiencies are expected. WL_#2 showed DPF regeneration events happened periodically throughout the day of operation. The DPF regeneration events are shown separately in the figure so that typical operational emissions between the different pieces of equipment can be compared without the added complexity of trying to estimate the regeneration contribution to overall emissions for each piece of equipment. NOx emissions for DPF regeneration events averaged around 0.75 g/bhp-hr, which is about 3 times higher than the certification standard. Previous studies have shown that higher NOx emissions during DPF regeneration are due to the reduction of the EGR rate, and reduced NOx reduction efficiency over the catalyst under high engine load and fuel-rich modes. (Bermúdez et al., 2011; Ko et al., 2016).

It is interesting to note that all equipment showed similar emission rates between the trench and backfill modes, except for EX_#3 and WL_#1. EX_#3 had higher emissions in the

trench mode than in backfill mode, and WL_#1 showed the opposite trend, with higher emissions for the backfill mode. Further real-time emissions analysis was done for both pieces of equipment to evaluate these differences. Figure 2.3(a-c) Real-time NOx emissions from Excavator_#3 shows the real-time data analysis for EX_#3 for a day of activity. Fig 3a provides information on engine speed and engine load in order to identify the engine stop events (engine speed and load both zero), idle events (constant low engine idle speed and low load), and work events (rapid changes in engine speed and load). This figure shows the sequence of modes performed as engine stop, work, idle, work, and then this sequence was repeated.

Figure 2.3(b) provides information on real-time NOx emissions and real-time exhaust temperature for EX_#3. The results show that NOx emissions spiked after the equipment was just beginning backfilling or trenching operations after the engine was off or idling, respectively. This corresponded to periods where the exhaust temperature was at its lowest level of 200℃. It is interesting to note that NOx emissions spiked higher after the idle event than after the engine stop, even though exhaust temperature was lower after the engine was off. For this piece of equipment, the trench mode was always performed after the idle period and the backfill mode was always performed following engine stop event, which explains the difference of NOx emissions between these two modes. Comparing NOx emissions on a time basis from the idle periods beginning around 12,000s and 17,000s indicates higher emissions can occur when the engine idles for a longer period of time. Figure 2.3 (c) provides a zoomed-in graph of the last repeat of the testing sequence. Figure 2.3 (c) shows that after the engine idles for a longer period of time that emissions start to increase, which coincides with the exhaust temperature decreasing to levels where the

aftertreatment is likely less effective. Interestingly, idle NOx emission rates for the period between 17,500 and 18,000 reached levels around 0.010 to 0.012 g/s, which is higher than the emission rates during a typical work mode, as represented from approximately 16,000 to 16,800 seconds.

Figure 2.4 provides information on real-time engine speed, engine load percentage, NOx emissions, and exhaust temperature for WL_#1. NOx emission spikes were found after the idle period for each sequence, similar to those for EX_#3. It is noted that there was a slight increase in exhaust temperature when the engine started which could be due to the release of the heat remaining in the engine block from the previous operation. This phenomenon was not found in other studies. SCR inlet temperature is known as a key indicator of SCR conversion efficiency (Jiang et al., 2018). The reduction efficiency is expected to be over 90% when the SCR inlet temperature is around or over 250℃. (Jiang et al., 2018; McCaffery et al., 2021; Mendoza-Villafuerte et al., 2017). This condition was rarely reached with WL_#1, however, and therefore higher emission rates were expected for this piece of equipment. In addition, the trench event happened right after the idle for all three testing sequences, causing NOx emissions to be higher for the backfill than trench modes.

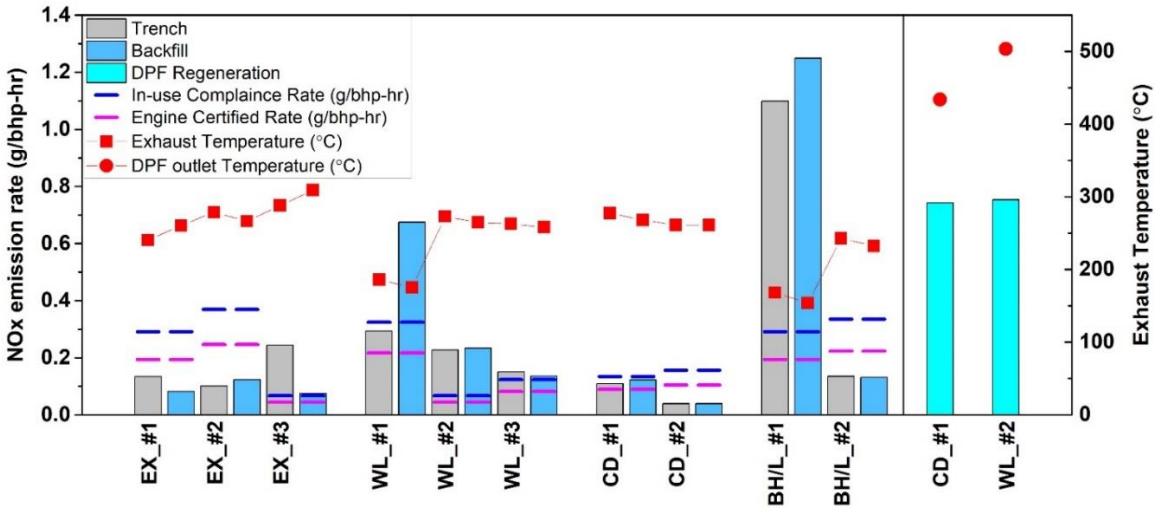

Figure 2.2 Averaged NOx emissions profile in units of g/bhp-hr, averaged exhaust temperature, and certification standard profile by modes and equipment types.

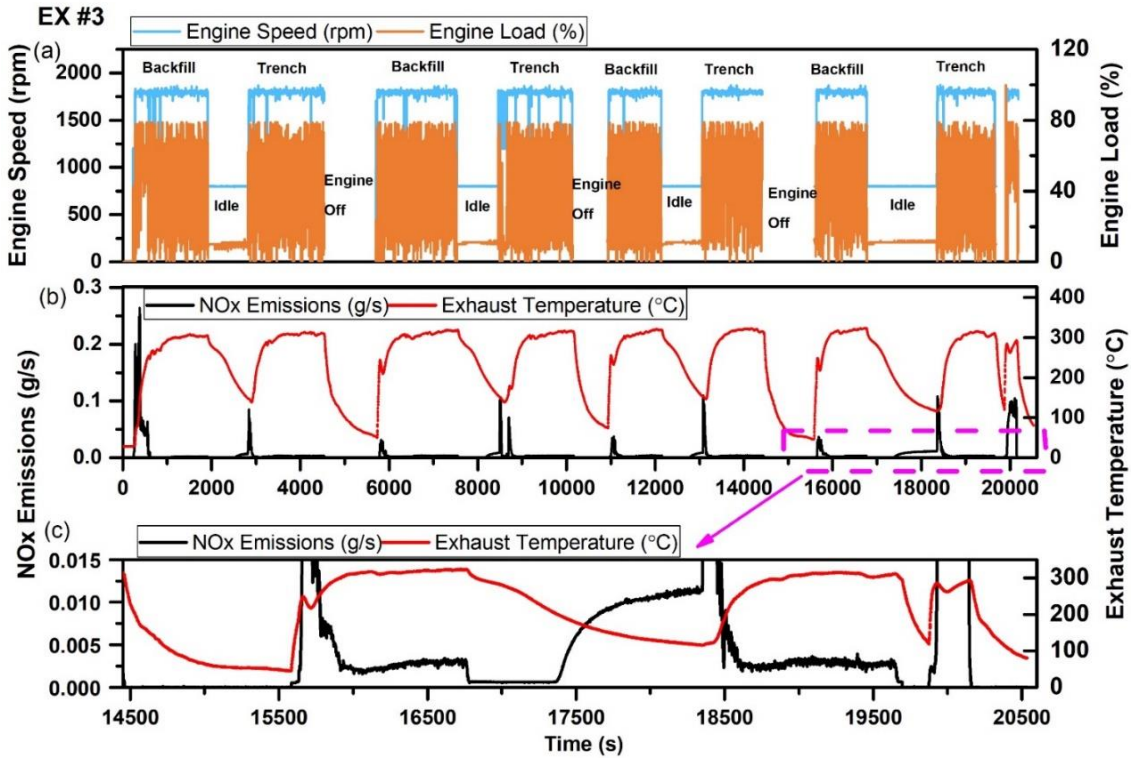

Figure 2.3(a-c) Real-time NOx emissions from Excavator_#3.

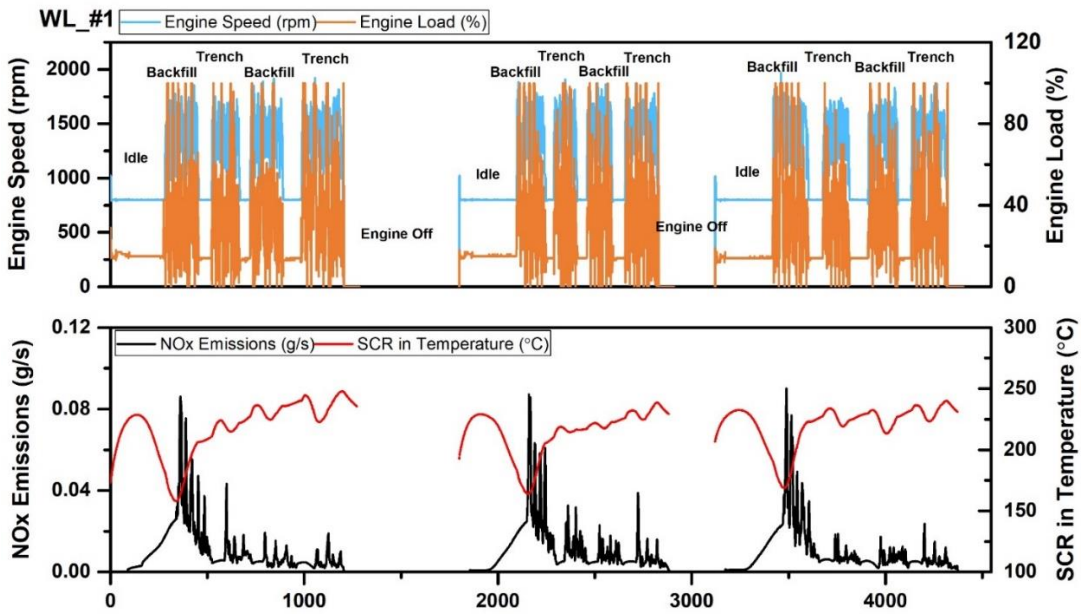

Figure 2.4 Real-time NOx emissions, engine speed and load profile, and exhaust temperature from Wheel Loader_#1.

2.4.3. NOx Emission Comparisons With Prior Studies

Frey et al. and Cao et al. (Cao et al., 2016; Cao et al., 2018; Frey et al., 2008a; Frey et al., 2008b; Frey et al., 2010) both measured emissions from a wide variety of off-road construction equipment. Some of the equipment tested in both studies included backhoes, wheel loaders and excavators. Figure 2.5 shows a comparison between the present study and previous studies by equipment type and work modes performed on each piece of equipment. Ex_#1_D denotes the excavator equipment category, "D" represents a "Digging" work mode, and "B" represents a "Backfilling" work mode. The results, including those from this study, are presented in g/gal units. The other studies focused on emissions measurements from mostly older Tier 2 and Tier 3 equipment. Overall, NOx emissions from older equipment ranged from 73 to 172 g/gal for Tier 2 equipment and from 58 to 96 g/gal for Tier 3 equipment. Under the present test conditions, NOx emissions from Tier 4 final construction equipment showed significant reductions on a g/gal basis,

with a range of 1 to 10 g/gal. Note that WL_#1_B, BH/L_#2_D, and BH/L_#2_B are the only three test articles/modes showing an emissions rate higher than 5 g/gal. Compared to the previous studies, the Tier 4 final equipment showed an average reduction of 91% for NOx emissions. This indicates a significant benefit could be achieved by deploying Tier 4 final advanced technology such as SCR and DPF from an emission reduction perspective.

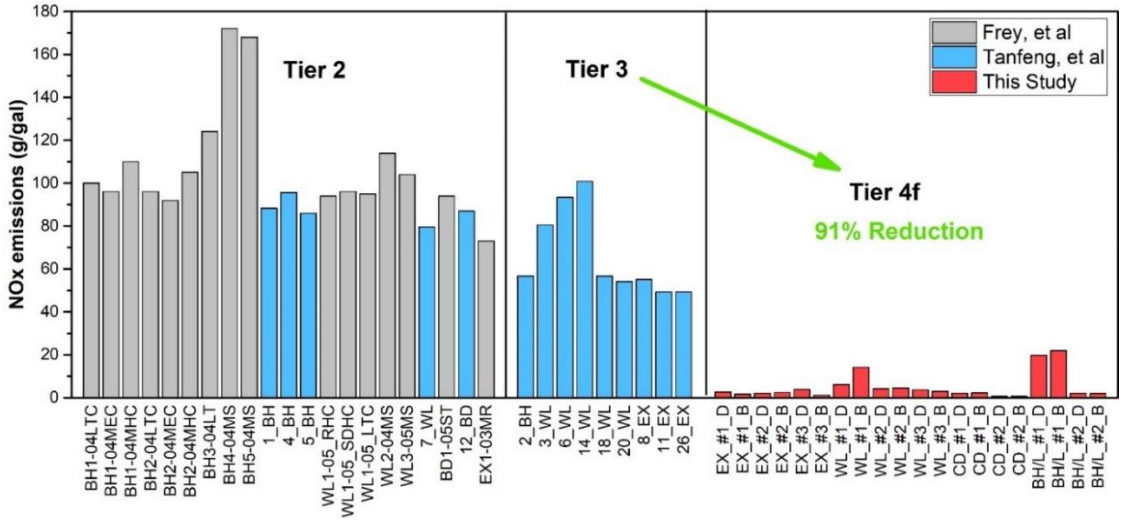

Figure 2.5 NOx emissions rates in units of g/gal.

2.4.4. **PM Emissions**

PM emissions for all the different types of equipment were below the certification standard. PM emissions ranged from 0.1 to 13 mg/bhp-hr, which is below the standard of 20 mg/bhp-hr for Tier 4 final off-road equipment. Detailed PM emissions results are provided in Figure 2.6. It is valuable to emphasize that DPF regeneration events were excluded from the dataset, particularly for WL_#2. On a fuel and time basis, PM emissions showed a range from 0.5 to 49 mg/kg-fuel and 10 to 436 mg/hour. Emissions from different test modes did not show much variance. However, emissions between different equipment categories did show some trends, with the backhoe/loaders being the highest, as both pieces of equipment in backhoe/loader category lacked a DPF to reduce PM emissions. Previous studies have

shown significant (over 90%) reductions in PM emissions for off-road equipment and on-road vehicles equipped with DPFs (Cao et al., 2018; Jiang et al., 2018).

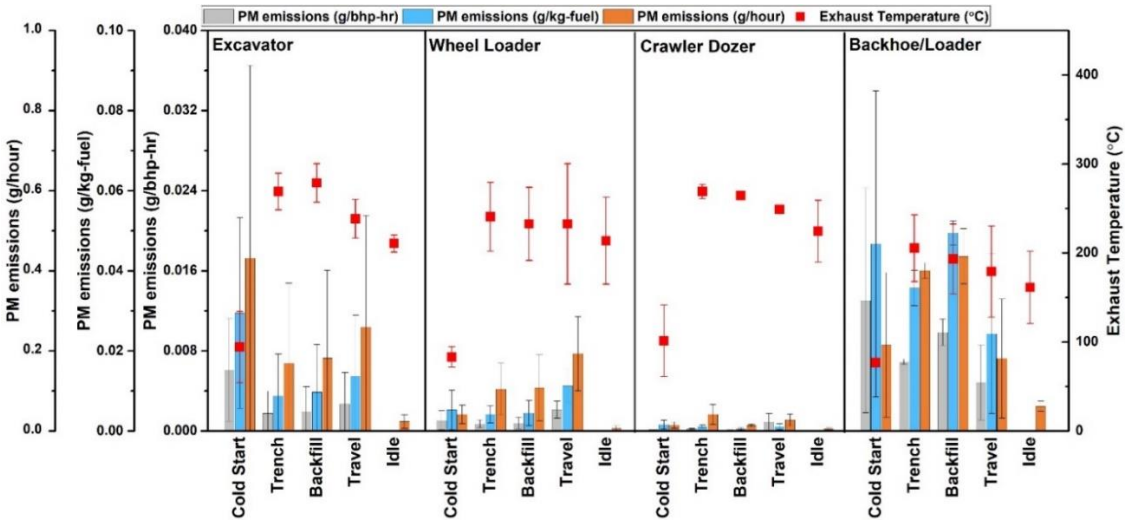

Figure 2.6 Averaged PM emissions profile in units of g/kg-fuel and g/hour and averaged exhaust temperature profile by modes and equipment types.

2.4.5. CO Emissions

CO emissions ranged from 0.11 to 1.90 g/bhp-hr, which was below the standard of 2.5 g/bhp-hr for Tier 4 final off-road equipment. On a fuel and time basis, CO emissions showed a range from 0.65 to 7.65 g/kg-fuel and 7.14 to 139 g/hour. Emissions from different test modes showed some variance with the cold-start being the mode with the highest emissions, ranging from 1.2 to 1.9 g/bhp-hr. Emissions from trench and backfill modes did not show much difference within each category.

2.4.6. Fuel Consumption

Fuel consumption rates for the different equipment types over different modes are presented in Figure 2.7 in units of kg/bhp-hr and kg/hour. Fuel consumption rates were generally consistent between different equipment categories over different modes, with a range around 0.2 kg/bhp-hr, except for the travel mode for the crawler dozer category. Cold-start phase fuel consumption was generally higher than other work modes due to

lower energy conversion efficiencies when the engine is operated under a cold condition. Idle emissions showed a time-based emissions factor ranging from 0.03 to 0.1 kg/hour. Previous studies have shown that by decreasing the ratio of idling to actual machine operation additional fuel use and excess carbon dioxide (CO_2) emissions can effectively be reduced (Lewis et al., 2012a; Lewis et al., 2012b).

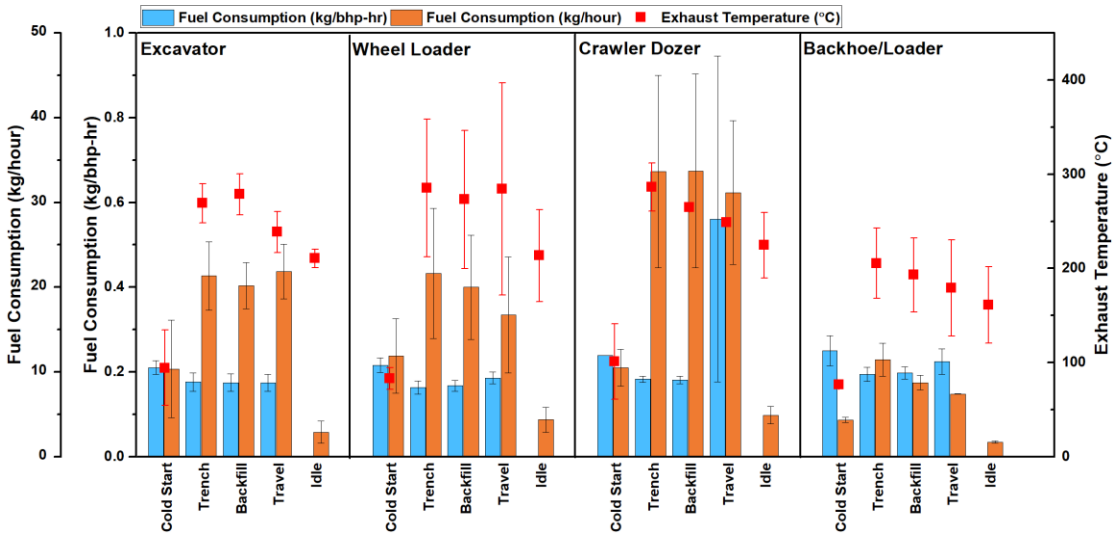

Figure 2.7 Averaged Fuel Consumption profile in units of kg/bhp-hr and kg/hour and averaged exhaust temperature profile by modes and equipment types.

2.4.7. **Comparisons With OFFROAD Model**

The OFFROAD model called "OFFROAD2017 – (ORION v1.0.1)" was developed by the California Air Resource Broad (CARB) as a tool for estimating emissions from off-road equipment. This model is part of the EMission FACtor (EMFAC) model that provides California's emissions inventories of on-road and off-road mobile sources and tools (CARB, 2017). Using the OFFROAD model, emission factors for different types of off-road equipment, from a certain calendar year, or within certain region can be derived in units of tons per day. In addition, the model also provides equipment fuel consumption on

a gallons per year basis and activity on a hours per year basis. Therefore, emission rates and fuel consumption rates on a time basis can be derived.

Figure 2.8 shows NOx emissions and PM emissions on a g/hour basis, and fuel consumption on a gal/hour basis for each piece of equipment that was tested for the work and idle mode operations. The work mode emissions were calculated based on the integrated emissions from all of the trench and backfill modes for each piece of equipment. The equipment tested in this study was categorized based on its engine power bin. The predicted emissions based on the OFFROAD model, which were derived based on equipment type, model year and HP bin, are also shown by the red line in the figure. Note that the OFFROAD model emission rates represent overall emission rates without differentiating between work and idle modes and other types of activity.

NOx emissions for the work modes are comparable to or less than the OFFROAD model prediction for most of the equipment, except for WL_#1, WL_#2 and BH/L_#1. As discussed in a previous section, NOx emissions from these three pieces of equipment were higher because of lower aftertreatment temperatures, and DPF regeneration events. The idle emission rates on a time basis for most of the equipment were comparable to or less than the work mode emissions, with the exception of WL_#1, WL_#2, and CD_#1. Overall, the results suggest that idle emissions could play an important role when designing the model.

PM emissions for the work modes are well below the OFFROAD model prediction for most of the equipment due to high PM emission reductions from the DPF system, except for EX_#3, BH/L_#1 and BH/L_#2. This trend indicates that the model may overestimate PM emissions in categories where DPFs are more prevalent than predicted.

Fuel consumption estimations from the model fall between those for the work and idle modes, being lower than the fuel consumption during work modes and higher than the fuel consumption for the idle modes. This is because the model predicts the emission factors based on real-world activity which consists of both work and idle mode operation.

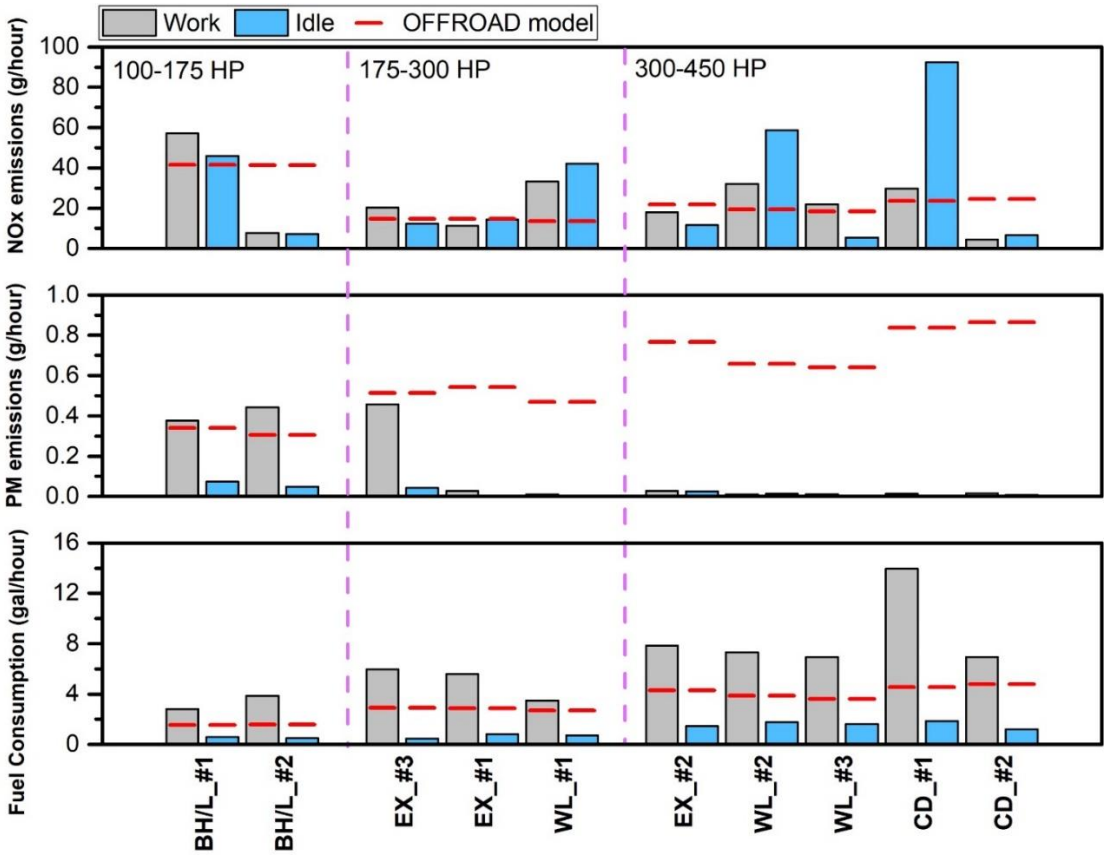

Figure 2.8 Comparison with the OFFROAD model in unit of g/hour

2.5. **Conclusions**

Emission Measurements were made for 10 pieces of Tier 4 final equipment with SCR and DPF aftertreatment systems which included 3 excavators, 3 wheel loaders, 2 backhoe/loaders, and 2 crawler tractors with PEMS. This information will be useful for developing emissions inventory models, understanding the differences between

certification levels and real-world emissions, and in understanding the effectiveness of advanced aftertreatment systems for off-road applications.

The main conclusion in this study can be summarized as follows:

For all types of equipment, the highest NOx emissions were seen for the cold-start phase due to exhaust temperatures being below the activation temperatures for the SCR system. This was followed by the travel mode operation. NOx emissions under idle ranged from 12.8 to 50 g/hour, which in many cases was higher than the NOx emissions for work modes on a time basis.

NOx emissions from all equipment categories for trench and backfill operations showed a range from 0.07 to 0.69 g/bhp-hr, and from 11.4 to 34.2 g/hour. NOx emissions for the trench and backfill modes were generally close to or below the in-use compliance emission rate, except for a few pieces of equipment that had higher NOx emissions due to cooler aftertreatment systems. NOx emissions for the work modes are comparable to the OFFROAD model prediction for most of the equipment. Compared to the previous studies, the Tier 4 final equipment showed an average reduction of 91% for NOx emissions. This indicates a significant benefit could be achieved for NOx emissions by deploying Tier 4 final advanced technology, such as SCR, from an emission reduction perspective.

PM and CO emissions for all the different types of equipment were below the certification standard. PM emissions for Backhoe/Loader are higher than other equipment categories because both pieces of equipment in Backhoe/Loader category lacked a DPF to reduce PM emissions. PM emissions were generally lower than those for the OFFROAD model, suggesting PM emissions might be overestimated in categories where DPFs are more prevalent than predicted.

2.6. **Acknowledgements**

The authors thank the staff of the Bourns College of Engineering-Center for Environmental Research and Technology (CE-CERT), include Mr. Don Pacocha, Mr. Mark Villela, Mr. Daniel Gomez for performing the tests and preparing the equipment for testing. The authors acknowledge Caltrans for funding this study.

2.7. **Reference**

Abolhasani S, Frey HC, Kim K, Rasdorf W, Lewis P, Pang S-h. Real-world in-use activity, fuel use, and emissions for nonroad construction vehicles: a case study for excavators. Journal of the Air & Waste Management Association 2008; 58: 1033-1046.

Bermúdez V, Lujan JM, Pla B, Linares WG. Effects of low pressure exhaust gas recirculation on regulated and unregulated gaseous emissions during NEDC in a light-duty diesel engine. Energy 2011; 36: 5655-5665.

Cao T, Durbin TD, Russell RL, Cocker III DR, Scora G, Maldonado H, et al. Evaluations of in-use emission factors from off-road construction equipment. Atmospheric environment 2016; 147: 234-245.

Cao T, Russell RL, Durbin TD, Cocker III DR, Burnette A, Calavita J, et al. Characterization of the emissions impacts of hybrid excavators with a portable emissions measurement system (PEMS)-based methodology. Science of The Total Environment 2018; 635: 112-119.

California Air Resources Board. "Mobile Source Emissions Inventory and Assessment," Los Angeles. http://www.arb.ca.gov/msei/msei.htm, accessed Sep. 2020

California Air Resource Board. "2017 Off-Road Diesel Emission Factor Update for NOx and PM," https://www.arb.ca.gov/msprog/offroad/cert/cert.php, accessed Oct 2020

California Air Resources Board, "EMFAC2014 Volume III Technical Documentation," https://www.arb.ca.gov/msei/downloads/emfac2014/emfac2014-vol3-technical-documentation-052015.pdf, accessed Sep 2020

California Air Resource Board, "Airborne Toxic Control Measure. Reduction Airborne Toxic Control Measure to Limit Diesel-Fueled Commercial Motor Vehicle Idling, 2004" https://ww2.arb.ca.gov/capp-resource-center/heavy-duty-diesel-vehicle-idling-information, accessed Sep 2020

Desouza C, Marsh D, Beevers S, Molden N, Green D. Real-world emissions from non-road mobile machinery in London. Atmospheric Environment 2020; 223: 117301.

Frey HC, Kim K, Pang S-H, Rasdorf WJ, Lewis P. Characterization of real-world activity, fuel use, and emissions for selected motor graders fueled with petroleum diesel and

B20 biodiesel. Journal of the Air & Waste Management Association 2008a; 58: 1274-1287.

Frey HC, Rasdorf W, Kim K, Pang S-h, Lewis P. Comparison of real-world emissions of B20 biodiesel versus petroleum diesel for selected nonroad vehicles and engine tiers. Transportation research record 2008b; 2058: 33-42.

Frey HC, Rasdorf W, Lewis P. Comprehensive field study of fuel use and emissions of nonroad diesel construction equipment. Transportation Research Record 2010; 2158: 69-76.

Fu M, Ge Y, Tan J, Zeng T, Liang B. Characteristics of typical non-road machinery emissions in China by using portable emission measurement system. Science of the Total Environment 2012; 437: 255-261.

Jiang Y, Yang J, Cocker III D, Karavalakis G, Johnson KC, Durbin TD. Characterizing emission rates of regulated pollutants from model year 2012+ heavy-duty diesel vehicles equipped with DPF and SCR systems. Science of The Total Environment 2018; 619: 765-771.

Khan AS, Clark NN, Gautam M, Wayne WS, Thompson GJ, Lyons DW. Idle emissions from medium heavy-duty diesel and gasoline trucks. Journal of the Air & Waste Management Association 2009; 59: 354-359.

Ko J, Si W, Jin D, Myung C-L, Park S. Effect of active regeneration on time-resolved characteristics of gaseous emissions and size-resolved particle emissions from light-duty diesel engine. Journal of Aerosol Science 2016; 91: 62-77.

Lewis P, Frey HC, Rasdorf W. Development and use of emissions inventories for construction vehicles. Transportation research record 2009a; 2123: 46-53.

Lewis P, Karimi B, Shan Y, Rasdorf W. Comparing the economic, energy, and environmental impacts of biodiesel versus petroleum diesel fuel use in construction equipment. International Journal of Construction Education and Research 2019; 15: 276-290.

Lewis P, Leming M, Frey HC, Rasdorf W. Assessing effects of operational efficiency on pollutant emissions of nonroad diesel construction equipment. Transportation research record 2011; 2233: 11-18.

Lewis P, Leming M, Rasdorf W. Impact of engine idling on fuel use and CO 2 emissions of nonroad diesel construction equipment. Journal of Management in Engineering 2012a; 28: 31-38.

Lewis P, Rasdorf W, Frey HC, Leming M. Effects of engine idling on national ambient air quality standards criteria pollutant emissions from nonroad diesel construction equipment. Transportation research record 2012b; 2270: 67-75.

Lewis P, Rasdorf W, Frey HC, Pang S-H, Kim K. Requirements and incentives for reducing construction vehicle emissions and comparison of nonroad diesel engine emissions data sources. Journal of Construction Engineering and management 2009b; 135: 341-351.

Marshall SK, Rasdorf W, Lewis P, Frey HC. Methodology for estimating emissions inventories for commercial building projects. Journal of Architectural Engineering 2012; 18: 251-260.

McCaffery C, Zhu H, Tang T, Li C, Karavalakis G, Cao S, et al. Real-world NOx emissions from heavy-duty diesel, natural gas, and diesel hybrid electric vehicles of different vocations on California roadways. Science of The Total Environment 2021; 784: 147224.

Mendoza-Villafuerte P, Suarez-Bertoa R, Giechaskiel B, Riccobono F, Bulgheroni C, Astorga C, et al. NOx, NH3, N2O and PN real driving emissions from a Euro VI heavy-duty vehicle. Impact of regulatory on-road test conditions on emissions. Science of The Total Environment 2017; 609: 546-555.

Miller, W., Johnson, K.C., Durbin, T., Dixit, P., “In-use emissions testing and demonstration of retrofit technology for control of on-road heavy-duty engines,” Final Report by University of California, Riverside to the South Coast Air Quality Management District Under Contract No. 11612, Sep 2013.

Misra C, Collins JF, Herner JD, Sax T, Krishnamurthy M, Sobieralski W, et al. In-use NO x emissions from model year 2010 and 2011 heavy-duty diesel engines equipped with aftertreatment devices. Environmental science & technology 2013; 47: 7892-7898.

Rasdorf W, Frey C, Lewis P, Kim K, Pang S-H, Abolhassani S. Field procedures for real-world measurements of emissions from diesel construction vehicles. Journal of Infrastructure Systems 2010; 16: 216-225.

Rasdorf W, Lewis P, Marshall SK, Arocho I, Frey HC. Evaluation of on-site fuel use and emissions over the duration of a commercial building project. Journal of infrastructure systems 2012; 18: 119-129.

Quiros, D.C., Ham, W.A., Ianni, R., Smith, J.D., "Assessing emission control system durability using ARB's pilot heavy-duty truck and bus surveillance program," Presentation at the 27th CRC Real World Emissions Workshop, Long Beach, CA, March, 2017.

Shao Z. Non-road emission inventory model methodology. The international council on clean transportation (Working paper) 2016; 4.

Tan D, Tan J, Peng D, Fu M, Zhang H, Yin H, et al. Study on real-world power-based emission factors from typical construction machinery. Science of The Total Environment 2021; 799: 149436.

U.S. Environmental Protection Agency, "2017 National Emissions Inventory Report," https://gispub.epa.gov/neireport/2017/, accessed Sep 2020

U.S. Environmental Protection Agency, "NONROAD2008 Model," https://www.epa.gov/moves/nonroad-technical-reports#2008a, accessed Sep. 2020

2.8. **Appendix**

Table 2.3 Equipment and Engine Specifications

Equipment Type	Equipment Model #		Engine Serial No.	Eng Model Year	Displ Liters	Rated Power (bhp)	Rated Speed (RPM)	HP Category	Odometer Reading (Hours)	Engine Model
Excavator_#1	Caterpillar	335F	D8T05549	2015	7.0	204	1800	175-300	2063	C7.1 ACERT
Excavator_#2	Caterpillar	336FL	SYE13070	2016	9.3	318	1600	300-450	1615	4045HT096
Excavator_#3	Hitachi	210 GLC	4HK1XDRAB-01	2017	5.2	172	2000	100-175	350	6135HT003
Wheel Loader_#1	Caterpillar	930M	D8T05679	2015	7.0	188	1800	175-300	2057	AR-4HK1X
Wheel Loader_#2	John Deere	744KII	RG6090U042695	2017	9.0	365	2100	300-450	359	6135HDW11
Wheel Loader_#3	John Deere	824KII	RG6135U002202	2014	13.5	397	2000	300-450	97	C15.2 ACERT
Crawler Dozer_#1	John Deere	1050K	RG6135U002084	2014	13.5	397	2000	300-450	1996	C9.3 ACERT
Crawler Dozer_#2	Caterpillar	D8T	ENG01073	2015	15.2	357	1700	300-450	3654	6090HDW36
Backhoe/Loader_#1	Caterpillar	430F2	W7N05800	2015	4.4	115	2200	100-175	1601	C7.1 ACERT
Backhoe/Loader_#2	John Deere	310SL	PE4045U049562	2017	4.5	126	2200	100-175	695	C4.4 ACERT

Table 2.4 Engine Certifications and Aftertreatment Devices

Equipment Type	Engine Certification g/bhp-hr				Aftertreatment Device
	NMHC	NOx	CO	PM	
Excavator_#1	0.007	0.19	0.969	0.001	CTOX-DPF-PASSIVE, SCR
Excavator_#2	0.015	0.25	0.075	0.015	PTOX-DPF-Active, SCR
Excavator_#3	0.022	0.04	0.022	0.002	DPF, SCR
Wheel Loader_#1	0.015	0.22	0.149	0.015	CTOX-DPF-PASSIVE, SCR
Wheel Loader_#2	0.022	0.04	0.022	0.002	PTOX-DPF-Active, SCR
Wheel Loader_#3	0.045	0.08	0.075	0.007	PTOX-DPF-Active, SCR
Crawler Dozer_#1	0.015	0.09	0.075	0.007	PTOX-DPF-Active, SCR

3. Characterizing Emission Rates of Regulated and Unregulated Pollutants From Two Ultra-Low NOx CNG Heavy-Duty Vehicles

3.1. Abstract

In this study, a goods movement vehicle equipped with the ISX12N 400 near-zero natural gas engine and a yard tractor equipped with the B6.7N 240 near-zero natural engine were evaluated over different test cycles on a heavy-duty chassis dynamometer. Both heavy-duty vehicles were operated stoichiometrically and equipped with a three-way catalyst (TWC). Experiments emphasized nitrogen oxide (NOx) emissions, greenhouse gases (GHGs), and particulate emissions. Results showed substantially low levels of NOx emissions of both vehicles and dramatic reductions of up to 90% compared to the 2010 certification standard. The cold-start period did not influence the overall NOx emissions, suggesting that real-world NOx formation during cold-start will not contribute to ground level ozone considering the vocations of these vehicles. Carbon monoxide (CO) emissions were found at relatively high levels. Solid particle number emissions from both vehicles were seen to be above the European particle number limit, indicating that current natural gas engines could be an important source of nanoparticles, especially those of the sub 23 nm range. Both vehicles demonstrated elevated methane (CH_4) and ammonia (NH_3) emissions. Nitrous oxide (N_2O) and NH_3 emissions were largely dependent of the cold-start fraction of the test cycles, showing greater emission concentrations compared to the hot-start tests.

Keywords: CNG vehicles; Ultra-low NOx emissions; On-road Vehicles; Cold start emissions; PN emissions

3.2. **Introduction**

Heavy-duty on-road vehicles represent one of the largest sources of nitrogen oxide (NOx) emissions and fuel consumption in North America (Frey, 2018; Herner et al., 2009). Heavy-duty vehicles are predominantly diesel-powered, although there is increasing interest in natural gas (NG) systems. As emissions and greenhouse gas (GHG) regulations continue to tighten, new opportunities for advanced fleet specific heavy-duty vehicles are becoming available with improved fuel economy. NOx emissions have dropped 90% for heavy-duty vehicles with the recent 2010 certification limit of 0.20 g/bhp-hr; however, additional NOx reductions of another 90% are desired for the South Coast Air basin (representing the greater Los Angeles area) to meet its 2023 and 2031 NOx inventory requirements. An ultra-low NOx standard was adopted by the California Air Recourses Board (CARB) that was primarily driven by the National Ambient Air Quality Standard requirements for ambient ozone that many urban areas in California currently do not meet without further NOx reductions from the heavy-duty diesel vehicle fleet. NOx emissions are key precursors to ozone (O_3) formation in the troposphere that is formed via the photolysis of nitrogen dioxide (NO_2) involving various reactive hydrocarbons (Monks et al., 2015).

Although the 2010 certification standards were designed to reduce NOx emissions, the in-use NOx emissions are actually much higher than certification standards for certain fleets (Monks et al., 2015; Quiros et al., 2016; Thiruvengadam et al., 2015). The magnitude is largely dependent on the duty cycle (Dixit et al., 2017). Since engines are certified at

moderate to high engine loads, low load duty cycles can show different emission rates (Misra et al., 2017). For diesel engines, low load duty cycles have a significant impact on NOx emissions. Cold-start emissions can be several times higher than the certification standard, and much higher than the corresponding hot-start emissions (Herner et al., 2009; Velders et al., 2011). The main cause for the high NOx emissions is low selective catalytic reduction (SCR) inlet temperatures resulting from low power operation (Bishop et al., 2013; Misra et al., 2013; Thiruvengadam et al., 2016). Stoichiometric natural gas engines equipped with three-way catalysts (TWCs) are not subjected to the limitations posed by the use of SCR systems, resulting in in-use emissions that are more comparable to the emission certification levels. Previous studies have shown NOx emissions benefits with heavy-duty CNG vehicles equipped with TWCs (Misra et al., 2017; Thiruvengadam et al., 2015).

New engine designs and alternative fuels are expected to play a major role in controlling NOx emissions and subsequently improving air quality. Several studies have shown the pathway for ultra-low NOx emissions from stoichiometric compressed natural gas (CNG) engines, capable of achieving sub 0.02 g/bhp-hr of NOx emissions(Sharp et al., 2017a; Sharp et al., 2017b). The use of natural gas has significantly increased in many fleets, such as refuse trucks, buses, delivery trucks, and yard tractors commonly used in on-terminal container movement (Fontaras et al., 2012; Karavalakis et al., 2013; Thiruvengadam et al., 2016). Natural gas is a clean-burning alternative fuel known for its soot-free combustion due to its lower carbon fraction compared to any other fossil fuel (Hesterberg et al., 2008; Korakianitis et al., 2011). Natural gas has a high octane number (up to 130) and relatively higher knock resistance compared to gasoline, which enables the

use of higher compression ratio engines that provide better efficiency (Korakianitis et al., 2011; Thiruvengadam et al., 2018). Legacy natural gas engines were built on a diesel engine block retrofitted with a spark ignition platform and operated with lean-burn combustion and an oxidation catalyst that served to control carbon monoxide (CO) and nonmethane hydrocarbon (NMHC) emissions. Legacy lean-burn natural gas engines produced comparable levels of NOx emissions to diesel vehicles without SCR systems (Korakianitis et al., 2011). Current natural engines operate with spark ignited stoichiometric combustion with exhaust gas recirculation (EGR) and three-way catalysts (TWCs) to control NOx, CO, and total hydrocarbon (THC) emissions. The simultaneous reductions in CO and NOx emissions in the TWC are favored from oxygen deficient exhaust conditions occurring during stoichiometric combustion (DeFoort et al., 2004). Studies have shown important reductions in NOx and THC emissions with stoichiometric natural gas engines compared to lean burn engines (Einewall et al., 2005; Hajbabaei et al., 2013; Yoon et al., 2013). Both Hajbabaei et al. and Yoon et al. showed that NOx emissions from stoichiometric natural gas engines equipped with a TWC were over 90% lower compared to lean-burn natural gas engines but showed higher CO emissions. Other studies have also shown that stoichiometric combustion is the most effective technology in reducing gaseous toxic pollutants, such as aldehydes and polycyclic aromatic hydrocarbons (Yoon et al., 2014). Recent investigations have reported dramatic NOx reductions with ultra-low NOx heavy-duty vehicles, even well below the 0.02 g/bhp-hr standard (Li et al., 2019).

The goal of this study is to evaluate and characterize two near-zero NOx stoichiometric ultra-low natural gas engines in different vocations. This demonstration of

this engine technology was done in a goods movement vehicle and a yard tractor. Both vocations represent a major source of NOx emissions and other pollutants within the heavy-duty vehicle population. Both types of vehicles operate in or closely adjacent to densely populated areas in the South Coast Air basin and in the port of Los Angeles and Long Beach complex, which is also the biggest container terminal in the United States (US). Increased port activity and maritime transportation related emissions have led to the necessity of reducing emissions from major emission sources such as cargo handling equipment (i.e., yard tractors). While about 95% of the port's yard tractors are diesel-powered, there is an increased interest in introducing near-zero NOx CNG platforms at marine and inland cargo handling terminals. In this study, we aim to characterize the relationship between NOx emissions and other pollutants from ultra-low NOx CNG engines when operated on different vocation cycles using a chassis dynamometer.

3.3. **Materials and Methods**

3.3.1. **Test Vehicles**

Two heavy-duty in-use vehicles equipped with different natural gas engines were tested in this study, as shown in Table 3.2, Supplementary Material (SM). The first test article was an ISX12N 400 Cummins Westport Inc. (CWI) 11.9-liter natural gas engine installed in a class 8 truck. The engine was developed to meet CARB's optional ultra-low NOx standard of 0.02 g/bhp-hr. The vehicle equipped with the ISX12N 400 engine was primarily a goods movement vehicle operated in the freight corridors of the South Coast Air Basin. The second test article was a B6.7N CWI 6.7-liter natural gas near zero (NZ) engine installed in a yard tractor. The engine was developed as a near zero low NOx engine with a NOx standard of 0.1 g/bhp-hr (50% below the 2010 NOx emissions standard). This

vehicle was a yard tractor equipped with a non-road short distance (<5 miles) goods movement engine with a limited top speed (governed to less than 30 mph) and typically found in transient fleet yard operation. Both vehicles were operated with compressed natural gas (CNG) pipeline fuel, which represents typical natural gas available in Southern California.

3.3.2. **Test Cycles**

Different test cycles were utilized for both vehicles in this study, as shown in Table 3.3. Some cycles were very short (less than 30 minutes), so a combined test cycle with two or three back to back iterations of the cycle was utilized in order to capture enough particulate matter (PM) mass to quantify emissions near 1 mg/bhp-hr (10 mg/mile).

The test vehicle that utilized the ISX12N NG engine was tested following the three Drayage Truck Port (DTP) cycles (Near Dock, Local, and Regional), the Urban Dynamometer Driving Schedule (UDDS), and the Heavy-Heavy Duty Diesel Truck (HHDDT) transient test cycles. These cycles are representative of Southern California driving vocations, especially typical for goods movement vehicles. The DTP cycles were developed by TIAX LLC in conjunction with the Ports of Long Beach and Los Angeles. The DTP cycles are classified based on whether the cargo is being moved around in the port terminal or distributed to local or regional distribution centers. The HHDDT cycles were developed by the California Air Recourses Board (CARB) and West Virginia University. The HHDDT cycles are representative of truck activity in Southern California and include three modes, named Creep, Transient, and Cruise.

The test vehicle equipped with a B6.7N NG engine was tested over several different cycles, including two yard tractor (YT) transient cycles representative of heavy loads

(YT1_H) and light loads (YT2), and the central business district (CBD) cycle. The YT1_H cycle was performed at 100% of the gross vehicle weight (GVW) and the light cycle YT_L was performed at both full 100% GVW and 50% GVW (YT2_H and YT2_L). The YT1_H cycle was performed as a cold-start and hot-start test. Because the YT cycles are short (less than 30 minutes), the hot-start YT transient cycles were repeated twice, while the cold-start YT was performed as a single cycle. The CBD cycle was developed to represent typical transit bus operation in a downtown business district and was performed in triplicate. Although the test vehicle was a yard tractor of typical port cargo handling operation, the 6.7-liter engine can also be used for transit bus operations, so the CBD cycle was also included. The bus cycle was performed at 80% of the GVW to represent a typical load on a bus in the South Coast Air Basin.

3.3.3. Emissions Measurements and Analysis

All testing was performed at CE-CERT's Heavy-Duty Chassis Dynamometer facility, consisting of an electric AC type design chassis dynamometer that can simulate inertia loads from 10,000 lb to 80,000 lb, which covers a broad range of in-use medium and heavy-duty vehicles. The vehicles were tested on the chassis dynamometer with a test weight of 65,000 lbs. Emissions measurements were obtained using CE-CERT's Mobile Emissions Laboratory (MEL). Detailed information of the facility and sampling setup have been discussed previously (Cocker et al., 2004). Basic emissions measurements included THC, NOx, CO, NMHC, methane (CH_4), carbon dioxide (CO_2), and PM mass. Measurements of NH_3 and nitrous oxide (N_2O) emissions were also obtained with a Horiba Quantum Cascade Laser (QCL) Spectroscopy.

The gravimetric PM mass was measured with the CVS and collected on 47 mm diameter 2 μm pore Teflo filters (Whatman brand). The filters were measured for net gains using a UMX2 ultra precision microbalance with buoyancy correction in accordance with the weighing procedure guidelines set forth in the Code of Federal Regulations (CFR). Real-time soot mass or black carbon emissions were measured using an AVL Micro-Soot Sensor (MSS). The MSS is an instrument that measures soot mass concentration at a frequency of one Hertz basis using a photo acoustic detection technique, where the light-absorbing PM components (such as soot particles) are exposed to laser light that is periodically modulated at the acoustical resonant frequency. Sampling for black carbon emissions was made in the raw exhaust (before the CVS). Real-time particle size distributions were obtained using an Engine Exhaust Particle Sizer (EEPS) spectrometer. The EEPS (TSI 3090, firmware version 8.0.0) was used to obtain real-time second-by-second size distributions between 5.6 to 560 nm. Particles were sampled at a flow rate of 10 L/min, which is considered to be high enough to minimize diffusional losses. They were then charged with a corona charger and sized based on their electrical mobility in an electrical field. Concentrations were determined through the use of multiple electrometers.

For the ISX12N NG engine, total particle number emissions were measured using a TSI 3776 ultrafine-Condensation Particle Counter (CPC) with a 2.5 nm cut point. The instrument operated at a flowrate of 1.5 L/min. Solid particle number emissions were measured with a catalytic stripper with a downstream a TSI 3776 ultrafine-CPC. The catalytic stripper removed the volatile components by oxidation on a catalytic coated substrate. For the B6.7N NG engine, total particle number were measured at the CVS using a TSI 3776 ultrafine-CPC. Solid particle number emissions were measured according to

the European Particle Measurement Programme (PMP) at the raw exhaust (before the CVS) using the AVL Particle Counter (APC plus) with a cut-off particle diameter of 23 nm (APC_23nm). For particles below the 23 nm diameter, a TSI 3776 ultrafine-CPC with a cut-off diameter of 2.5 nm was used downstream of the APC plus (APC_3).

3.4. **Results**

3.4.1. **NOx Emissions**

The NOx emissions of both vehicles over the different duty cycles are presented in Figure 3.1. For both vehicles, the results show that NOx emissions were below or close to the CARB optional low NOx standard of 0.02 g/bhp-hr for the all the hot-start tests and below the in-use not-to-exceed (NTE) zone standard of 0.03 g/bhp-hr. The latter is a defined boundary used to monitor emissions compliance under real-world conditions. For the 12L goods movement vehicle, NOx emissions ranged from 0.012 to 0.006 g/bhp-hr for the port activity cycles and from 0.001 to 0.02 g/bhp-hr for the HHDDT transient cycles. The lower NOx emissions were found even for the HHDDT Creep cycle, which represents very low speed operation. The HHDDT transient mode showed NOx emissions slightly above the optional low NOx standard due to some relatively high NOx episodes during truck start and stop events at moderate speed. For the drayage port cycles, the higher NOx emissions were seen during the regional mode, which represents truck operation at distances greater than 20 miles from the ports, indicating higher NOx emissions exposures to populated areas including regional roads, driving in traffic, and short travel in freeways. Overall, stoichiometric combustion offers high exhaust temperatures even for the low load driving conditions which resulted in high NOx conversions in the fully warmed-up TWC. This is not a typical observation with SCR equipped diesel trucks where NOx emissions

can be significantly higher compared to stoichiometric natural gas vehicles when operated in low load conditions with the SCR system being inactivated (Quiros et al., 2016; Thiruvengadam et al., 2015). The cold-start NOx emissions were statistically significantly higher than the hot-start tests. During cold-start, the NOx emission conversion efficiency is expected to be lower due to the TWC being below its light-off temperature.

For the 6.7L yard tractor, the hot-start NOx emissions were also below the CARB optional NOx standard, ranging from 0.017 to 0.003 g/bhp-hr. The highest NOx emissions were seen for the CBD cycle and were likely due to high NOx spikes produced during accelerations from idle resulting in imperfect air-fuel ratio control and occasional lean combustion(Grigoratos et al., 2016; Pelkmans et al., 2001). The high engine load operation for the yard tractor cycles (YT2_H vs YT2_L) also appeared to have an impact on NOx emissions, with higher engine loading resulting in more NOx. It is therefore expected that when this equipment is handling cargo and operating at low speeds at the marine terminal it will produce higher NOx emissions compared to low load operation. Similar to the 12L engine, the cold-start NOx emissions for the 6.7L engine showed strong, statistically significant increases compared to the hot-start tests.

The hot-start real-time transient NOx accumulated mass emissions for the 12L goods movement vehicle over the two repeated UDDS cycles and for the 6.7L yard tractor over the two repeated YT1_H cycles are shown in Figure 3.2, respectively. For the 12L goods movement vehicle, all the spikes occurred at similar times and during de-accelerations within the test cycle, suggesting that NOx emissions were essentially zero (less than 0.0007 g/bhp-hr) except during sharp de-accelerations. For the 6.7L yard tractor, all the spikes occurred at different times within the test cycle during hard accelerations

from idle conditions. Results indicate that the variability in the measurements was not due to instrument accuracy, but due to variability in the test article, suggesting that NOx emissions were essentially zero except for the acceleration events. Figure 3.3 shows the accumulated NOx emissions during cold-start operation for both vehicles. Cold-start NOx emissions represented a significant part of the total emissions due to the inactive TWC, but as the engine warmed up NOx emissions dropped and remained constant. For 12L goods movement vehicle, approximately 90% of the NOx emissions occurred in the first 100 seconds of the UDDS cycle, whereas for the 6.7L yard tractor about 90% of the NOx emissions occurred in the first 59 seconds. Given that the cold-start period lasted on average 60 to 100 seconds out of 1060 seconds (total cycle length) for the UDDS and 1200 seconds for the YT1_H cycles, the real weighted in-use cold-start emissions for a 4-hr shift for these vehicles would be 0.4% and 0.7% for the goods movement vehicle and yard tractor, respectively. This finding suggests a very small contribution of cold-start to the total in-use NOx emissions for each vocation, despite the high emissions on a per bhp-hr basis.

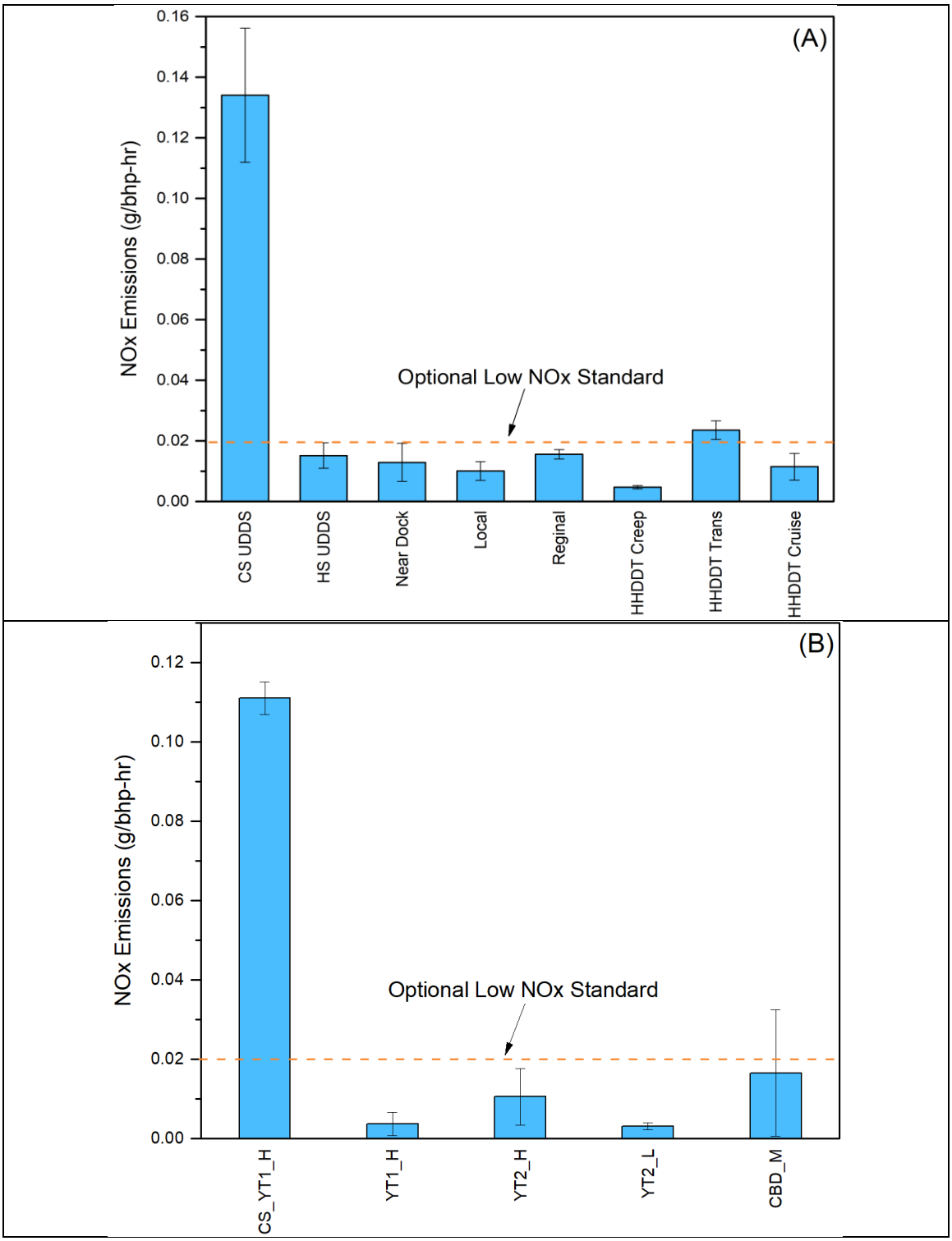

Figure 3.1(a-b) NOx emissions for the 12L goods movement vehicle (top panel) and the 6.7L yard tractor (bottom panel) over different test cycles

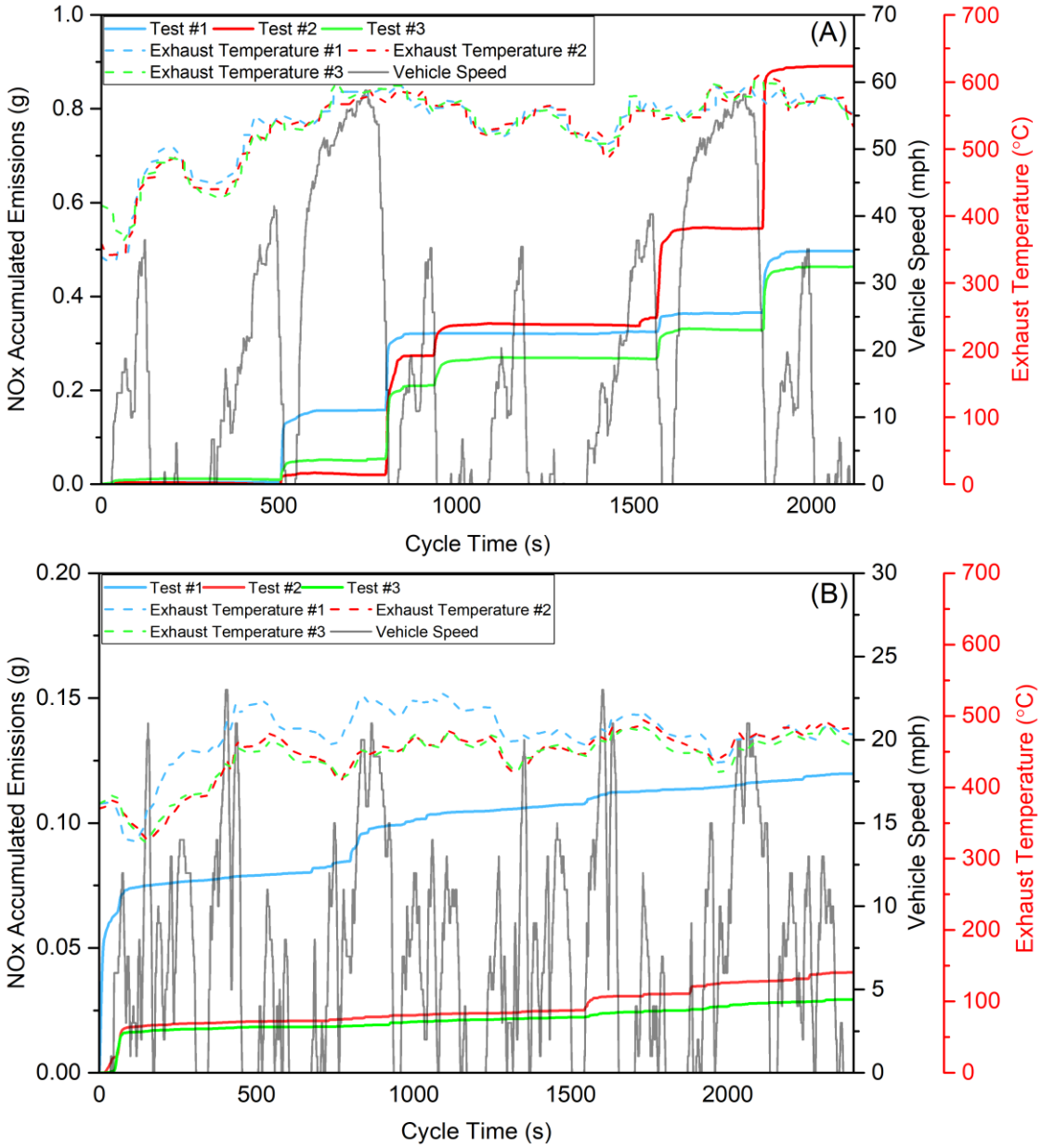

Figure 3.2(a-b) Real-time NOx emissions for the 12L goods movement over duplicate hot-start UDDS (top panel) and for the 6.7L yard tractor over duplicate hot-start YT1_H (bottom panel)

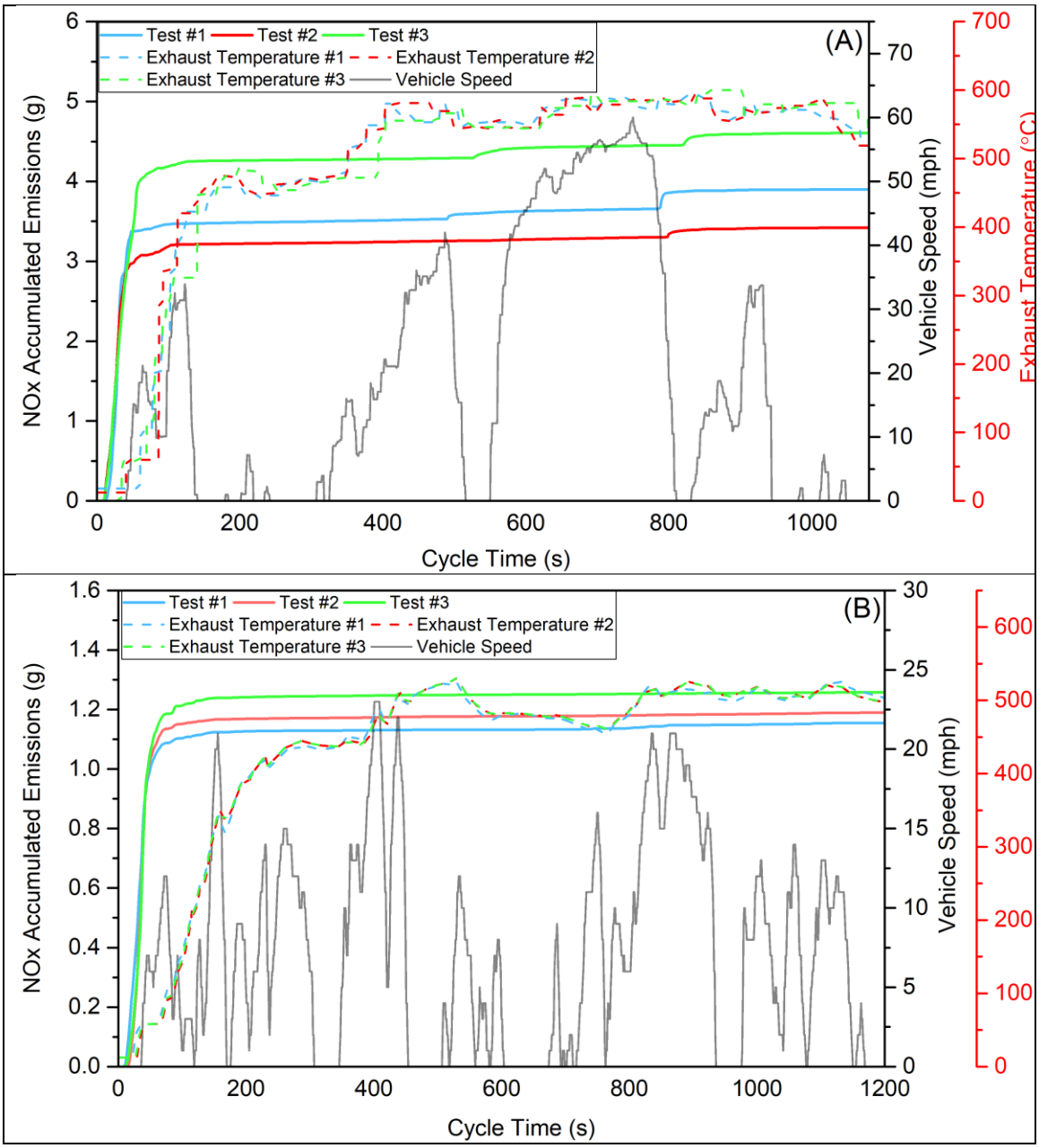

Figure 3.3(a-b) Real-time NOx emissions for the 12L goods movement over a single cold-start UDDS (top panel) and for the 6.7L yard tractor over a single cold-start YT1_H (bottom panel)

3.4.2. **PM Mass, Particle Number Emissions, and Particle Size Distribution**

Figure 3.4 shows the PM mass emissions for the 12L goods movement vehicle and the 6.7L yard tractor. The total PM mass emissions from the 12L goods movement vehicle

shows that PM mass ranged from 1 mg/bhp-hr (CS_UDDS) to 4 mg/bhp-hr (Regional), whereas that from 6.7L yard tractor ranged from 0.9 mg/bhp-hr (CBD_M) to 5.3 mg/bhp-hr (YT2_H). For the 12L goods movement vehicle, PM mass emissions levels were found to be very low including those for the cold-start tests, being 80% below the certification standard (0.01 g/bhp-hr). For the 12L goods movement vehicle, the highest PM mass emissions were found for the cold-start UDDS and the HHDDT creep mode. The latter can be explained because the work (denominator) for the creep cycle was small. The higher PM emissions during the cold-start cycle could be due to the enrichment of the air-fuel ratio, which leads to incomplete combustion combined with the lower efficiency of the TWC (Giechaskiel, 2018). For the 6.7L yard tractor, the PM mass emissions for all test cycles were 80% to 50% below the 2010 certification standard (10 mg/bhp-hr). PM mass emissions formation appeared to be independent of the test conditions (i.e., cold-start vs hot-start), but dependent on engine loading conditions, with the higher load cycle producing more PM emissions than the low load cycle. In general, PM emissions from CNG engines are expected to be very low, but not necessarily lower than those from heavy-duty diesel vehicles equipped with diesel particulate filters (DPFs) (Giechaskiel, 2018). Findings from this study are in agreement with previous studies that have shown low PM mass emissions from stoichiometric CNG vehicles (Hajbabaei et al., 2013; Karavalakis et al., 2016; Li et al., 2019). Fuel contribution to PM formation is considered to be minimal due to the fact that natural gas primarily consists of methane, which is the simplest, lowest molecular-weight hydrocarbon, with no carbon-carbon molecular bonds, which lowers the probability of benzene ring formation (McTaggart-Cowan et al., 2006; Wang et al., 1997). The source of PM emissions from CNG engines could likely be explained by the entrance

of lubrication oil into the combustion chamber, resulting in metallic ash particles (Feist et al., 2010; Khalek et al., 2018; Thiruvengadam et al., 2014).

Figure 3.5 shows the total and solid particle number emissions for both vehicles over the different duty cycles. Results from 12L goods movement vehicle show that the total particle number emissions were highest (2E14 #/mile) for the Creep cycle and lowest on the Regional and Cruise cycles (8E12 #/mile). For the Drayage Truck Port cycles, the percent of solid particles >23 nm in diameter was highest for the Near Dock and lowest for the regional cycle (71% vs 52%) suggesting that as the duty cycle increases in load, the fraction of solid particles decreases. The opposite trend was observed for the CARB HHDDT cycles. The cold-start UDDS showed higher total and solid particle number emissions than the hot-start UDDS, which can be attributed to the lubrication oil entering into the combustion chamber and favoring the formation of particles. A recent study by Khalek et al. also reported elevated solid particle number emissions from a stoichiometric natural gas engine and suggested they originated from the lubrication oil as well as engine wear (Khalek et al., 2018).

Results from the 6.7L yard tractor show that the CVS-based total particle number transient measurements (TPN_3) were highest (4.3E13 #/mi) for the cold-start YT1_H cycle and lowest (1.2E13 #/mi) for the CBD_M cycle. However, solid particle number emissions were not found to be higher for the cold-start YT1_H compared to the hot-start YT1_H. This finding could be quite common for diesel engines equipped with SCR systems downstream of the DPFs, attributing the higher hot-start particle number to the additional formation of nitrates and sulfates (Amanatidis et al., 2014). Under the present test conditions, no precise explanation can be offered at this time. It is worth noted that

solid particle number emissions sized between 2-23 nm were significantly higher during the first 400 seconds of the cold-start YT1_H cycle compared to those above 23 nm (Figure 3.10). This finding suggests that smaller diameter solid particles are formed when the engine and TWC are cold due to the increased penetration of lubrication oil. The solid particle number emissions (>23 nm) exceeded the Euro 6 standard by a factor of 32 to 2 with an average of 9 times higher for all the tests. Solid particle number emissions between 3-23 nm (calculated from SPN_3 and SPN_23) were found in substantially higher concentrations compared to solid particle number >23 nm for all cycles except for the YT1_H cycle and showed 15 times higher average particle number emissions than the Euro 6 standard.

Average real-time particle size distributions for the 12L goods movement vehicle are illustrated in Figure 3.6 (a-h). The cold-start UDDS showed the highest population of nucleation mode particles at around 5-20 nm in diameter compared to the other cycles. The bulk of the nucleation mode particles occurred during the wake of the main acceleration event of the cycle. The cold-start period of the cycle (first 50 seconds) favored the formation of both nucleation and accumulation mode particles, peaking at 10-15 nm and 50-80 nm, respectively. The hot-start UDDS (duplicate) showed an order of magnitude lower particle number concentrations, as a result of the engine warmup and warmer exhaust surfaces, and the more efficient operation of the TWC, which contributed to the removal of semi-volatile gas-phase compounds promoting evaporation of nucleation mode particles. The majority of the particle peaks were observed during acceleration events in the 20-80 nm in diameter. The Near Dock cycle showed higher concentrations of accumulation mode particles at 60-70 nm compared to nucleation mode particles in the 5-

10 nm range. Similarly, the Local cycle showed higher populations of accumulation mode particles at 60-80 nm during the hard acceleration hills of the test cycle, but also a clear bimodal distribution with nucleation mode particles at 10 nm or below to be formed during the entire cycle. The Regional cycle, on the other hand, showed a strong population of accumulation mode particles at about 70 nm during deceleration, as well as presence of smaller particles in the 10 nm or below range. According to Tonegawa et al., deceleration events favor the infusion of lubrication oil into the combustion chamber, resulting in higher particle emissions (Tonegawa et al., 2006). The HHDDT Creep mode showed elevated accumulation mode particles at about 60 nm in diameter during the deceleration of the first and third climbing hill of the test cycle, as well as lower concentrations of particles below 10 nm. Particle concentrations decreased considerably in between the first and third climbing hills of the cycle, with the nucleation mode being practically non-existence and likely removed by coagulation. For the HHDDT Transient mode, the formation of particles coincided with acceleration events. The particle peaks were largely centered in the accumulation mode at about 50-60 nm in diameter. The HHDDT Cruise mode showed slightly lower concentrations of accumulation mode particles than the other CARB HHDDT cycles. The major spikes of accumulation mode particles at 60 nm occurred during the first and second deceleration events after a relatively steady-state engine operation. Thiruvengadam et al. also reported similar findings and also highlighted that during steady-state operation lubrication oil is inhibited in entering the combustion chamber due to the better sealing of the piston rings and valves. Our results over the HHDDT Cruise mode confirm this hypothesis and also the fact that particle formation from lubrication oil is favored during deceleration.

For the 6.7L yard tractor, particle size concentrations were found to be in lower levels than the 12L goods movement vehicle, as shown in Figure 3.7(a-e). Particle size distributions were largely bimodal for all test cycles, with the nucleation mode particles dominating the particle size distribution. Overall, higher particle populations were seen for the hot-start YT2_H and YT2_L cycles and the cold-start YT1_H compared to the hot-start YT1_H and CBD. The cold-start YT1_H clearly demonstrated higher particle number concentrations compared to the hot-start YT1_H (duplicate), with the dominating nucleation mode peaking at about 5-20 nm in diameter. It is evident that YT2_H cycle produced higher particle concentrations in both the nucleation and accumulation modes compared to YT2_L, indicating that engine load conditions will significantly affect the concentrations and sizing of particle emissions. For the YT2_H cycle, nucleation mode particles at about 10 nm dominated the particle size profile, with some accumulation mode particles at 60-70 nm occurring during acceleration events. For the YT2_L cycle, the nucleation mode particles below 10 nm clearly dominated the particle size distribution, with their concentrations being higher than those of the accumulation mode particles. The CBD cycle showed small concentrations of particles, mainly in the 10-15 nm size range.

Results reported here for both vehicles agree with previous studies that showed elevated particle concentrations during heavy acceleration events, especially in the nucleation mode regime (Amirante et al., 2015; Jayaratne et al., 2012; Tonegawa et al., 2006). Higher particle concentrations during accelerations are generally favored from the vaporization and combustion of the lubrication oil on the surface, the exhaust, and the cylinder. Overall, the predominance of nucleation mode particles during accelerations was likely a result of the in-cylinder combustion of the lubricant oil additives (originated from the metal additive

package) that underwent volatilization and consequently re-nucleation forming nanoparticles (Abdul-Khalek et al., 1998). Hallquist et al. suggested that the enhanced nucleation mode for natural gas engines could likely be a result of the lack of larger (soot) particles in the exhaust that will cause a decrease in the available surface area, favoring nucleation over adsorption/condensation of supersaturated vapors (Hallquist et al., 2013). Previous studies using stoichiometric natural gas engines also found nucleation mode particles centered between 10-15 nm that were dominating the particle size distribution and had their origin to lubrication oil ash (Hallquist et al., 2013; Jayaratne et al., 2012; Thiruvengadam et al., 2014; Tonegawa et al., 2006).

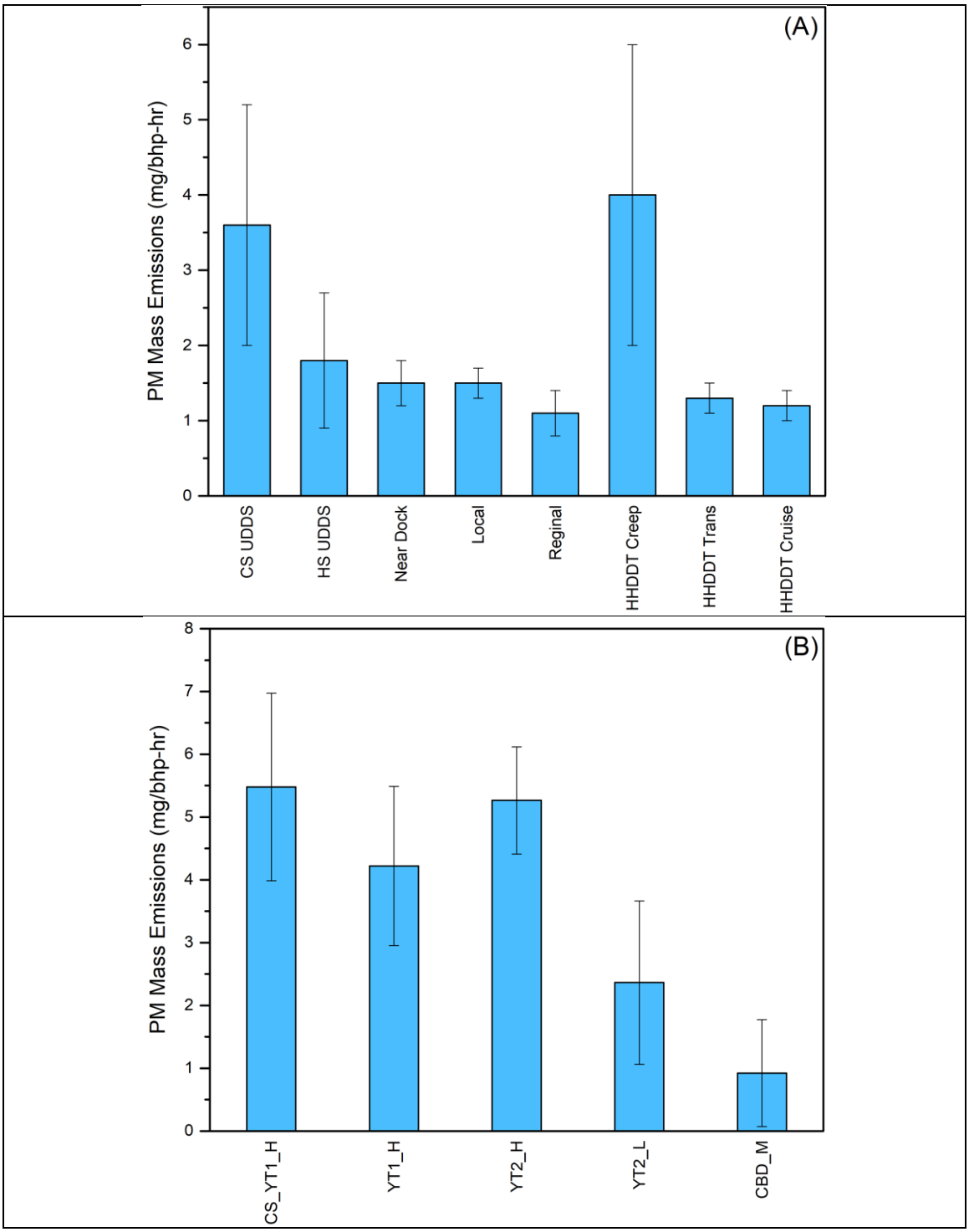

Figure 3.4(a-b) PM mass emissions for the 12L goods movement vehicle (top panel) and the 6.7L yard tractor (bottom panel) over different test cycles

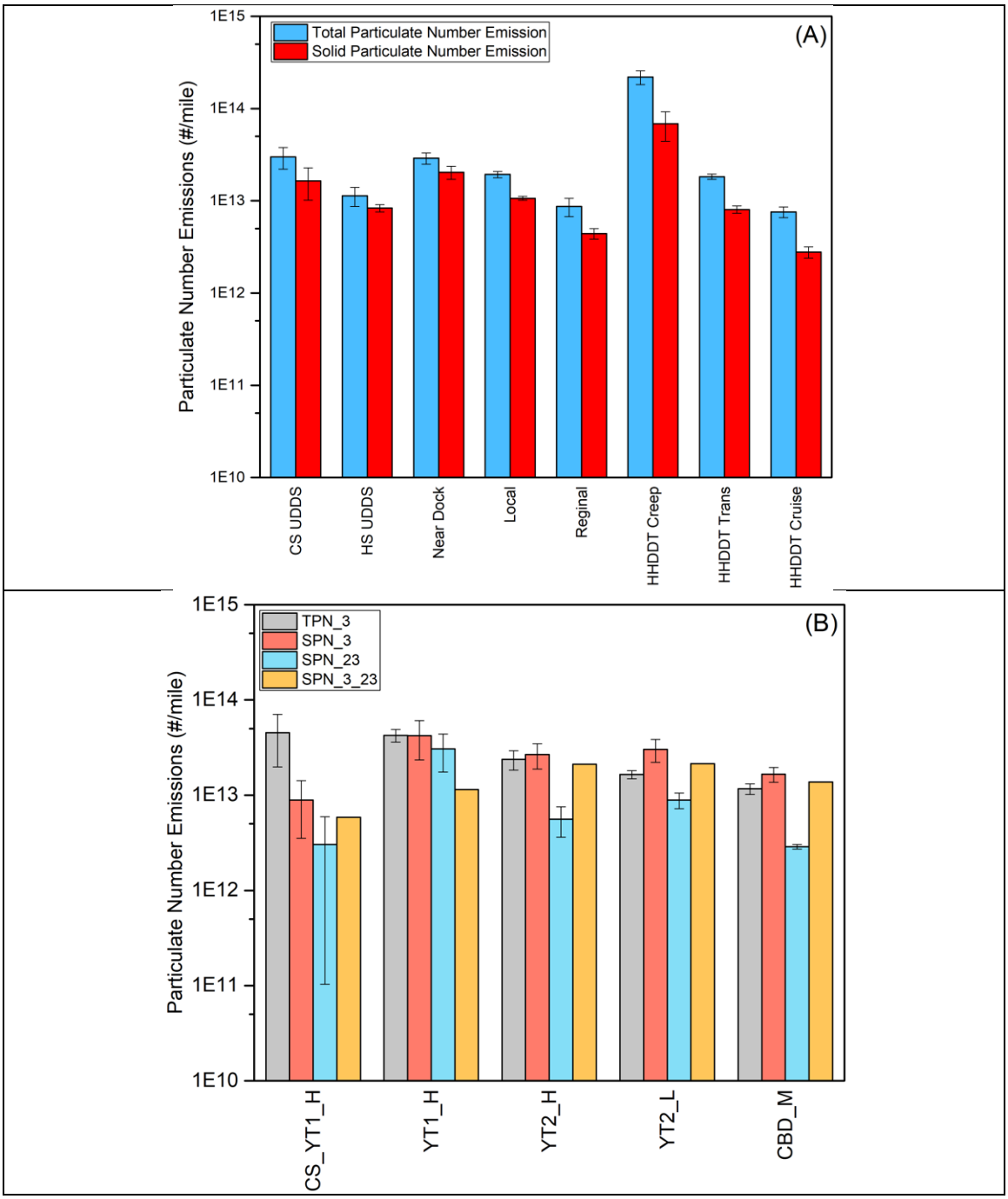

Figure 3.5(a-b) Total and solid particle number emissions for the 12L goods movement vehicle (top panel) and the 6.7L yard tractor (bottom panel) over different test cycles

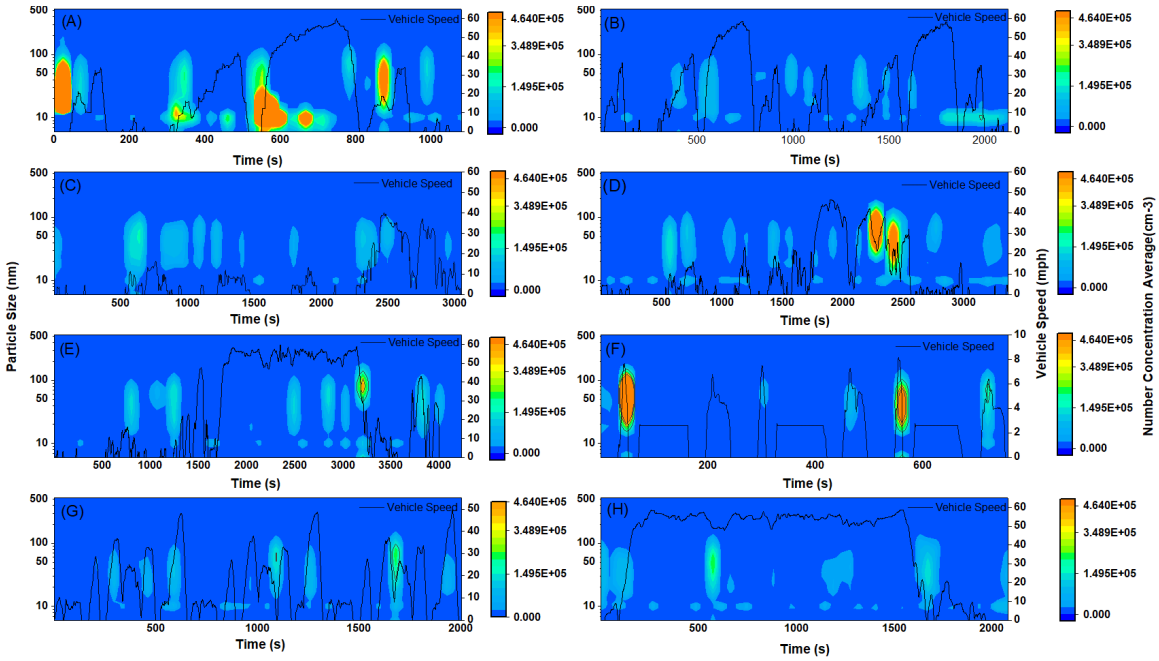

Figure 3.6(a-h) Particle size distributions for the 12 L goods movement vehicles for the cold-start UDDS (A), hot-start UDDS (B), Near Dock (C), Local (D), Regional (E), HHDDT Creep (F), HHDDT Transient (G), and HHDDT Cruise (H) test cycles

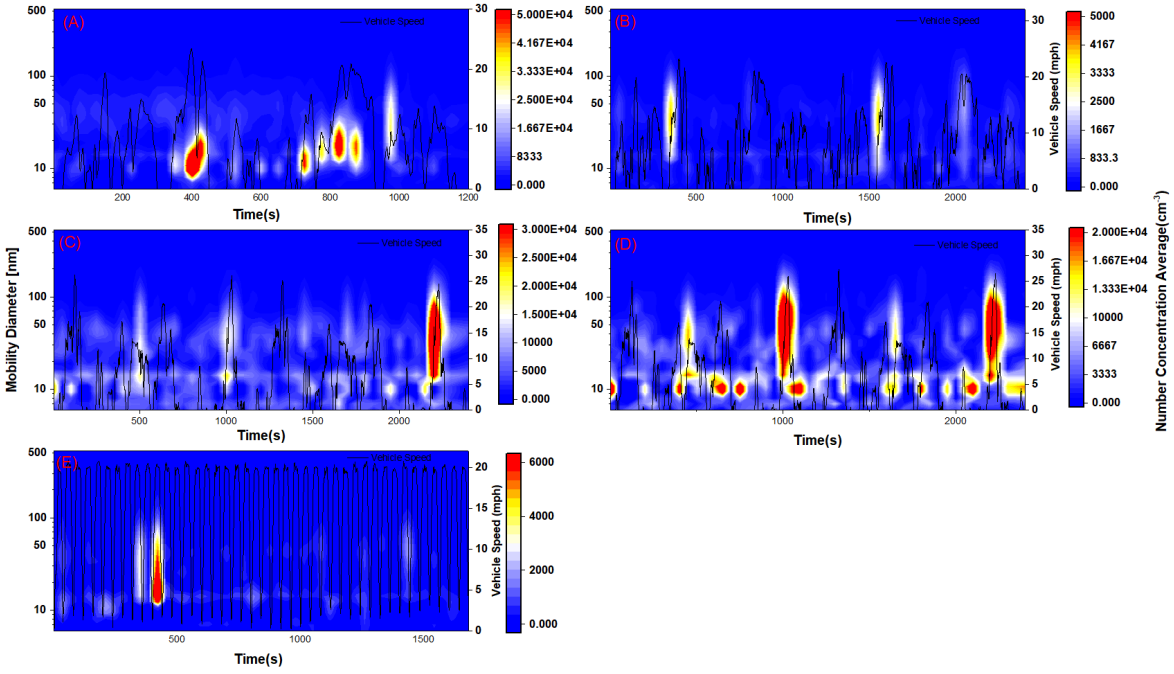

Figure 3.7(a-e) Particle size distributions for the 6.7L yard tractor for the cold-start YT1_H (A), hot-start YT1_H (B), YT2_H (C), YT2_L (D), and CBD (E) test cycles

3.4.3. **THC and CO Emissions**

THC and NMHC emissions are shown in Figure 3.11(a-b) THC and NMHC emissions for the 12L goods movement vehicle (top panel) and the 6.7L yard tractor (bottom panel) over the different driving cycles. For the 12L goods movement vehicle, THC emissions ranged between 0.4-0.01 g/bhp-hr. The cold-start UDDS produced higher THC emissions compared to the hot-start start UDDS, followed by the Regional and HHDDT Creep and Cruise cycles. The NMHC emissions were found in very low levels and for the cold-start and hot-start cycles. The NMHC emissions were well below the standard (0.14 g/bhp-hr) and were slightly above the certification value (0.004 g/bhp-hr) for this engine family. For the 6.7L yard tractor, THC emissions were found to be higher than those of the goods movement vehicle, and ranged from 1.2-0.18 g/bhp-hr. The cold-start cycle did not appear to affect THC emissions when compared to the hot-start cycle. However, the higher engine loading resulted in higher THC emissions compared to the same cycle with lower engine loading. NMHC emissions did not show significant differences between the test cycles, and remained below the standard, but slightly above the certification value for this engine family.

CO emissions were found in relatively high concentrations for both vehicles, as shown in Figure 3.8 (a-b). The relatively high CO emissions for these engines can be attributed to the richer operating conditions of the stoichiometric combustion compared to lean burn conditions, resulting in less oxygen availability for the oxidation of CO to CO_2 during combustion or over the TWC (Yoon et al., 2013). For both vehicles, CO emissions were strongly dependent on the cold-start when the TWC was less efficient for the oxidation of CO. For the 12L goods movement vehicle, CO emissions ranged between 0.23 to 1.93

g/bhp-hr. The CO emission levels for the 12L goods movement vehicle were found to be lower compared to previous studies with stoichiometric CNG heavy-duty vehicles, indicating significant progress in engine calibration optimization and catalyst efficiency (Hajbabaei et al., 2013; Karavalakis et al., 2016). For the 6.7L yard tractor, CO emissions ranged from 0.43-5.7 g/bhp-hr, with the higher engine loading showing higher CO emissions (YT2_H vs YT2_L). The CO emissions from the yard tractor were somewhat comparable to those of previous studies employed a near-zero NOx emissions natural gas platform (Li et al., 2019). For both vehicles, CO emissions were found to be below the current CO emissions standard of 15.5 g/bhp-hr.

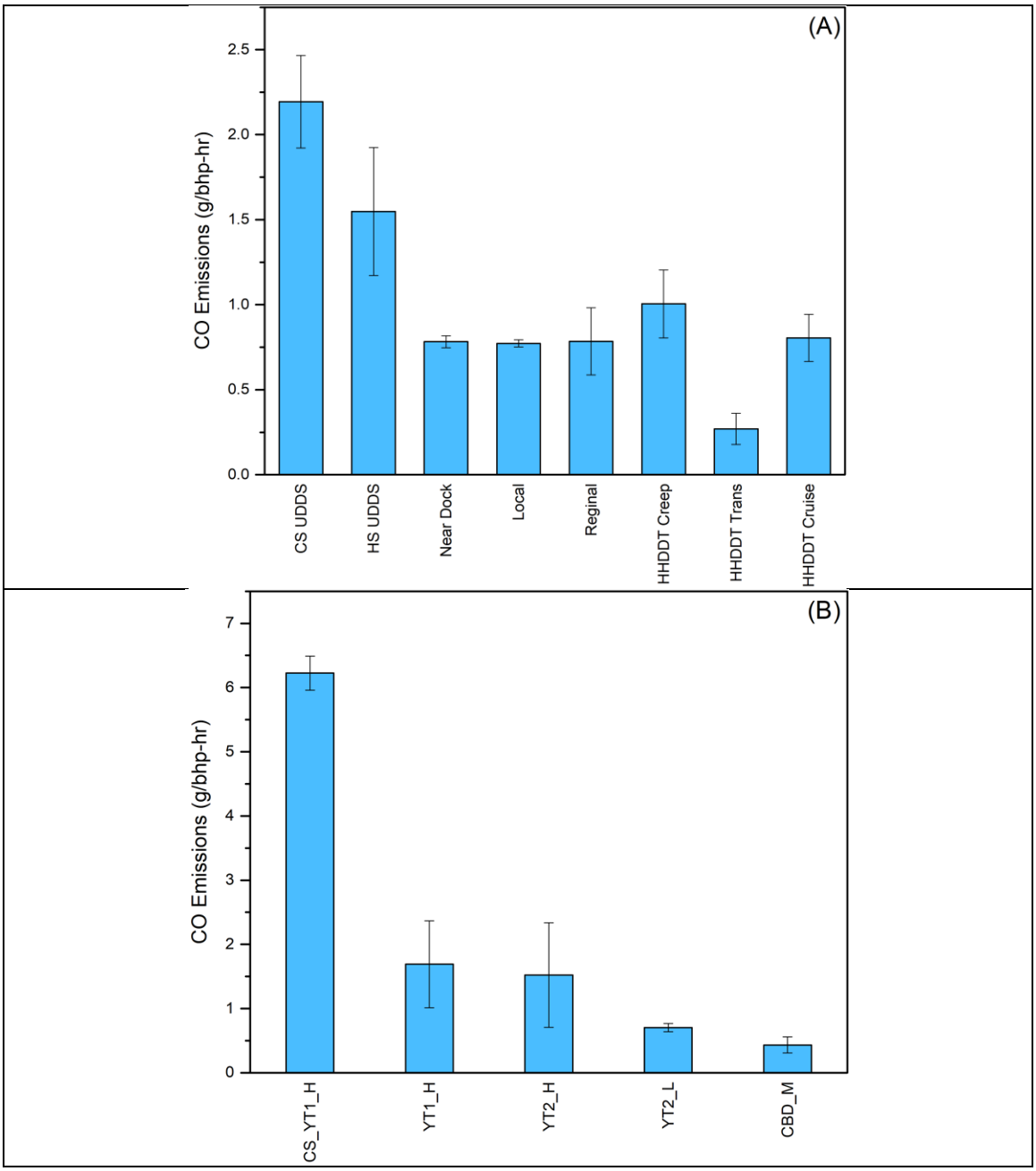

Figure 3.8(a-b) CO emissions for the 12L goods movement vehicle (top panel) and the 6.7L yard tractor (bottom panel) over different test cycles

3.4.4. **Greenhouse Gas (GHG) Emissions**

Greenhouse gas (GHG) emissions of CO_2, CH_4, and nitrous oxide (N_2O) are currently regulated for heavy-duty on-road vehicles. In particular, CO_2 emissions are regulated for model year (MY) 2014 and newer heavy-duty on-road engines, and CH_4 and N_2O

emissions are regulated for MY 2015 and newer engines. Table 3.1 shows the GHG emissions and their global warming potential (GWP) for both vehicles on all test cycles. For the 12L goods movement vehicle, the highest CO_2 emissions and corresponding lower fuel economy were seen for the low-load, low-speed Near Dock, Local, and HHDDT Creep cycles. Our results indicate that most of the CO_2 emissions from freight transport vehicles will occur during queuing, on-dock movements, and congested traffic in local roads. CO_2 emissions for the 6.7L yard tractor were higher than those of the 12L goods movement vehicle, with the YT2_H cycle that represents a full 100% GVW showing higher CO_2 emissions compared to the cycle that represented 50% GVW (YT2_L). It is evident that yard tractors significantly contribute to the total CO_2 emissions at port terminals during the process of loading and unloading containers or when these vehicles operate in congestion and stop-and-go driving.

Natural gas engines are generally characterized by their relatively high CH_4 emissions (Hajbabaei et al., 2013; Quiros et al., 2017). Since CH_4 is the major hydrocarbon component in natural gas, CH_4 emissions mainly come from unburned fuel compared to gasoline combustion where CH_4 derives from the incomplete combustion of the fuel after a series of reactions leading to the formation of smaller hydrocarbon radicals. The high CH_4 emissions from stoichiometric natural gas engines is also a consequence of the TWCs being less efficient in oxidizing the CH_4 molecule due to the lack of oxygen in the exhaust. A recent study reported significantly higher CH_4 emissions from a stoichiometric natural gas engine equipped with a TWC compared to conventional and hybrid diesel engines equipped with DPF and SCR systems (Quiros et al., 2017). For the 12L goods movement, the cold-start UDDS showed significantly higher CH_4 emissions compared to the hot-start

UDDS, indicating that improvements in the TWC after reaching its light-off temperature, such as larger size and higher precious metals loadings, will promote CH_4 conversion. Similar to the cold-start UDDS cycle, the highest CH_4 emissions were also seen over the Regional and HHDDT Cruise cycles, which is an indication that most of the CH_4 slip occurs under more transient conditions with higher engine speeds. Increased CH_4 emissions at higher engine speeds and when the in-cylinder residence time is lowest were also observed in a previous study (Stettler et al., 2016). For the 6.7L yard tractor, CH_4 emissions were not influenced by the cold-start and were generally found to be higher for the more transient cycles compared to the lighter load CBD cycle and the steady-state operation.

N_2O is the most common tropospheric nitrogen species aside from molecular nitrogen and is considered to be a more powerful GHG on a unit basis compared to CO_2 and CH_4. N_2O has a lifetime of approximately 121 years in the atmosphere and GWP of 265 based on a 100-year time horizon (265 times more powerful than CO_2 in terms of heat trapping effects) (IPCC, 2013; Ravishankar et al., 2009). It is also the single most important ozone-depleting compound (Ravishankara et al., 2009). As shown in Table 3.1, N_2O emissions for both vehicles were strongly influenced by the cold-start cycles, since N_2O is formed during the reduction of NOx over the surface of the TWC during its initial warm up period and it is not an in-cylinder combustion product (Huai et al., 2004; Prigent and De Soete, 1989; Thiruvengadam et al., 2016). For the 12L goods movement vehicle, cold-start N_2O emissions represented 95% of the total emissions for the entire cycle and were attributed to a single spike during the first 50 seconds of the cycle. For the 6.7L yard tractor, the cold-start N_2O emissions predominantly occurred in the first 164 seconds, representing

99% of the total emissions. Emissions of N_2O for the hot-start tests and when the TWC system was efficiently operated were very low or found to be close to the detection limits of the test method. The results reported here agree with previous studies that have shown higher N_2O emissions with corresponding higher CO emissions, largely due to reactions of CO and hydrogen on the catalyst surface ($2NO + CO \rightarrow N_2O + CO_2$; $2NO + H_2 \rightarrow N_2O + H_2O$) that would promote the formation of N_2O (Behrentz et al., 2004; Gong and Rutland, 2013; Karavalakis et al., 2016). A less apparent observation was that N_2O emissions trended higher during the more transient and hotter cycles, which is in agreement with findings from previous studies shown higher N_2O emissions over cold-start and transients (Quiros et al., 2017; Rahman et al., 2011).

The GWP, expressed in equivalent CO_2 (CO_2eq) units, was calculated by assuming CH_4 to be 25 times higher than CO_2 over a 100-year time horizon and for N2O to be 265 times over a 100-year time horizon. CO_2 emissions dominated the tailpipe GHG emissions for both vehicles. For the 12L goods movement vehicle, the Near Dock, Local, and HHDDT Creep mode showed the highest GWP compared to the other cycles. The cold-start UDDS also produced higher CO_2eq emissions compared to the hot-start UDDS. For the 6.6L yard tractor, CO_2eq emissions were higher than the goods movement vehicle, with the hot-start YT1_H, YT2_H, and YT2_L cycles having the greatest GWP compared to the other test cycles. Emissions of CH_4 contributed to less than 2% for the 12L goods movement vehicle and were between 0.65-3.8% for the 6.7L yard tractor. N_2O emissions for both vehicles showed very little or negligible contribution to the total GWP of the tailpipe emissions. our results are in line with previous studies that have shown

insignificant contribution of N_2O and small contribution of CH_4 to the total GWP, respectively (Yoon et al., 2013; Thiruvengadam et al., 2016).

Table 3.1: GHG emissions (CO_2, CH_4, and N_2O) and global warming potential (GWP) for both vehicles over the different test cycles

Vehicle	Trace	CO_2	CH_4	N_2O	GWP (CO_2 eq)	CO_2 Eq. Impact (%)	
						CH_4	N_2O
12L Goods Movement	CS UDDS	540.5	0.43	0.0192	556.3	1.93%	0.91%
	UDDS	534.1	0.18	0.0000	538.6	0.84%	0.00%
	Near Dock	608.5	0.18	0.0001	613.0	0.73%	0.00%
	Local	611.3	0.14	0.0001	614.8	0.57%	0.00%
	Regional	555.4	0.41	0.0005	565.8	1.81%	0.02%
	HHDDT Creep	612.0	0.37	0.0001	621.3	1.49%	0.00%
	HHDDT Trans	548.7	0.02	0.0001	549.2	0.09%	0.00%
	HHDDT Cruise	534.4	0.35	0.0003	543.2	1.61%	0.01%
6.7L Yard Tractor	CS YT1_H	730.0	0.93	0.0278	760.7	3.06%	0.97%
	YT1_H	778.0	1.09	0.0010	805.6	3.38%	0.03%
	YT2_H	781.9	1.23	0.0031	813.4	3.78%	0.10%
	YT2_L	791.8	1.07	0.0022	819.1	3.27%	0.07%
	CBD_M	725.8	0.19	0.0009	730.8	0.65%	0.03%

3.4.5. **Ammonia Emissions**

Ammonia (NH_3) emissions are of great interest and concern as they are considered precursors to secondary inorganic aerosol formation (Liu et al., 2015). Ammonia emissions are characteristic of stoichiometric natural gas engines equipped with TWC. It has been shown that stoichiometric natural gas engines emit significantly higher NH_3 levels than

diesel engines equipped with SCR, which control NH_3 emissions by optimizing urea dosing and NH_3 storage in the SCR system (Thiruvengadam et al., 2016). NH_3 formation in stoichiometric engines is attributed to NO reacting with hydrogen that is produced by the reaction of CO with water (Gong and Rutland, 2013; Livingston et al., 2009). As shown in Figure 3.9 (a-b), NH_3 emissions for both vehicles were higher for the cold-start cycles. For the 12L goods movement vehicle, the Near Dock cycle and the HHDDT Creep mode showed the highest NH_3 emissions compared to the other Drayage Port cycles and CARB HHDDT cycles, respectively. This finding suggests that the majority of NH_3 emissions will be produced during low-speed, increased idling, and stop-and-go conditions, typical of port activities or urban driving in congested roads. For the 6.7L yard tractor, NH_3 emissions did not show any differences between the yard tractor cycles and the CBD. However, NH_3 emissions were found at low concentrations for the steady-state tests. It is worth noting that NH_3 emissions exhibited a good relationship with N_2O emissions formation. Overall, it was observed that cold-start N_2O emissions were higher in the presence of NH_3 in the exhaust, likely due to oxidation mechanisms.

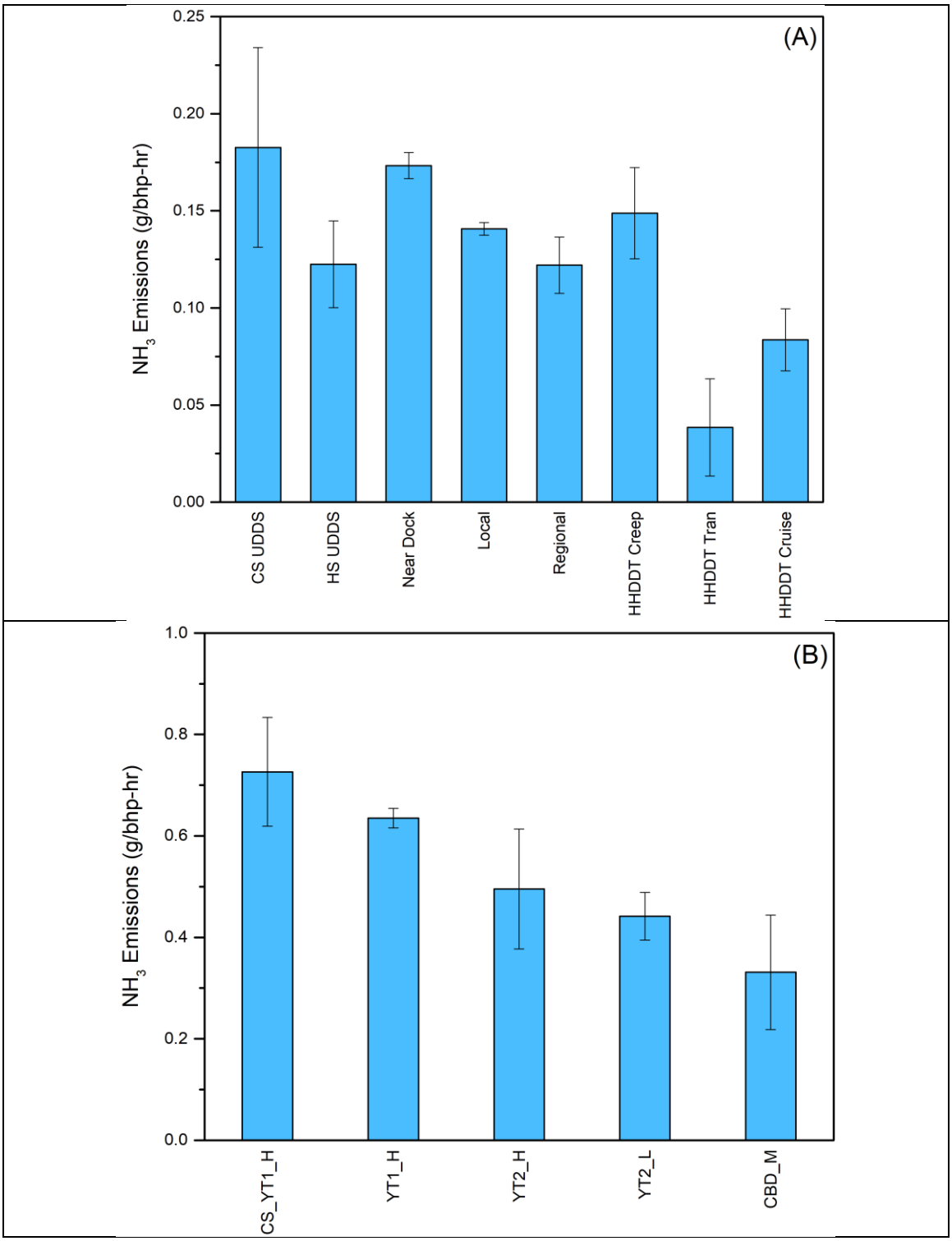

Figure 3.9(a-b) NH_3 emissions for the 12L goods movement vehicle (top panel) and the 6.7L yard tractor (bottom panel) over different test cycles

3.5. **Conclusions**

This work investigated the emissions impacts from two near-zero NOx emissions natural gas heavy-duty vehicles in different vocations. Both vehicles were exercised over different driving cycles on a chassis dynamometer. The results reported here showed very low NOx emissions levels for both vehicles and dramatic reductions of up to 90% compared to the 2010 certification standard. This study highlighted the potential importance of using ultra-low NOx stoichiometric natural gas platforms in captive fleets, seaport equipment, and goods movement vehicles to alleviate ground-level ozone formation in urban areas of the South Coast Air basin. The impact of the cold-start period on NOx emissions was found to be relatively small considering the real-world fraction of time natural gas heavy-duty vehicles of any vocation operate in cold mode compared to hot mode. Both vehicles showed elevated solid particle number emissions that were above the European particle number limit, indicating that significant work should be undertaken to reduce solid particle number emissions from natural gas vehicles to levels comparable to those of diesel vehicles equipped with DPFs. In addition, a significant fraction of smaller sub 23 nm particles exists in natural gas engine exhaust, which could be a major concern from regulatory and health effects perspectives. For the 12L goods movement vehicle, the profile of the particle size distribution was highly dependent on the test cycle. For some test cycles, high particle concentrations in the nucleation mode regime were observed during acceleration events, whereas for other test cycles particles in the accumulation mode were seen during deceleration. Both driving patterns favor the infusion of lubrication oil via the piston ring into the combustion chamber, which will result in particle formation. For the 6.7L yard tractor, nucleation mode particles in the 5-10 nm diameter dominated the

particle size distribution, with the higher load cycle producing greater populations of both nucleation and accumulation mode particles than the lower load cycles. CO emissions were found in relatively high levels, but lower than older technology stoichiometric natural gas engines, indicating significant improvements in engine calibration and catalyst formulation. Emissions of N_2O and NH_3 were highly dependent of the cold-start cycles showing higher concentrations for both vehicles compared to the hot-start tests. CH_4, the principal component of natural gas, showed elevated emission levels associated with the incomplete combustion of CH_4, especially during transient operation and at higher engine speeds.

3.6. **Acknowledgements**

This study was performed for Cummins Westport, Inc. as part of a South Coast Air Quality Management District (SCAQMD) Contract No. 16205 with Cummins Westport, Inc. We acknowledge Mr. Don Pacocha, Mr. Mark Villela, and Mr. Daniel Gomez of the University of California, Riverside for performing the emissions testing.

3.7. **Reference**

Abdul-Khalek IS, Kittelson DB, Graskow BR, Wei Q, Brear F. Diesel exhaust particle size: measurement issues and trends. SAE transactions 1998: 683-696.

Amanatidis S, Ntziachristos L, Giechaskiel B, Bergmann A, Samaras Z. Impact of selective catalytic reduction on exhaust particle formation over excess ammonia events. Environmental science & technology 2014; 48: 11527-11534.

Amirante R, Distaso E, Tamburrano P, Reitz RD. Measured and predicted soot particle emissions from natural gas engines. SAE Technical Paper, 2015.

Behrentz E, Ling R, Rieger P, Winer AM. Measurements of nitrous oxide emissions from light-duty motor vehicles: a pilot study. Atmospheric Environment 2004; 38: 4291-4303.

Bishop GA, Schuchmann BG, Stedman DH. Heavy-duty truck emissions in the South Coast Air Basin of California. Environmental science & technology 2013; 47: 9523-9529.

DeFoort M, Olsen D, Willson B. The effect of air-fuel ratio control strategies on nitrogen compound formation in three-way catalysts. International Journal of Engine Research 2004; 5: 115-122.

Dixit P, Miller JW, Cocker III DR, Oshinuga A, Jiang Y, Durbin TD, et al. Differences between emissions measured in urban driving and certification testing of heavy-duty diesel engines. Atmospheric Environment 2017; 166: 276-285.

Einewall P, Tunestål P, Johansson B. Lean burn natural gas operation vs. stoichiometric operation with EGR and a three way catalyst. SAE technical paper 2005: 0250.

Feist MD, Landau M, Harte E. The effect of fuel composition on performance and emissions of a variety of natural gas engines. SAE International Journal of Fuels and Lubricants 2010; 3: 100-117.

Fontaras G, Martini G, Manfredi U, Marotta A, Krasenbrink A, Maffioletti F, et al. Assessment of on-road emissions of four Euro V diesel and CNG waste collection trucks for supporting air-quality improvement initiatives in the city of Milan. Science of the total environment 2012; 426: 65-72.

Frey HC. Trends in onroad transportation energy and emissions. Journal of the Air & Waste Management Association 2018; 68: 514-563.

Giechaskiel B. Solid particle number emission factors of Euro VI heavy-duty vehicles on the road and in the laboratory. International journal of environmental research and public health 2018; 15: 304.

Gong J, Rutland C. Three way catalyst modeling with ammonia and nitrous oxide kinetics for a lean burn spark ignition direct injection (SIDI) gasoline engine. SAE Technical Paper, 2013.

Grigoratos T, Fontaras G, Martini G, Peletto C. A study of regulated and green house gas emissions from a prototype heavy-duty compressed natural gas engine under transient and real life conditions. Energy 2016; 103: 340-355.

Hajbabaei M, Karavalakis G, Johnson KC, Lee L, Durbin TD. Impact of natural gas fuel composition on criteria, toxic, and particle emissions from transit buses equipped with lean burn and stoichiometric engines. Energy 2013; 62: 425-434.

Hallquist Å, Jerksjö M, Fallgren H, Westerlund J, Sjödin Å. Particle and gaseous emissions from individual diesel and CNG buses. Atmospheric Chemistry and Physics 2013; 13: 5337-5350.

Herner JD, Hu S, Robertson WH, Huai T, Collins JF, Dwyer H, et al. Effect of advanced aftertreatment for PM and NO x control on heavy-duty diesel truck emissions. Environmental science & technology 2009; 43: 5928-5933.

Hesterberg TW, Lapin CA, Bunn WB. A comparison of emissions from vehicles fueled with diesel or compressed natural gas. Environmental science & technology 2008; 42: 6437-6445.

Huai T, Durbin TD, Miller JW, Norbeck JM. Estimates of the emission rates of nitrous oxide from light-duty vehicles using different chassis dynamometer test cycles. Atmospheric Environment 2004; 38: 6621-6629.

Jayaratne E, Meyer N, Ristovski Z, Morawska L. Volatile properties of particles emitted by compressed natural gas and diesel buses during steady-state and transient driving modes. Environmental science & technology 2012; 46: 196-203.

Karavalakis G, Hajbabaei M, Durbin TD, Johnson KC, Zheng Z, Miller WJ. The effect of natural gas composition on the regulated emissions, gaseous toxic pollutants, and ultrafine particle number emissions from a refuse hauler vehicle. Energy 2013; 50: 280-291.

Karavalakis G, Hajbabaei M, Jiang Y, Yang J, Johnson KC, Cocker DR, et al. Regulated, greenhouse gas, and particulate emissions from lean-burn and stoichiometric natural gas heavy-duty vehicles on different fuel compositions. Fuel 2016; 175: 146-156.

Khalek IA, Badshah H, Premnath V, Brezny R. Solid particle number and ash emissions from heavy-duty natural gas and diesel w/SCRF engines. SAE Technical Paper, 2018.

Korakianitis T, Namasivayam A, Crookes R. Natural-gas fueled spark-ignition (SI) and compression-ignition (CI) engine performance and emissions. Progress in energy and combustion science 2011; 37: 89-112.

Li C, Han Y, Jiang Y, Yang J, Karavalakis G, Durbin TD, et al. Emissions from advanced ultra-low-NOx heavy-duty natural gas vehicles. 2019.

Liu T, Wang X, Deng W, Zhang Y, Chu B, Ding X, et al. Role of ammonia in forming secondary aerosols from gasoline vehicle exhaust. Science China Chemistry 2015; 58: 1377-1384.

Livingston C, Rieger P, Winer A. Ammonia emissions from a representative in-use fleet of light and medium-duty vehicles in the California South Coast Air Basin. Atmospheric Environment 2009; 43: 3326-3333.

McTaggart-Cowan G, Reynolds C, Bushe W. Natural gas fuelling for heavy-duty on-road use: current trends and future direction. International journal of environmental studies 2006; 63: 421-440.

Misra C, Collins JF, Herner JD, Sax T, Krishnamurthy M, Sobieralski W, et al. In-use NO x emissions from model year 2010 and 2011 heavy-duty diesel engines equipped with aftertreatment devices. Environmental science & technology 2013; 47: 7892-7898.

Misra C, Ruehl C, Collins J, Chernich D, Herner J. In-use NOx emissions from diesel and liquefied natural gas refuse trucks equipped with SCR and TWC, respectively. Environmental science & technology 2017; 51: 6981-6989.

Monks PS, Archibald A, Colette A, Cooper O, Coyle M, Derwent R, et al. Tropospheric ozone and its precursors from the urban to the global scale from air quality to short-lived climate forcer. Atmospheric Chemistry and Physics 2015; 15: 8889-8973.

Pelkmans L, De Keukeleere D, Bruneel H, Lenaers G. Influence of vehicle test cycle characteristics on fuel consumption and emissions of city buses. SAE Transactions 2001: 1388-1398.

Prigent M, De Soete G. Nitrous Oxide N_2O in Engines Exhaust Gases-A First Appraisal of Catalyst Impact. SAE transactions 1989: 281-291.

Quiros DC, Smith J, Thiruvengadam A, Huai T, Hu S. Greenhouse gas emissions from heavy-duty natural gas, hybrid, and conventional diesel on-road trucks during freight transport. Atmospheric Environment 2017; 168: 36-45.

Quiros DC, Thiruvengadam A, Pradhan S, Besch M, Thiruvengadam P, Demirgok B, et al. Real-world emissions from modern heavy-duty diesel, natural gas, and hybrid

diesel trucks operating along major California freight corridors. Emission Control Science and Technology 2016; 2: 156-172.

Rahman M, Hara K, Nakatani S, Tanaka Y. Emission testing of N 2 O (bag sampling) from diverse vehicles by laser spectroscopic motor exhaust gas analyzer. SAE Technical Paper, 2011.

Ravishankara A, Daniel JS, Portmann RW. Nitrous oxide (N2O): the dominant ozone-depleting substance emitted in the 21st century. science 2009; 326: 123-125.

Sharp C, Webb CC, Neely G, Carter M, Yoon S, Henry C. Achieving ultra low NOx emissions levels with a 2017 heavy-duty on-highway TC diesel engine and an advanced technology emissions system-thermal management strategies. SAE International Journal of Engines 2017a; 10: 1697-1712.

Sharp C, Webb CC, Yoon S, Carter M, Henry C. Achieving ultra low NOx emissions levels with a 2017 heavy-duty on-highway TC diesel engine-comparison of advanced technology approaches. SAE International Journal of Engines 2017b; 10: 1722-1735.

Stettler ME, Midgley WJ, Swanson JJ, Cebon D, Boies AM. Greenhouse gas and noxious emissions from dual fuel diesel and natural gas heavy goods vehicles. Environmental Science & Technology 2016; 50: 2018-2026.

Thiruvengadam A, Besch M, Carder D, Oshinuga A, Pasek R, Hogo H, et al. Unregulated greenhouse gas and ammonia emissions from current technology heavy-duty vehicles. Journal of the Air & Waste Management Association 2016; 66: 1045-1060.

Thiruvengadam A, Besch M, Padmanaban V, Pradhan S, Demirgok B. Natural gas vehicles in heavy-duty transportation-A review. Energy Policy 2018; 122: 253-259.

Thiruvengadam A, Besch MC, Thiruvengadam P, Pradhan S, Carder D, Kappanna H, et al. Emission rates of regulated pollutants from current technology heavy-duty diesel and natural gas goods movement vehicles. Environmental science & technology 2015; 49: 5236-5244.

Thiruvengadam A, Besch MC, Yoon S, Collins J, Kappanna H, Carder DK, et al. Characterization of particulate matter emissions from a current technology natural gas engine. Environmental science & technology 2014; 48: 8235-8242.

Tonegawa Y, Oguchi M, Tsuchiya K, Sasaki S, Ohashi T, Goto Y. Evaluation of regulated materials and ultra fine particle emission from trial production of heavy-duty CNG engine. SAE Technical Paper, 2006.

Velders GJ, Geilenkirchen GP, de Lange R. Higher than expected NOx emission from trucks may affect attainability of NO2 limit values in the Netherlands. Atmospheric environment 2011; 45: 3025-3033.

Wang WG, Clark N, Lyons D, Yang R, Gautam M, Bata R, et al. Emissions comparisons from alternative fuel buses and diesel buses with a chassis dynamometer testing facility. Environmental science & technology 1997; 31: 3132-3137.

Yoon S, Collins J, Thiruvengadam A, Gautam M, Herner J, Ayala A. Criteria pollutant and greenhouse gas emissions from CNG transit buses equipped with three-way catalysts compared to lean-burn engines and oxidation catalyst technologies. Journal of the Air & Waste Management Association 2013; 63: 926-933.

Yoon S, Hu S, Kado NY, Thiruvengadam A, Collins JF, Gautam M, et al. Chemical and toxicological properties of emissions from CNG transit buses equipped with three-way catalysts compared to lean-burn engines and oxidation catalyst technologies. Atmospheric Environment 2014; 83: 220-228.

3.8. **Supplemental Materials**

Table 3.2 SM1 Technical specifications of the test engines

Manufacturer	Cummins Westport, Inc.	Cummins Westport, Inc.
Model	B6.7N240	ISX12N
Year	2019	2019
VIN Number	1T9TSNA83KR825001	75053847
Rated Power	179kW at 2400 rpm	298kW at 2100 rpm
Peak Torque	759Nm	1,966Nm
Number of Cylinders	6	6
Displacement	6.7L	11.9L
Adv NOx Standard	0.1 g/bhp-hr	0.02 g/bhp-hr
PM Standard	0.01 g/bhp-hr	0.01 g/bhp-hr
Aftertreatment	Three-way catalyst	Three-way catalyst

Table 3.3 SM3: Test cycles characteristics for both vehicles

Test Cycle	Distance (miles)	Average Speed (mph)	Duration (sec)
Cold-start UDDS (UDDS_CS)	5.55	18.8	1061
Duplicate hot-start UDDS (UDDSx2)	11.1	18.8	2122
Near Dock	5.61	6.6	3046
Local	8.71	9.3	3362
Regional	27.3	23.2	3661
HHDDT_Creep (triplicate)	0.372	1.75	768
HHDDT_Transient (triplicate)	8.55	15.4	2004
HHDDT_Cruise	23.1	39.9	2083
CS_YT1_H	2.37	7.12	1200
YT1_H (duplicate)	2.37 x 2	7.12	2400
YT2_H (duplicate)	1.76 x 2	5.27	2400
YT2_L (duplicate)	1.76 x 2	5.27	2400
CBD_M (triplicate)	6.0	12.6	1680

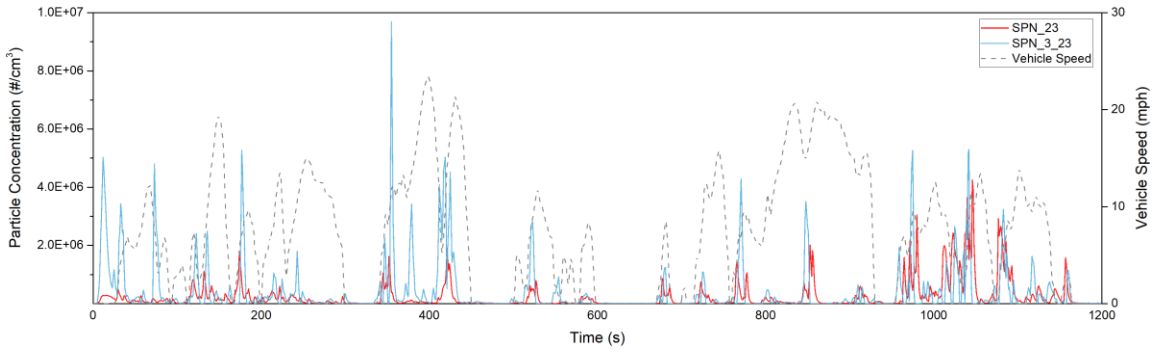

Figure 3.10 SM 1 Real-time solid particle number emission concentrations for the 6.7L yard tractor over the cold-start YT1_H cycle

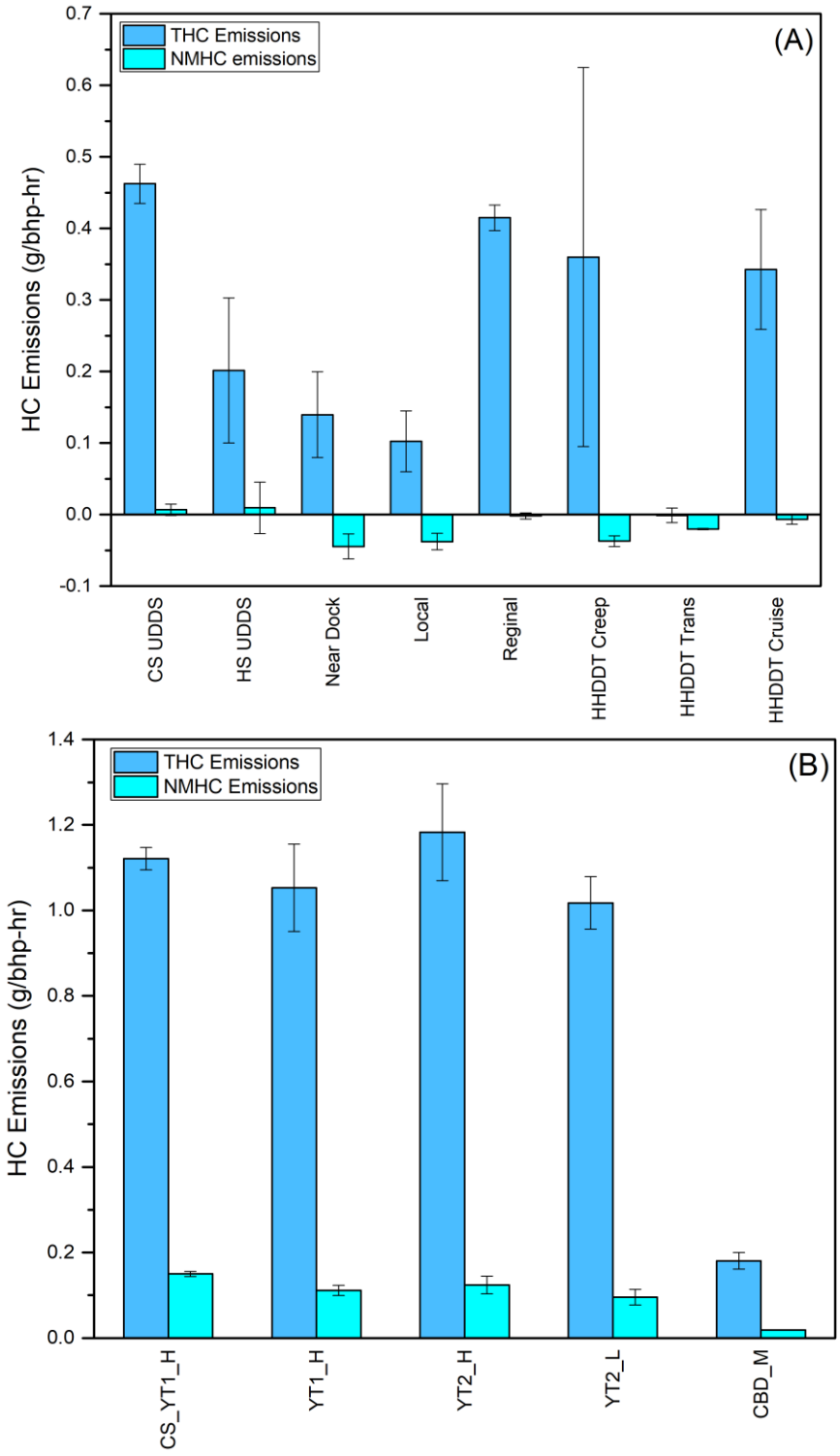

Figure 3.11(a-b) THC and NMHC emissions for the 12L goods movement vehicle (top panel) and the 6.7L yard tractor (bottom panel) over the different driving cycles

4. Emissions From In-Use Heavy-Duty Diesel, Natural Gas and Diesel-Electric Hybrid Trucks - Part. 1 NOx, N_2O and NH_3 Emissions

4.1. Abstract

The current study characterized in-use NOx, N_2O and NH_3 emissions from a fleet of 14 heavy-duty vehicles of different vocations (school bus, transit bus, refuse hauler, delivery vehicle, and goods movement vehicle), fuels (diesel, hydrogenated vegetable oil [HVO]/renewable diesel (RD), and CNG), engine types, and aftertreatment controls (SCR or TWC), and over different drive cycles using a chassis dynamometer. This study is part of a larger effort that included over 200 in-use heavy-duty vehicles, which is one of the most extensive studies of emissions from modern HDDVs to date. For the UDDS cycle, NOx emissions varied depending on the vocation and the technology. Average NOx emissions across all vehicles ranged from 0.003 to 6.16 g/bhp-hr and from 0.02 to 17.2 g/mile. The in-use PEMS NOx emissions were higher than those over the vocational and UDDS cycles for most vehicles, except for goods movement vehicles 0.2Diesel #3 and #5. NOx emissions for the HHDDT cruise cycles showed similar or lower NOx emissions compared to those for the UDDS cycles, the vocational cycles, and the in-use PEMS testing for all the vehicles in delivery and goods movement categories, except for the goods movement vehicle 0.2Diesel #5. NH_3 and N_2O emissions are also pollutants of concern for air quality and global warming, which were also further discussed.

Keywords: CNG vehicles; Diesel Vehicles; NOx, N_2O, NH_3 Emissions, Chassis Dynamometer Testing.

4.2. **Introduction**

Heavy-duty diesel vehicles (HDDVs) and heavy-duty diesel engines (HDDEs) are the largest sources of NOx emissions in transportation sector in the United States (U.S.) (EPA, 2008). In California, on-road heavy-duty vehicles are estimated to contribute 31 percent of all statewide NOx emissions in the transportation category, which represents the largest single source category of NOx emissions. NOx is considered a precursor of ozone formation through photochemical reactions with volatile organic compounds. NOx also reacts with ammonia, moisture, and other compounds to form small particles that can penetrate deeply into sensitive parts of the lungs and can cause or worsen respiratory disease (EPA, 2015b). In some regions of California, there are still extreme challenges in meeting the most recent federal ozone and PM2.5 standards. Therefore, the reductions of NOx emissions are critical for meeting the current and future air quality standards.

As part of efforts to reduce emissions from on-road heavy-duty engines, more stringent U.S. EPA emissions standards of 0.20 g/bhp-hr NOx were introduced for 2010 and newer on-road heavy-duty engines. Since then, the heavy-duty vehicle population has included vehicles with more advanced engines and technologies, such as Selective Catalyst Reduction (SCR) for diesel vehicles. SCR utilizes ammonia that is hydrolyzed from an aqueous urea solution as a reactant to convert NOx into nitrogen and water (Guan et al., 2014). Although SCR catalysts provide good NOx emissions reductions under certain conditions, the conversion efficiency is highly dependent on the catalyst materials and conditions, urea injection timing and volume, etc. Many studies have shown elevated NOx emissions when the SCR inlet temperature is below 250 °C under various driving conditions (Tan et al., 2019). Studies have also shown that NOx emissions under real-world

conditions can significantly differ from those under more controlled laboratory conditions using an engine or chassis dynamometer. Real-world conditions, such as frequent stop-go events, extended idling, and low load/speed operation can have a large impact on SCR efficiency and tailpipe NOx emissions (Grigoratos et al., 2019; Kotz et al., 2016; Mendoza-Villafuerte et al., 2017). Studies have also found higher NOx emissions during cold start operation when the SCR catalyst is well below its light-off temperature (Weilenmann et al., 2009; Weilenmann et al., 2005).

Natural gas engines are another technology that can meet not only the 0.2 g/bhp-hr NOx standard, but also an optional 0.02 g/bhp-hr NOx standard, which is 90% below 2010 certification standard. Current natural engines technologies utilized spark-ignited, stoichiometric combustion with a three-way catalysts (TWC) aftertreatment system, as well as exhaust gas recirculation (EGR) to control NOx emissions. Several chassis dynamometer studies have demonstrated that late-model, stoichiometric, compressed natural gas (CNG) engines can achieve emissions at or below 0.02 g/bhp-hr NOx levels under a variety of conditions (Li et al., 2019; Zhu et al., 2020). Data from vehicles equipped with 0.2 and 0.02 g/bhp-hr CNG engines is still relatively limited in terms of the number of vehicles and testing over a wide range of mileages, so it is uncertain how effective these engines are over a wide range of applications and over the full useful vehicle lifespan. Additional data is also needed for emissions inventory models that are used for policy development.

Aside from NOx emissions, NH_3 and N_2O emissions are also pollutants of concern. NH_3 is considered to be a precursor to secondary inorganic aerosol formation (Liu et al., 2015). N_2O is an important greenhouse gas (GHG), which has a lifetime of about 121 years

in the atmosphere and a GWP of 298 based on a 100-year time horizon (Seyboth, 2013). Both NH_3 and N_2O are generally formed through reactions over the surfaces of the catalyst. A number of studies have demonstrated the formation of NH_3 over the surfaces of TWCs or other catalytic surfaces (Bae et al., 2022; Wang et al., 2015). Relatively high NH_3 emissions have been observed from heavy-duty CNG vehicles with TWCs in several studies (Thiruvengadam et al., 2016). For SCR-equipped diesel vehicles, overdosing of urea can also lead to "ammonia slip" that can in turn lead to elevated tailpipe NH_3 emissions. In spark-ignited engines, elevated N_2O emissions have been observed primarily during the initial warm-up period of the catalyst between temperatures of 300 °C to 500 °C. The formation of N_2O emissions under higher temperatures is minimal unless deterioration of the catalyst happens. Over the SCR catalyst, N_2O emissions form preliminarily due to both ammonia oxidation and decomposition of ammonium nitrate particles (Thiruvengadam et al., 2016). While the potential importance of NH_3 and N_2O emissions from heavy-duty vehicles is recognized, data for these two pollutants is still limited from heavy-duty vehicles, particularly over a wide range of operating conditions, and for vehicles with different mileages.

The objective of the current study is to characterize in-use NOx, N_2O and NH_3 emissions from a fleet of 14 heavy-duty vehicles of different vocations (school bus, transit bus, refuse hauler, delivery vehicle, and goods movement vehicle), fuels (diesel, hydrogenated vegetable oil [HVO]/renewable diesel (RD), and CNG), engine types, and aftertreatment controls (SCR or TWC), and over different drive cycles using a chassis dynamometer. This study is part of a larger effort that included over 200 in-use heavy-duty vehicles, which is one of the most extensive studies of emissions from modern HDDVs to

date. The goal was to better understand in-use NOx emissions, to evaluate a variety of technologies for vehicles in different vocations, and to provide information for the development of future regulations. This information has also been used as a key basis for the development of CARB's current and future EMissionFACtor (EMFAC) models. The focus of this paper is on the results and implications of the emissions of nitrogenous species that were measured during the chassis dynamometer testing part of this larger study.

4.3. Materials and Methods

4.3.1. Test Vehicles

The main technical specifications for each of the fourteen vehicles in this study are provided in Table 4.1. All test vehicles were equipped with model year 2009 and later engines, with the exception of one earlier model year 2000 engine which was retrofitted with a DPF in 2013. They included a variety of different vocations, including transit buses, school buses, refuse haulers, delivery trucks, and goods movement trucks.

It should be noted that a subset of eight CNG vehicles were also tested but are not included in this paper due to a measurement issue that was identified. In particular, it was found that these CNG vehicles showed some exhaust leaks that caused ambient air to be drawn into the tailpipe section prior to the TWC under the vacuum created by the CVS system. This in turn created an oxygen-rich environment for the catalyst, such that NOx emissions were not converted over the catalyst, resulting in unrepresentatively high idle emissions. Note that this issue would not be observed under typical operating conditions, where the exhaust is not subject to a CVS vacuum, and this was demonstrated by some additional tests. This issue is discussed in greater detail in the supporting information. It should be noted that the observation of an inward leak under idle conditions raises the

possibility that outward leaks of pre-catalyst exhaust emissions could be leaking outward under higher load conditions. The evaluation of this possibility was beyond the scope of the current study, however, but will likely be further explored in future studies.

Table 4.1 Testing Vehicles Specification

Test ID	Vocation	MY	Disp. (L)	Mileage	Test Fuel	Aftertreatment System
Diesel (No SCR) #1	School Bus	2000	7.2	312,185	ULSD/RD	DOC/DPF
Diesel (No SCR) #2	Goods Movement	2009	12.8	18,071	ULSD/RD	DOC/DPF
0.2Diesel #1	Delivery	2011	11.9	79,246	ULSD/RD	DOC/DPF/SCR
0.2Diesel #2	Delivery	2016	8.9	31,816	ULSD/RD	DOC/DPF/SCR
0.2Diesel #3	Goods Movement	2014	12.8	475,197	ULSD/RD	DOC/DPF/SCR
0.2Diesel #4	Goods Movement	2015	11.9	329,480	ULSD/RD	DOC/DPF/SCR
0.2Diesel #5	Goods Movement	2015	12.8	123,647	ULSD	DOC/DPF/SCR
Diesel-Electric	Delivery	2013	5.1	72,388	ULSD	DOC/DPF/SCR
0.2CNG high emitter	Transit Bus	2011	8.9	392,006	CNG	TWC (likely nonfunctional)
0.2CNG #1	Transit Bus	2009	8.9	376,912	CNG	TWC
0.2CNG #2	Delivery	2017	11.9	255,619	CNG	TWC
0.02CNG #1	Refuse	2017	8.9	33,358	CNG	TWC
0.02CNG #2	Goods Movement	2017	11.9	119,514	CNG	TWC
0.02CNG #3	Goods Movement	2018	11.9	58,205	CNG	TWC

4.3.2. **Test Cycles**

Each vehicle selected for chassis dynamometer testing was tested over several driving cycles. All vehicles were tested over the Urban Dynamometer Driving Schedule (UDDS), allowing the UDDS test results to serve as a cross-vocational comparison point for all vehicles. Additionally, each vehicle was tested over one or more vocational cycles. The vocational test cycles were assigned based on the vehicle vocation, as shown in Table 4.2. Delivery and goods movement vehicles were also tested with HHDDT cruise cycles. Test cycles were conducted as hot starts in triplicate with a 20-minute soak between tests. One cold start was conducted on the UDDS cycle for each vehicle. The test weights utilized for testing were based on average test weights obtained during the activity data collection portion of this study, with the exception of one box truck that had a considerably lower GVWR.

Table 4.2 Test cycles and test weights

Test ID	UDDS (CS+3xHS)	Vocational Cycle (HSx3)	HHDDT Cruise (HSx3)	Test weight
Diesel (No SCR) #1	Yes	School Bus Cycle	No	32500
Diesel (No SCR) #2	Yes	Goods Movement Cycle	Yes	69500
0.2Diesel #1	Yes	Delivery Cycle	Yes	56000
0.2Diesel #2	Yes	Delivery Cycle	Yes	56000
0.2Diesel #3	Yes	Goods Movement Cycle	Yes	69500
0.2Diesel #4	Yes	Goods Movement Cycle	Yes	69500
0.2Diesel #5	Yes	Goods Movement Cycle	Yes	69500
Diesel-Electric	Yes	Delivery Cycle	Yes	16000
0.2CNG high emitter	Yes	OCTA	No	32500
0.2CNG #1	Yes	OCTA	No	32500
0.2CNG #2	Yes	Delivery Cycle	Yes	56000
0.02CNG #1	Yes	Refuse Cycle (w grade change)	No	56000
0.02CNG #2	Yes	Goods Movement Cycle	Yes	69500
0.02CNG #3	Yes	Goods Movement Cycle	Yes	69500

4.3.3. Test Fuels

The diesel vehicles were tested with commercial grade #2, ultra-low sulfur diesel fuel. Commercially available fuel was considered to be more representative of what in-use vehicles would be using during normal in-use operation than certification fuel. Similarly, for the CNG vehicles, locally supplied, commercially available CNG was used in the testing. A subset of the diesel vehicles was also tested on a retail HVO/RD.

4.3.4. Emissions Measurements and Analysis

All testing was performed at CE-CERT's Heavy-Duty Chassis Dynamometer facility, consisting of an electric AC type design chassis dynamometer that can simulate inertia loads from 10,000 lb to 80,000 lb, which covers a broad range of in-use medium and heavy-duty vehicles. Emissions measurements were obtained using CE-CERT's Mobile Emissions Laboratory (MEL). At the entrance to the CVS, an exhaust flow rate meter was installed to provide exhaust flow measurements that were used in conjunction with the raw exhaust concentration measurements to determine the raw exhaust mass emission rates. Detailed information of the facility and sampling setup have been discussed previously (Cocker et al., 2004).

The focus of the emissions measurements for this study are NOx, NH_3 and N_2O. NOx was measured using UCR's MEL with a chemiluminescence analyzer. Tailpipe NH_3 and N_2O measurements were made using a Horiba MEXA-ONE-QCL-NX quantum cascade laser infrared spectrometer (QCL). An FTIR was used for the measurement of engine out emissions. The FTIR used was a Horiba FTX-ONE-CS with a rate of one scan per 0.2 seconds, a cell volume of approximately 65 milliliters, and a pathlength of 2.4 meters. For the engine-out measurements, a section of the exhaust pipe between the

turbocharger to the aftertreatment system was removed and was replaced with a fabricated exhaust pipe that had provisions for installing a sample probe for the FTIR. In conjunction with these measurements, additional measurements were made of total hydrocarbon (THC), carbon monoxide (CO), non-methane hydrocarbon (NMHC), methane (CH_4), carbon dioxide (CO_2), and PM mass, which will be discussed elsewhere.

4.4. **Results and Discussion**

4.4.1. **NOx Emissions**

NOx emissions for the test vehicles by vocation/technology group are shown for the cold start and hot start UDDS on a g/bhp-hr basis in Figure 4.1, on a g/mile basis in Table 4.3. Figure 4.2 shows the hot start NOx emissions for the UDDS cycles, vocational cycles based on each vehicle's vocation, and the HHDDT cruise cycles for delivery and goods movement vehicles on a g/mile basis. In-use PEMS data based on real-driving conditions and activities are also included in Figure 2 to provide a comparison between the chassis dynamometer and actual driving. The in-use, real-world PEMS data are discussed in greater detail in a previously published paper (McCaffery et al., 2021). Figure 4.1 and Figure 4.2 also include a zoomed in figure for the 0.02 g CNG vehicles to better show their low emission rates.

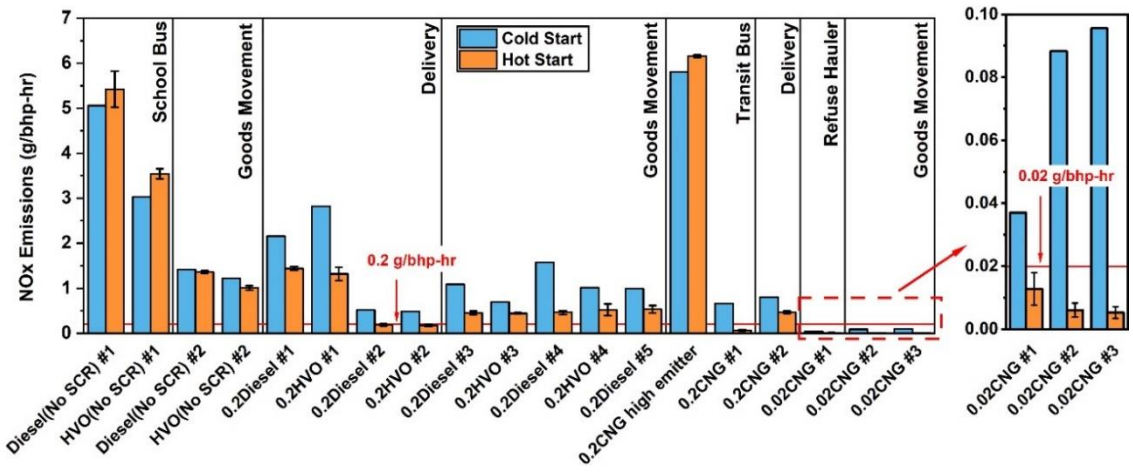

Figure 4.1 Chassis NOx emissions for UDDS cycle (g/bhp-hr)

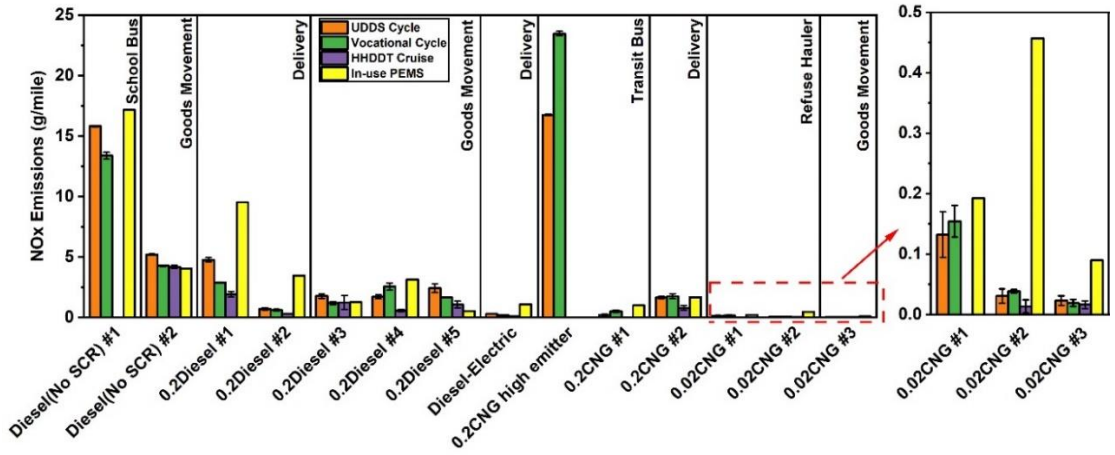

Figure 4.2 Chassis NOx emissions for UDDS cycles, Vocational cycles, HHDDT cruise cycles and in-use PEMS (g/mile)

Table 4.3 Chassis NOx emissions for UDDS cycle (g/bhp-hr and g/mile)

		NOx			
		g/bhp-hr		g/mile	
		Cold Start	Hot Start	Cold Start	Hot Start
School Bus	Diesel (No SCR) #1	5.06	5.42 ± 0.40	15.74	15.80 ± 0.06
	HVO (No SCR) #1	3.03	3.54 ± 0.11	9.31	9.70 ± 0.39
Goods Movement Vehicle	Diesel (No SCR) #2	1.42	1.36 ± 0.03	5.91	5.18 ± 0.06
	HVO (No SCR) #2	1.22	1.01 ± 0.05	5.68	4.32 ± 0.10
Delivery Vehicle	0.2Diesel #1	2.16	1.44 ± 0.04	7.32	4.75 ± 0.17
	0.2HVO #1	2.82	1.32 ± 0.15	9.67	4.48 ± 0.48
	0.2Diesel #2	0.52	0.19 ± 0.02	2.21	0.69 ± 0.10
	0.2HVO #2	0.49	0.18 ± 0.02	2.02	0.67 ± 0.09
Goods Movement Vehicle	0.2Diesel #3	1.09	0.45 ± 0.04	4.84	1.75 ± 0.19
	0.2HVO #3	0.70	0.44 ± 0.02	3.60	1.70 ± 0.01
	0.2Diesel #4	1.58	0.46 ± 0.04	5.10	1.70 ± 0.17
	0.2HVO #4	1.01	0.52 ± 0.13	3.85	1.77 ± 0.23
	0.2Diesel #5	0.99	0.53 ± 0.08	4.74	2.40 ± 0.36
Delivery Vehicle	Diesel-Electric*	-	- -	1.58	0.27 ± 0.01
Transit Bus	0.2CNG high emitter	5.81	6.16 ± 0.03	17.21	16.74 ± 0.06
	0.2CNG #1	0.66	0.07 ± 0.01	2.24	0.20 ± 0.04
Delivery Vehicle	0.2CNG #2	0.80	0.47 ± 0.03	3.47	1.62 ± 0.10
Refuse Hauler	0.02CNG #1	0.04	0.01 ± 0.01	0.17	0.13 ± 0.04
Goods Movement Vehicle	0.02CNG #2	0.09	0.01 ± 0.00	0.43	0.03 ± 0.01
	0.02CNG #3	0.10	0.01 ± 0.00	0.43	0.02 ± 0.01

*Power based emissions factor may not be applicable for diesel-electric hybrid vehicles

For the UDDS cycle, NOx emissions varied depending on the vocation and the technology. Average NOx emissions across all vehicles ranged from 0.003 to 6.16 g/bhp-hr and from 0.02 to 17.2 g/mile. Based on the hot start UDDS cycle, the highest NOx emissions were found for the transit bus 0.2CNG high emitter. The diesel (No SCR) and

HVO (No SCR) school bus showed the second highest NOx emissions, ranging around 3.5 to 5.42 g/bhp-hr (9.7 to 15.8 g/mile). The diesel/HVO (no SCR) goods movement vehicle also had relatively high emissions, but these were comparable to the 1.2 g/bhp-hr certification standard for that engine vintage. The SCR-equipped 0.2 g diesel/HVO vehicles in the delivery and goods movement categories showed significantly lower hot start UDDS emissions than the Diesel/HVO (No SCR) vehicles in the school bus and goods movement categories except for 0.2Diesel/HVO #1. The 0.2 g diesel vehicles excluding 0.2Diesel/HVO #1 showed a range of 0.18 to 0.46 g/bhp-hr for the hot start UDDS, which is within 2.5 times higher than the certification standard. The SCR-equipped delivery vehicle 0.2Diesel/HVO #1, on the other hand, showed an even higher emissions rate than the no SCR-equipped goods movement vehicle Diesel/HVO (No SCR) #2. For the other 0.2 g diesel vehicles, the NOx emissions reduction efficiencies for SCR systems were around 80% for the hot start UDDS. The 0.2Diesel #1 vehicle, however, had an SCR efficiency of 60% and showed NOx emissions rates up to seven times higher than the standard of 0.2 g/bhp-hr. This can be attributed to lower aftertreatment temperature conditions (much below 250 °C), as discussed below. The cold start UDDS emissions for all the 0.2 g diesel vehicles were higher than those for the hot start UDDS, ranging from 0.49 to 1.58 g/bhp-hr, for the vehicles excluding 0.2Diesel/HVO #1.

From Figure 4.2, emissions from both diesel (no SCR) vehicles for the vocational cycles and the in-use PEMS testing were similar to the UDDS cycles, suggesting engine-out emissions were not heavily cycle dependent. In contrast, the vocational cycle NOx emissions for most of the 0.2 g diesel vehicles were lower than those for the UDDS cycle, ranging from 0.6 to 2.9 g/mile, except for goods movement vehicle 0.2Diesel #4. For the

0.2 g diesel vehicles, the in-use PEMS NOx emissions were higher than those over the vocational and UDDS cycles, except for goods movement vehicles 0.2Diesel #3 and #5, suggesting, for most of cases, that there were elements of the in-use operations that are still not necessarily captured in the vocational cycles. The higher emissions from the in-use PEMS testing can be attributed to many factors, such as the strong influence of SCR temperature on NOx reduction efficiencies, frequent stop-go events, and long idling times or engine on/off events, which have been explained in more detail in a previously published paper (McCaffery et al., 2021). In addition, during the in-use PEMS testing, some of the highest emitting diesel vehicles, NOx emissions remained elevated even during periods when the SCR temperature was above 250 °C during the in-use PEMS testing, suggesting the possible malfunction or deterioration of the SCR system or inadequate urea dosing (McCaffery et al., 2021). NOx emissions for 0.2 g diesel vehicles tested in this study appeared to be more dependent on the engines/aftertreatment conditions and vehicle group, rather than the pattern of test cycles (i.e., transient, cruise, idling).

NOx emissions for the HHDDT cruise cycles showed similar or lower NOx emissions compared to those for the UDDS cycles, the vocational cycles, and the in-use PEMS testing for all the vehicles in delivery and goods movement categories, except for the goods movement vehicle 0.2Diesel #5. This vehicle in particular showed lower NOx emissions for in-use PEMS testing than those for the HHDDT cruise cycles due to higher exhaust temperatures. The HHDDT cruise cycle is essentially a steady-state cycle, which stimulates highway driving with a high engine speed and catalyst temperature. As the SCR generally operates at a higher temperature, NOx emissions for HHDDT cruise are expected to be lower for most vehicles compared to the more urban/vocational cycles. Several

researchers have conducted emissions testing for MY2010+ heavy-duty diesel trucks (Jiang et al., 2018). Results from these studies have shown comparable emission rates to most of the vehicles in this study except for 0.2Diesel/HVO #1, with emission rates in general within 2 times of the 0.2 g/bhp-hr standard.

The potential benefits of biomass derived renewable diesel were also evaluated in the study. The results from Figure 4.1 show that HVO provided significant reductions in NOx emissions for the diesel (no SCR) vehicles. HVO showed reductions of 35% and 26% for the Diesel no SCR#1 and Diesel no SCR #2 vehicles, respectively. The results in this study agree with those at other studies that have shown lower NOx emissions with HVO compared to diesel fuel for no SCR engines/vehicles (Heikkilä et al., 2012; Karavalakis et al., 2016b; Mueller et al., 2009; Murtonen et al., 2010; Na et al., 2015). The lower NOx emissions with HVO are due to the absence of aromatics in the fuel, resulting in lower combustion temperatures and less formation of thermal NOx (Glaude et al., 2010). Additionally, the higher cetane number of HVO reduces ignitions delay, which can reduce the fraction of fuel burned during the premixed phase of the combustion event (Happonen et al., 2012; Heikkilä et al., 2012). The 0.2 g diesel vehicles with model years newer than 2010 showed more similar emissions between diesel fuel and HVO, that were generally comparable within the experimental variability for the hot start UDDS. Results were more mixed for the cold start UDDS, with some vehicles showing higher emissions for the diesel fuel (0.2Diesel/HVO#3 and 0.2Diesel/HVO#4) and others showing higher emissions for the HVO (0.2Diesel/HVO#1).

The diesel hybrid delivery vehicle seen in Figure 4.2 showed emission rates of 1.58 g/mile for the cold start UDDS and 0.27 g/mile for the hot start UDDS. Note that the diesel

electric vehicle is not included in Figure 1, since the bhp-hr values only account for the work done by the engine, and not the electric motor, and hence these values would not be representative of the full work being performed by the vehicle. The diesel electric vehicle showed emissions that were lower than the other 0.2 g diesel vehicles for the UDDS and vocational cycles, and that were also comparable to or lower than those for the 0.2 g CNG vehicles. It is also noted from Table 4.4 that the cold start UDDS emissions for diesel-electric hybrid were more comparable to those the 0.2 g diesel and 0.2 g CNG vehicles.

NOx emission results for the 0.2 g CNG vehicles differed for each vehicle over both cold and hot start UDDS. The 0.2CNG high emitter showed tailpipe NOx emissions levels of around 5.81 g/bhp-hr for the cold start UDDS cycle and 6.16 g/bhp-hr for the hot start UDDS cycle, which were close to the engine-out levels. This vehicle did not show any on board diagnostic (OBD) error codes before the testing, although was likely equipped with a damaged or fully deteriorated TWC that needed to be maintained/replaced. Follow-up discussions with the fleet indicated that the engine was rebuilt and a new TWC was installed in this vehicle. Transit bus 0.2CNG #1, on the other hand, showed significantly lower emissions than the delivery vehicle over the hot start UDDS cycle, with an emissions rate of 0.07 g/bhp-hr and 0.2 g/mile. Compared to the 0.2 g diesel vehicles, the transit bus 0.2CNG#1 showed good NOx reductions. Emission rates for delivery vehicle 0.2CNG#2 were higher than the 0.2 engine certification level, with an emissions rate of 0.47 g/bhp-hr and 1.62 g/mile. NOx emissions from the 0.2 g CNG vehicles for the in-use PEMS testing showed mixed results compared to the UDDS cycle, with the delivery vehicle 0.2CNG#2 showing similar emissions to the UDDS cycle, while the transit bus 0.2CNG#1 showed higher emissions than the UDDS cycle. Previous studies have shown the potential for lower

NOx emissions for 0.2 g CNG vehicles compared to diesel vehicles. Many researchers have conducted emissions testing for 0.2 g stoichiometric natural gas vehicles with TWC using chassis dynamometers and PEMS, which have shown the NOx emissions rates vary from around 1 g/mile over cruise cycles and around 10 g/mile over more transient cycles (Hajbabaei et al., 2013; Li et al., 2019)

The 0.02 g CNG vehicles generally showed emissions that were considerably lower than those for the other vehicle technologies. The 0.02 g CNG vehicles in the refuse and goods movement category showed much lower emissions with emission rates ranging from 0.04 to 0.1 g/bhp-hr and from 0.17 to 0.43 g/mi for the UDDS cold start phase and around 0.01 g/bhp-hr and from 0.02 to 0.13 g/mi for the UDDS hot start. NOx emissions from 0.02 g CNG vehicles for in-use PEMS showed similar emissions to the UDDS for the refuse hauler 0.02CNG#1, and with the goods movement 0.02CNG #2 and #3 showing higher emissions for the in-use PEMS compared to the UDDS. Several recent studies have showed NOx emissions below or close to the CARB optional low NOx emission standard of 0.02g/bhp-hr for several heavy-duty vehicles over a range of hot-start cycles (Li et al., 2019; Zhu et al., 2020).

4.4.2. **Nitrous Oxide (N_2O) and Ammonia (NH_3) Emissions**

NH_3 and N_2O emissions are also pollutants of concern for air quality and global warming. NH_3 and N_2O emissions for cold start and hot start UDDS cycles in g/bhp-hr and g/mile units for all tested vehicles are provided in Table 4.4. It is shown that the no SCR equipped vehicles tested with both diesel fuel and HVO had very low or close to measurement limit emissions of NH_3 and N_2O. This is expected as both NH_3 and N_2O are mostly formed on the surface of the catalyst, such as TWC for the CNG vehicles or DPF-

SCR for the 0.2 g diesel vehicles, rather than as direct products of combustion (Heeb et al., 2006). The low level of engine out emission levels of N_2O and NH_3 emissions (below 5 ppm for the entire cycle) for the diesel (no SCR) vehicles, are shown in greater detail in Figure 4.3 and Figure 4.4 below.

The delivery and goods movement diesel vehicles equipped with SCR and diesel-electric hybrid vehicle showed similarly low or close to measurement limit levels of NH_3 emissions, except for 0.2Diesel/HVO #1 and 0.2Diesel/HVO #3 over hot start UDDS cycle. Studies have shown that improper urea injection in an SCR catalyst or general catalyst degradation can lead to excess NH_3 emissions, which is termed as "ammonia slip". Higher NH_3 emissions are mainly attributed to catalyst temperature, catalyst degradation and optimization of urea injection (Girard et al., 2007; Johnson, 2010; Lambert, 2019; Thiruvengadam et al., 2015). The delivery vehicle 0.2Diesel #1 and goods movement vehicle 0.2Diesel #3 had NH_3 emissions of about 0.19 (0.63 g/mile) and 0.02 g/bhp-hr (0.08 g/mile), respectively, for the hot start UDDS cycle. The cold start NH_3 UDDS emissions, on the other hand, were lower for these vehicles compared to the hot start UDDS results, since urea is not injected until later in the cycle when the catalyst was warmed up. In addition, NH_3 emissions for the hot start UDDS cycle from 0.2Diesel/HVO #1 equipped with a MY2011 engine were about 10 times higher than those from 0.2Diesel/HVO #3 with a MY 2014 engine. Interestingly, higher NOx emissions were found for 0.2diesel/HVO #1, which suggests that the higher NH_3 emissions, which could be due to more catalyst degradation for the older engine resulting in a lower SCR catalyst reduction efficiency. The 0.2HVO #1 vehicle showed lower NH_3 emissions than 0.2Diesel #1, but the opposite trend was found for 0.2 Diesel/HVO #3, suggesting that fuel effects may play a less important

role in NH_3 formation than other factors, such as catalyst conditions and optimization of urea injection. The comparable or low NH_3 emissions results seen from this study agree with the findings from other studies that NH_3 emissions can form for diesel vehicles equipped with SCR (Girard et al., 2007; Livingston et al., 2009; Thiruvengadam et al., 2016).

Unlike SCR equipped diesel vehicles, CNG vehicles have characteristically high NH_3 emissions due to NH_3 formation across the TWC catalyst under slightly rich conditions for stoichiometric engines. Specifically, NH_3 forms in the catalyst from the reaction of NO and H_2 through the water gas shift reaction, as discussed in section 3.3. Except for the 0.2CNG high emitter vehicle, NH_3 emissions for the hot start UDDS cycle for the 0.2 g CNG and 0.02 g CNG vehicles ranged from 0.13 to 0.34 g/bhp-hr and from 0.44 to 0.97 g/mile. The NH_3 emission rates were comparable to the NOx emission rates for the 0.2 g CNG vehicles, while NH_3 emission rates were higher than the NOx emission rates for the 0.02g CNG vehicles, indicating the importance of NH_3 emissions for CNG vehicles. NH_3 emissions from cold start UDDS cycles did not show any correlation to hot start cycle NH_3 emissions for the same vehicle, which is likely due to the catalyst temperature being below the light-off temperatures when NH_3 can form for a greater percentage of the cycle for the cold-start tests. NH_3 emissions for the 0.2CNG high emitter, on the other hand, were very low, consistent with the NOx emission findings that the TWC showed no catalytic activity. NH_3 emissions from this study are comparable to those from previous studies on heavy-duty CNG vehicles equipped with TWC, which ranged from 0.8 to 1.2 g/mile for most of the vehicles, although some vehicles did show higher NH_3 emissions (Thiruvengadam et al, 2016,Karavalakis et al, 2016a, Zhu et al, 2020).

N_2O emissions exhibited some correlation with NH_3 emissions for most of the diesel vehicles. For the 0.2Diesel/HVO #1 and 0.2Diesel/HVO #3 vehicles, which had higher NH_3 emissions, their N_2O emission rates were also high, with emissions rates of 0.60 g/bhp-hr (1.98 g/mile) and 0.19 g/bhp-hr (0.74 g/mile), respectively. The 0.2Diesel/HVO #2, 0.2Diesel/HVO #4 and diesel-electric hybrid vehicles, on the other hand, emitted very low or close to measurement limit levels for N_2O and NH_3 emissions. Interestingly, 0.2Diesel #5 showed low NH_3 emissions, but high N_2O emissions. Studies have shown that N_2O emissions for SCR equipped diesel vehicles can be formed from the oxidation of NH_3 at high temperatures or the decomposition of ammonium nitrite at lower temperatures and relatively high NO_2/NO ratios (~50%) (Madia et al., 2002). Therefore, the phenomenon of high N_2O emissions and low NH_3 emissions for 0.2Diesel #5 could be attributed to these reactions at lower catalyst temperatures and high N_2O/NO ratios. This phenomenon will be further discussed in the following sections.

N_2O emissions for natural gas vehicles showed some variance between vehicles with different engine technologies. N_2O also forms via reactions on the TWC surface, as discussed in section 3.3. Hot start UDDS N_2O emissions ranged from 0.09 g/bhp-hr (0.25 g/mile) to 0.16 g/bhp-hr (0.55 g/mile) for the 0.2 g CNG vehicles, except for the 0.2CNG high emitter, and from 0.01 g/bhp-hr (0.06 g/mile) to 0.02 g/bhp-hr (0.08 g/mile) for the 0.02 g CNG vehicles. N_2O emissions for the 0.2CNG high emitter, on the other hand, were very low, consistent with TWC not showing any catalytic activity. N_2O emissions were more prevalent for the cold-start cycles, which is consistent with previous studies that have shown N_2O is generally formed over the surface of the TWC during its initial warm up period (Huai et al., 2004). Cold start UDDS emissions for 0.2 g CNG vehicles range from

0.11 g/bhp-hr (0.37 g/mile) to 0.17 g/bhp-hr (0.73 g/mile), which are around 10 times higher than those from the 0.02 g CNG vehicles, which had emissions rates ranging from 0.01 g/bhp-hr (0.06 g/mile) to 0.02 g/bhp-hr (0.08 g/mile). Many studies have found that N_2O emissions from gasoline and natural gas stoichiometric burn spark-ignited engines are correlated with air fuel ratio (Hiroyasu and Kadota, 1976; Li et al., 2021). The lower N_2O emissions seen from the 0.02 g CNG vehicles compared to the 0.2 g CNG vehicles could be attributed to the better air-fuel ratio control for the more advanced engine technology. The N_2O emission levels found in this study are comparable to those seen in previous studies. For example, (Karavalakis et al., 2016a)found N_2O emissions for two 0.2 g CNG vehicles equipped with stochiometric burn 9L and 12L Cummins engines were on the order of 0.12 g/mi and 0.35 g/mile, respectively.

Table 4.4 NH_3 and N_2O emissions for cold start and hot start UDDS cycle in units of g/bhp-hr and g/mile

		NH_3							
		g/bhp-hr				g/mile			
		Cold Start	Hot Start			Cold Start	Hot Start		
School Bus	Diesel (No SCR) #1	0.00	0.00	±	0.00	0.00	0.00	±	0.00
	HVO (No SCR) #1	0.00	0.00	±	0.00	0.00	0.00	±	0.00
Goods Movement Vehicle	Diesel (No SCR) #2	0.00	0.00	±	0.00	0.00	0.00	±	0.00
	HVO (No SCR) #2	0.00	0.00	±	0.00	0.00	0.00	±	0.00
Delivery Vehicle	0.2Diesel #1	0.09	0.19	±	0.02	0.30	0.63	±	0.05
	0.2HVO #1	N/A	0.15	±	0.01	N/A	0.50	±	0.03
	0.2Diesel #2	0.00	0.00	±	0.00	0.00	0.00	±	0.00
	0.2HVO #2	0.00	0.00	±	0.00	0.00	0.00	±	0.00
Goods Movement Vehicle	0.2Diesel #3	0.01	0.02	±	0.00	0.03	0.08	±	0.01
	0.2HVO #3	0.00	0.03	±	0.01	0.00	0.11	±	0.02
	0.2Diesel #4	0.00	0.00	±	0.00	0.00	0.02	±	0.00
	0.2HVO #4	0.00	0.00	±	0.00	0.00	0.00	±	0.00
	0.2Diesel #5	0.00	0.00	±	0.00	0.00	0.01	±	0.01
Delivery Vehicle	Diesel-Electric	0.00	0.00	±	0.00	0.00	0.00	±	0.00
Transit Bus	0.2CNG high emitter	0.00	0.00	±	0.00	0.00	0.01	±	0.00
	0.2CNG #1	0.27	0.34	±	0.06	0.92	0.97	±	0.16
Delivery Vehicle	0.2CNG #2	0.13	0.13	±	0.04	0.56	0.44	±	0.12
Refuse Hauler	0.02CNG #1	0.19	0.17	±	0.02	0.87	0.79	±	0.08
Goods Movement Vehicle	0.02CNG #2	0.18	0.17	±	0.01	0.86	0.87	±	0.06
	0.02CNG #3	0.10	0.16	±	0.01	0.47	0.70	±	0.05

Table 4.4 (continued) NH_3 and N2O emissions for cold start and hot start UDDS cycle in units of g/bhp-hr and g/mile

		N_2O							
		g/bhp-hr				g/mile			
		Cold Start	Hot Start			Cold Start	Hot Start		
School Bus	Diesel (No SCR) #1	0.01	0.01	±	0.00	0.02	0.04	±	0.01
	HVO (No SCR) #1	0.01	0.01	±	0.01	0.04	0.03	±	0.02
Goods Movement Vehicle	Diesel (No SCR) #2	0.00	0.00	±	0.00	0.00	0.00	±	0.00
	HVO (No SCR) #2	0.01	0.01	±	0.00	0.03	0.04	±	0.01
Delivery Vehicle	0.2Diesel #1	0.22	0.60	±	0.13	0.75	1.98	±	0.40
	0.2HVO #1	N/A	0.47	±	0.02	N/A	1.61	±	0.08
	0.2Diesel #2	0.01	0.02	±	0.00	0.06	0.09	±	0.02
	0.2HVO #2	0.03	0.06	±	0.01	0.12	0.21	±	0.03
Goods Movement Vehicle	0.2Diesel #3	0.28	0.19	±	0.02	1.24	0.74	±	0.08
	0.2HVO #3	0.15	0.23	±	0.03	0.79	0.90	±	0.11
	0.2Diesel #4	0.04	0.00	±	0.01	0.14	0.00	±	0.03
	0.2HVO #4	0.00	0.05	±	0.01	0.00	0.19	±	0.03
	0.2Diesel #5	0.16	0.16	±	0.03	0.74	0.70	±	0.16
Delivery Vehicle	Diesel-Electric	0.03	0.04	±	0.00	0.06	0.06	±	0.00
Transit Bus	0.2CNG high emitter	0.03	0.03	±	0.00	0.08	0.09	±	0.00
	0.2CNG #1	0.11	0.09	±	0.03	0.37	0.25	±	0.10
Delivery Vehicle	0.2CNG #2	0.17	0.16	±	0.01	0.73	0.55	±	0.03
Refuse Hauler	0.02CNG #1	0.02	0.01	±	0.00	0.08	0.06	±	0.02
Goods Movement Vehicle	0.02CNG #2	0.01	0.00	±	0.00	0.06	0.00	±	0.01
	0.02CNG #3	0.02	0.01	±	0.00	0.07	0.04	±	0.01

4.4.3. Real-Time Emissions Profiles

4.4.3.1. Real-Time Emissions Profile for Diesel Vehicle

Figure 4.3(a-g) shows real-time emissions profiles for NOx, NH_3, and N_2O emissions, including engine out emissions, and the SCR inlet temperature and vehicle speed profiles for the 0.2Diesel#1 delivery vehicle on a hot start UDDS cycle. This is the 0.2 diesel vehicle that had the highest NOx, NH_3, and N_2O emissions, so it provides a good example of the formation mechanisms of these pollutants. Figure 4.3 (a) shows that NOx emissions accumulated during the cold start phase during the first 400s where the SCR catalyst was below 250 °C. Figure 4.3 (c) also shows that the tailpipe NO concentrations in this period are similar in magnitude with the engine out NO concentrations, indicating that the SCR is not providing significant reductions under these conditions. At 400s, the catalyst reached around 250 °C and NH_3 emissions started to accumulate, suggesting that urea injection began. Accordingly, the SCR efficiency for NO and NO_2 emissions improved, as seen by comparing the engine out and tailpipe emissions concentrations in Figure 4.3 (d). As the urea injection and NOx reduction reaction began, from approximately cycle time 400s to 450s, a corresponding increase in NH_3 emissions was seen. NH_3 emissions remained at a high level for the rest of the cycle with a peak concentration of 150 ppm, which is comparable to the tailpipe NO emissions level peaking around 200 ppm.

Figure 4.3f shows that tailpipe N_2O emissions were only observed for a limited number of driving conditions, with peaks right after the cold start and a peak at around 450 seconds. The engine-out N_2O emissions emitted by this engine were less than 2 ppm, which is consistent with the expectation that most N_2O emissions form on the catalyst surface, as

opposed to during combustion. Studies have shown that the formation mechanism for N_2O on a SCR catalyst surface can be understood in the context of the following reactions at temperatures above 200 °C (Madia et al., 2002). The N_2O emissions peak between 400 to 450 seconds could be attributed to this pathway, as the SCR is warmed up to a temperature range of above 200 °C and as NH_3 emissions are present on the catalyst surface. Smaller N_2O peaks were also seen around 600 and 700 seconds, which is where NOx also tended to peak during the main highest speed driving portion of the cycle.

$$2NH_3 + 2O_2 \rightarrow N_2O + 3H_2O$$

$$4NH_3 + 4NO + 3O_2 \rightarrow 4N_2O + 6H_2O$$

There is also a spike in N_2O emissions at the beginning of the test, when the catalyst was below 200 °C, and N_2O emissions would not form from these reactions. The N_2O emissions formed near the beginning of the test could form from decomposition of nitrite particles. As the urea is injected prior to the SCR, it can generate NH_4NO_3 particles that will decompose and generate N_2O emissions at lower temperatures of around 100°C to 200°C. This reaction is also favored under higher NO_2/NO ratios (Zhang et al., 2018). The elevated N_2O emissions during the start of the test are attributed to residual NH_4NO_3 particles. It is known that controlled thermal decomposition of NH_4NO_3 at low temperatures is a standard laboratory method of generating N_2O (Wallington and Wiesen, 2014).

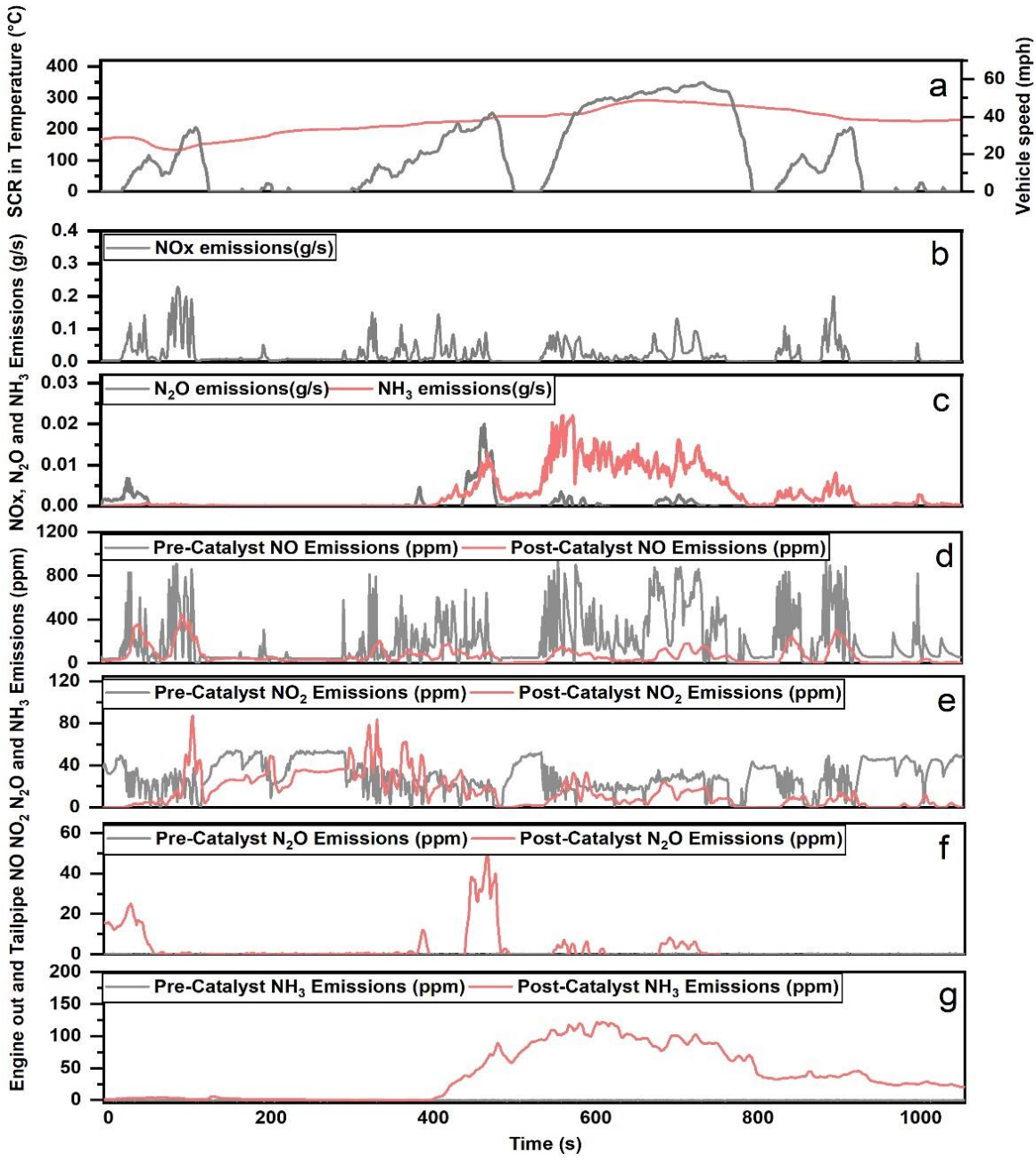

Figure 4.3 Real time tailpipe emissions(g/s), pre-catalyst and post catalyst emissions concentration(ppm) and catalyst intake temperature(°C) and cycle trace (mph) for 0.2Diesel #1 hot start UDDS cycle

4.4.3.2. **Real-Time Emissions Profile for Natural Gas Vehicle**

Figure 4.4(a-g) shows real-time emissions profiles for NOx, NH_3, and N_2O emissions, including engine out emissions, and the TWC inlet temperature and vehicle

speed profiles for the 0.02CNG#1 goods movement vehicle on a cold start UDDS cycle. Figure 4.4 shows higher NOx emissions were also seen during the cold start phase before 100s, when the TWC was below its light-off temperature. Once the TWC reaches its light-off temperature, NOx emissions drop significantly and remain at very low levels for the rest of the cycle. Compared to the SCR-equipped diesel vehicle, the CNG vehicle with a TWC took a shorter time to warm up, suggesting temperature fluctuations have less impact for the TWC-equipped CNG vehicles compared to the SCR-equipped diesel vehicles. This finding suggests the potential for CNG vehicles in reducing NOx emissions under certain more idling or stop-go conditions that can lead to cooler catalyst temperatures for diesel vehicles.

Higher NH_3 emissions from CNG vehicles are attributed to the following reaction of NO-H_2 and NO-CO under rich conditions and at temperatures above 250 °C:

$$2NO + 5H_2 \rightarrow 4NH_3 + 2H_2O$$

$$4NO + 4CO + 2H_2O + 2H_2 \rightarrow 2NH_3 + 4CO_2$$

Where H_2 is generally generated from the water-gas shift reaction and steam methane reforming as follows:

$$CO + H_2O \rightarrow CO_2 + H_2 \text{ (Water-Gas Shift)}$$

$$CH_4 + H_2O \rightarrow CO + 3H_2 \text{ (Steam Methane Reforming)}$$

N_2O is another byproduct from reactions of NO with CO and H_2 on the catalyst surface (Cant et al., 1998; Hirano et al., 1992; Prigent and De Soete, 1989).The formation of N_2O is favored at catalyst temperatures below 350°C (Nevalainen et al., 2018). It is clearly observed from Figure 4.4 that N_2O emissions from CNG vehicles form during the initial part of the cold start test (0 to 100 s) when the catalyst temperatures were below

350°C, and then remain at low levels for the rest of the cycle after the catalyst has lite-off. The observation in this study of N_2O emissions forming under lower temperature conditions is consistent with the findings from other studies (Hirano et al., 1992; Huai et al., 2004).

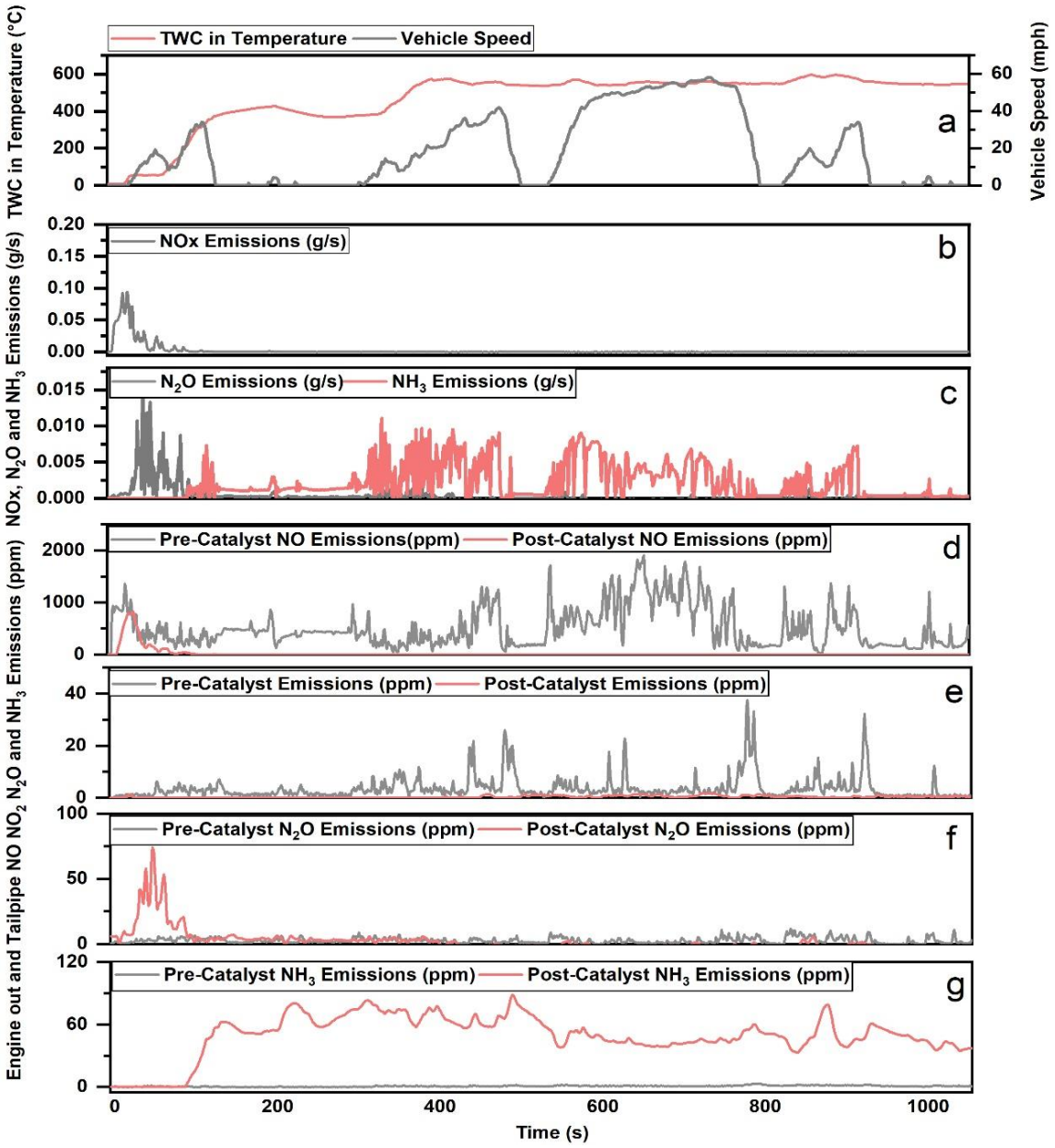

Figure 4.4 Real time tailpipe emissions (g/s), pre-catalyst and post catalyst emissions concentration(ppm) and catalyst intake temperature(°C) and cycle trace (mph) for 0.02 CNG #3 cold start UDDS cycle

4.5. **Conclusions**

NOx, N_2O and NH_3 emissions were measured from a fleet of 14 different heavy-duty vehicles over different drive cycles using a chassis dynamometer. The results showed that the UDDS NOx emissions varied depending on the vocation and the technology with average NOx emissions across all vehicles ranged from 0.003 to 6.16 g/bhp-hr. NOx emissions for vocational cycle and HHDDT cruise cycles showed some variances compared with the UDDS cycle but in the same range. For the 0.2 g diesel vehicles, the in-use PEMS NOx emissions were higher than those over the vocational and UDDS cycles, except for goods movement vehicles 0.2Diesel #3 and #5, suggesting, for most of cases, that there were elements of the in-use operations that are still not necessarily captured in the vocational cycles. HVO provided significant reductions in NOx emissions for diesel (no SCR) vehicles. The 0.2 g diesel vehicles with model years newer than 2010 showed more similar emissions between diesel fuel and HVO, that were generally comparable within the experimental variability for the hot start UDDS. NH_3 and N_2O emissions are also pollutants of concern for air quality and global warming, which originates from the catalyst reaction. N_2O emissions from SCR equipped diesel vehicles originate from the catalyst reaction involving NH_3 and NOx emissions as well as the decomposition of nitrite particles. The formation of N_2O for CNG vehicles is favored at catalyst temperatures below 350°C.

4.6. **Acknowledgements**

We acknowledge funding from the California Energy Commission (CEC), the South Coast Air Quality Management District (South Coast AQMD), Southern California Gas Company (SoCalGas), and the California Air Resources Board (CARB) under South Coast

AQMD contract number 17286. The authors thank Mark Villela, Daniel Gomez, and Dan Hartnett of the University of California, Riverside for their contribution in conducting the emissions testing for this program.

4.7. **Reference**

Bae WB, Byun SW, Hazlett M, Jung C, Kim CH, Kang SB. Emission of NH3 and N2O during NO reduction over commercial aged three-way catalyst (TWC): Role of individual reductants in simulated exhausts. Chemical Engineering Journal Advances 2022; 9: 100222.

Cant NW, Angove DE, Chambers DC. Nitrous oxide formation during the reaction of simulated exhaust streams over rhodium, platinum and palladium catalysts. Applied Catalysis B: Environmental 1998; 17: 63-73.

Cocker DR, Shah SD, Johnson K, Miller JW, Norbeck JM. Development and application of a mobile laboratory for measuring emissions from diesel engines. 1. Regulated gaseous emissions. Environmental science & technology 2004; 38: 2182-2189.

Girard JW, Cavataio G, Lambert CK. The Influence of Ammonia Slip Catalysts on Ammonia, N_2O and NO x Emissions for Diesel Engines. SAE Transactions 2007: 182-186.

Glaude P-A, Fournet R, Bounaceur R, Molière M. Adiabatic flame temperature from biofuels and fossil fuels and derived effect on NOx emissions. Fuel Processing Technology 2010; 91: 229-235.

Gong J, Rutland C. Three way catalyst modeling with ammonia and nitrous oxide kinetics for a lean burn spark ignition direct injection (SIDI) gasoline engine. SAE Technical Paper, 2013.

Grigoratos T, Fontaras G, Giechaskiel B, Zacharof N. Real world emissions performance of heavy-duty Euro VI diesel vehicles. Atmospheric environment 2019; 201: 348-359.

Guan B, Zhan R, Lin H, Huang Z. Review of state of the art technologies of selective catalytic reduction of NOx from diesel engine exhaust. Applied Thermal Engineering 2014; 66: 395-414.

Hajbabaei M, Karavalakis G, Johnson KC, Lee L, Durbin TD. Impact of natural gas fuel composition on criteria, toxic, and particle emissions from transit buses equipped with lean burn and stoichiometric engines. Energy 2013; 62: 425-434.

Happonen M, Heikkilä J, Murtonen T, Lehto K, Sarjovaara T, Larmi M, et al. Reductions in particulate and NO X emissions by diesel engine parameter adjustments with HVO fuel. Environmental science & technology 2012; 46: 6198-6204.

Heeb NV, Forss A-M, Brühlmann S, Lüscher R, Saxer CJ, Hug P. Three-way catalyst-induced formation of ammonia—velocity-and acceleration-dependent emission factors. Atmospheric Environment 2006; 40: 5986-5997.

Heikkilä J, Happonen M, Murtonen T, Lehto K, Sarjovaara T, Larmi M, et al. Study of Miller timing on exhaust emissions of a hydrotreated vegetable oil (HVO)-fueled diesel engine. Journal of the air & waste management association 2012; 62: 1305-1312.

Hirano H, Yamada T, Tanaka K, Siera J, Cobden P, Nieuwenhuys B. Mechanisms of the various nitric oxide reduction reactions on a platinum-rhodium (100) alloy single crystal surface. Surface science 1992; 262: 97-112.

Hiroyasu H, Kadota T. Models for combustion and formation of nitric oxide and soot in direct injection diesel engines. SAE transactions 1976: 513-526.

Huai T, Durbin TD, Miller JW, Norbeck JM. Estimates of the emission rates of nitrous oxide from light-duty vehicles using different chassis dynamometer test cycles. Atmospheric Environment 2004; 38: 6621-6629.

Jiang Y, Yang J, Cocker III D, Karavalakis G, Johnson KC, Durbin TD. Characterizing emission rates of regulated pollutants from model year 2012+ heavy-duty diesel vehicles equipped with DPF and SCR systems. Science of The Total Environment 2018; 619: 765-771.

Johnson TV. Review of diesel emissions and control. SAE International Journal of Fuels and Lubricants 2010; 3: 16-29.

Karavalakis G, Hajbabaei M, Jiang Y, Yang J, Johnson KC, Cocker DR, et al. Regulated, greenhouse gas, and particulate emissions from lean-burn and stoichiometric natural gas heavy-duty vehicles on different fuel compositions. Fuel 2016a; 175: 146-156.

Karavalakis G, Johnson KC, Hajbabaei M, Durbin TD. Application of low-level biodiesel blends on heavy-duty (diesel) engines: Feedstock implications on NOx and particulate emissions. Fuel 2016b; 181: 259-268.

Kotz AJ, Kittelson DB, Northrop WF. Lagrangian hotspots of in-use NOx emissions from transit buses. Environmental Science & Technology 2016; 50: 5750-5756.

Lambert CK. Perspective on SCR NO x control for diesel vehicles. Reaction Chemistry & Engineering 2019; 4: 969-974.

Li C, Han Y, Jiang Y, Yang J, Karavalakis G, Durbin TD, et al. Emissions from advanced ultra-low-NOx heavy-duty natural gas vehicles. 2019.

Li M, Tian H, Wei Z, Zhang Q, Shen B. Ammonia and nitrous oxide emissions of a stoichiometric natural gas engine operating with high caloric value and low caloric value fuels. Fuel 2021; 285: 119166.

Liu T, Wang X, Deng W, Zhang Y, Chu B, Ding X, et al. Role of ammonia in forming secondary aerosols from gasoline vehicle exhaust. Science China Chemistry 2015; 58: 1377-1384.

Livingston C, Rieger P, Winer A. Ammonia emissions from a representative in-use fleet of light and medium-duty vehicles in the California South Coast Air Basin. Atmospheric Environment 2009; 43: 3326-3333.

Madia G, Koebel M, Elsener M, Wokaun A. Side reactions in the selective catalytic reduction of NO x with various NO2 fractions. Industrial & Engineering Chemistry Research 2002; 41: 4008-4015.

McCaffery C, Zhu H, Tang T, Li C, Karavalakis G, Cao S, et al. Real-world NOx emissions from heavy-duty diesel, natural gas, and diesel hybrid electric vehicles of different vocations on California roadways. Science of The Total Environment 2021; 784: 147224.

Mendoza-Villafuerte P, Suarez-Bertoa R, Giechaskiel B, Riccobono F, Bulgheroni C, Astorga C, et al. NOx, NH_3, N_2O and PN real driving emissions from a Euro VI heavy-duty vehicle. Impact of regulatory on-road test conditions on emissions. Science of The Total Environment 2017; 609: 546-555.

Mueller CJ, Boehman AL, Martin GC. An experimental investigation of the origin of increased NOx emissions when fueling a heavy-duty compression-ignition engine with soy biodiesel. SAE International Journal of Fuels and Lubricants 2009; 2: 789-816.

Murtonen T, Aakko-Saksa P, Kuronen M, Mikkonen S, Lehtoranta K. Emissions with heavy-duty diesel engines and vehicles using FAME, HVO and GTL fuels with and without DOC+ POC aftertreatment. SAE International Journal of Fuels and Lubricants 2010; 2: 147-166.

Na K, Biswas S, Robertson W, Sahay K, Okamoto R, Mitchell A, et al. Impact of biodiesel and renewable diesel on emissions of regulated pollutants and greenhouse gases on a 2000 heavy duty diesel truck. Atmospheric Environment 2015; 107: 307-314.

Nevalainen P, Kinnunen NM, Kirveslahti A, Kallinen K, Maunula T, Keenan M, et al. Formation of NH3 and N2O in a modern natural gas three-way catalyst designed for heavy-duty vehicles: the effects of simulated exhaust gas composition and ageing. Applied Catalysis A: General 2018; 552: 30-37.

Prigent M, De Soete G. Nitrous Oxide N_2O in Engines Exhaust Gases-A First Appraisal of Catalyst Impact. SAE transactions 1989: 281-291.

Quiros DC, Thiruvengadam A, Pradhan S, Besch M, Thiruvengadam P, Demirgok B, et al. Real-world emissions from modern heavy-duty diesel, natural gas, and hybrid diesel trucks operating along major California freight corridors. Emission Control Science and Technology 2016; 2: 156-172.

Seyboth K. Intergovernmental panel on climate change (IPCC). Encyclopedia of Energy, Natural Resource, and Environmental Economics 2013.

Tan Y, Henderick P, Yoon S, Herner J, Montes T, Boriboonsomsin K, et al. On-board sensor-based NO x emissions from heavy-duty diesel vehicles. Environmental science & technology 2019; 53: 5504-5511.

Thiruvengadam A, Besch M, Carder D, Oshinuga A, Pasek R, Hogo H, et al. Unregulated greenhouse gas and ammonia emissions from current technology heavy-duty vehicles. Journal of the Air & Waste Management Association 2016; 66: 1045-1060.

Thiruvengadam A, Besch MC, Thiruvengadam P, Pradhan S, Carder D, Kappanna H, et al. Emission rates of regulated pollutants from current technology heavy-duty diesel and natural gas goods movement vehicles. Environmental science & technology 2015; 49: 5236-5244.

Wallington T, Wiesen P. N2O emissions from global transportation. Atmospheric Environment 2014; 94: 258-263.

Wang J, Chen H, Hu Z, Yao M, Li Y. A review on the Pd-based three-way catalyst. Catalysis Reviews 2015; 57: 79-144.

Weilenmann M, Favez J-Y, Alvarez R. Cold-start emissions of modern passenger cars at different low ambient temperatures and their evolution over vehicle legislation categories. Atmospheric environment 2009; 43: 2419-2429.

Weilenmann M, Soltic P, Saxer C, Forss A-M, Heeb N. Regulated and nonregulated diesel and gasoline cold start emissions at different temperatures. Atmospheric environment 2005; 39: 2433-2441.

Zhang Y, Lou D, Tan P, Hu Z. Experimental study on the particulate matter and nitrogenous compounds from diesel engine retrofitted with DOC+ CDPF+ SCR. Atmospheric Environment 2018; 177: 45-53.

Zhu H, McCaffery C, Yang J, Li C, Karavalakis G, Johnson KC, et al. Characterizing emission rates of regulated and unregulated pollutants from two ultra-low NOx CNG heavy-duty vehicles. Fuel 2020; 277: 118192.

5. Emissions From In-Use Heavy-Duty Diesel and Natural Gas Trucks - Part. 2 PM, Unregulated, and Greenhouse Gas (GHG)

5.1. Abstract

This study characterized particulate matter (PM), greenhouse gases (GHG), total hydrocarbon (THC), carbon monoxide (CO), and carbonyl emissions from a fleet of fourteen in-use heavy-duty vehicles of different vocations (school bus, transit bus, refuse hauler, delivery vehicle, and goods movement vehicle), fuels (diesel, hydrogenated vegetable oil [HVO], and CNG), engine types, and aftertreatment controls (SCR or TWC), and over Urban Dynamometer Driving Schedule (UDDS) cycles using a chassis dynamometer. Results showed PM emissions were below the 10 mg/bhp-hr certification for all vehicles over both cold and hot start cycles, with the exception for the goods movement vehicle Diesel (No SCR) #2 and one CNG vehicle with a non-functional catalysts. CNG vehicles showed generally higher total particle number emissions than the DPF diesel vehicles except for the vehicle equipped with a non-functional catalyst. CO_2 emissions are the main contributor to GHG emissions for all vehicles. CH_4 contributes the second largest to GHG emissions for CNG vehicles over most cycles. THC and CO emissions levels for diesel vehicles were at or below the background levels. Compared to the 0.2 CNG vehicles, the 0.02 CNG vehicles have lower N_2O CH_4 and CO emissions, which is attributed to more optimized air-fuel ratio. Formaldehyde and acetaldehyde emissions were comparable to other studies.

Keywords: CNG vehicles; Diesel vehicles; PM emissions; PN emissions; Greenhouse gas Emissions

5.2. **Introduction**

Particulate matter (PM) is considered an important risk factor for adverse health effects (WHO, 2013). Particulate matter with a diameter less than 2.5 μm ($PM_{2.5}$) represented the largest environmental risk for human health in 2019(Murray et al., 2020). Ultra-fine particles, which have diameters less than 100 nm, are also associated with short-term cardiorespiratory and nervous system disease. Compared to fine particles ($PM_{2.5}$), these smaller particles have higher surface area, which cause more pulmonary inflammation and stay longer in the lung(Schraufnagel, 2020).

Regulators and policy makers worldwide have been implementing regulations that will control the PM emissions. Particle emission standards worldwide are generally based on the PM mass emissions. In the United States (U.S.), the Environmental Protect Agency (EPA) has imposed more stringent emissions standards for light-duty or heavy-duty vehicles to regulate PM mass emissions in the recent years. More advanced emissions control systems such as diesel particulate filters (DPFs) for diesel vehicles and alternative fuels such as compressed natural gas, have been playing an important role in meeting PM mass standards. However, these advanced systems may be limited in reducing particle number emissions. Many recent studies have found that both DPF-equipped diesel vehicles and compressed natural gas vehicles emit more particle number emissions for the ultra-fine particles than larger size particles (Toumasatos et al., 2021). The European Union (EU) introduced solid particle number (SPN) emissions standards for diesel light-duty vehicles in 2011, which utilized the Particle Measurement Program (PMP) method to measure SPN

with a cut size of 23 nm (Giechaskiel et al., 2017). There are still questions about the methodology of measuring "real" particle number emissions, however, due to different sampling artifacts (i.e. the sampling system, sampling location, instrument measurement accuracy, and particle loss rates) that may lead to significantly different results. The U.S. has also been considering total particle number emissions as key factor of PN regulation. Therefore, it is important to show total particle number emissions with different cut size to compare the PM and PN emissions standards and provide insights on setting the appropriate cut size for PN emissions.

Greenhouse gas emissions have become more and more important due to global climate change. Carbon-dioxide (CO_2), nitrous oxide (N_2O) and methane (CH_4) are combustion products or catalyst artifacts from diesel or natural gas engines that need to be considered. Starting from 2017, U.S. EPA has regulated GHG emissions from medium- or heavy- duty vehicles based on the vocations of the engine (EPA, 2011). In 2020, the transportation sector accounted for 27% of total greenhouse gas emissions, representing the largest source of GHG emissions in the transportation sector (EPA, 2022). CO_2 emissions come mostly from burning fossil fuels such as diesel or natural gas in the combustion process, which represent the largest contributor of GHG emissions (EPA, 2020). CH_4 emissions in the transportation sector mainly come from natural gas vehicles, since the major component of natural gas fuel is CH_4. N_2O emissions are mostly observed during the cold start operation for spark-ignited engines. N_2O emissions are also commonly seen for TWC-equipped vehicles where N_2O is a byproduct of catalyst reactions.

The chemical and toxicological properties of emissions from vehicles with more advanced technologies are also a concern. Many studies have been investigating the impact

of advanced engine/aftertreatment technologies or fuel composition on emissions components with high toxicity(Li et al., 2021; Yoon et al., 2013). Yoon et al. showed stochiometric combustion with a three-way catalyst can be effective for reducing particulate compounds. Another recent study showed that renewable natural gas (RNG) may also be a strategy that could lead to reductions in the toxicity of the emissions.

The objective of this study is to evaluate THC, CO, greenhouse gases, carbonyls, and particulate mass/number emissions from 14 heavy-duty vehicles over UDDS cycle using a chassis dynamometer. These vehicles have different vocations (school bus, transit bus, refuse hauler, delivery vehicles, and goods movement vehicles), powered by different fuel (ultra-low sulfur diesels [ULSD], hydrogenated vegetable oil [HVO], and CNG), different engine types, and emissions control aftertreatment systems (SCR or TWC). The characteristics of the particulate emissions were also characterized to understand their formation mechanism.

5.3. **Materials and Methods**

5.3.1. **Test Vehicles**

The main technical specifications for each of the 13 vehicles in this study are given in Table 5.1. All test vehicles were equipped with model year 2009 and later engines, except for one earlier model year 2000 diesel engine. The vehicle matrix was designed to include a variety of different vocations, such as transit buses, school buses, refuse haulers, delivery trucks, and goods movement trucks. All the diesel vehicles were equipped with DOC, DPF, and SCR systems to control THC and CO emissions, PM emissions, and NOx emissions, respectively. All the CNG vehicles were equipped with TWCs. Two exceptions

were Diesel (No SCR) #1 and Diesel (No SCR) #2, which were only equipped with DOC/DPF systems.

Table 5.1 Test vehicles main specifications

	Vocation	MY	Disp. (L)	Mileage	Test Fuel	Aftertreatment System
Diesel (No SCR) #1	School Bus	2000*	7.2	312,185	ULSD/RD	DOC/DPF
Diesel (No SCR) #2	Goods Movement	2009	12.8	18,071	ULSD/RD	DOC/DPF
0.2Diesel #1	Delivery	2011	11.9	79,246	ULSD/RD	DOC/DPF/SCR
0.2Diesel #2	Delivery	2016	8.9	31,816	ULSD/RD	DOC/DPF/SCR
0.2Diesel #3	Goods Movement	2014	12.8	475,197	ULSD/RD	DOC/DPF/SCR
0.2Diesel #4	Goods Movement	2015	11.9	329,480	ULSD/RD	DOC/DPF/SCR
0.2Diesel #5	Goods Movement	2015	12.8	123,647	ULSD	DOC/DPF/SCR
Diesel-Electric	Delivery	2013	5.1	72,388	ULSD	DOC/DPF/SCR
0.2CNG #1	Transit Bus	2009	8.9	376,912	CNG	TWC
0.2CNG #2	Delivery	2017	11.9	255,619	CNG	TWC
0.2CNG #3	Transit Bus	2011	8.9	392,006	CNG	TWC
0.02CNG #1	Refuse	2017	8.9	33,358	CNG	TWC
0.02CNG #2	Goods Movement	2017	11.9	119,514	CNG	TWC
0.02CNG #3	Goods Movement	2018	11.9	58,205	CNG	TWC

* This vehicle is equipped with retrofitted engine in 2013.

5.3.2. **Test Cycles and Fuels**

Each vehicle was tested over cold start and hot start Urban Dynamometer Driving Schedule UDDS cycles on a heavy-duty chassis dynamometer. Test cycles were conducted as hot starts in triplicate with a 20-minute soak between tests. One cold start was conducted on the UDDS cycle for each vehicle. The test weights utilized for testing were based on

average test weights obtained during the activity data collection portion of this study. Test weight was set based on the vocation of each vehicle, with 32,500 lbs. for school bus and transit bus, 56,000 lbs. for delivery vehicle and 69,500 lb for goods movement vehicles. It should be noted that the diesel-electric truck in delivery vehicle category was tested at 16,000 lbs., as its gross vehicle weight rating (GVWR) rating was considerably lower than the specified test weight of 56,000 lbs.

The diesel vehicles were tested with commercial ultra-low sulfur diesel fuel (ULSD). Commercially available fuel was more representative of what in-use vehicles would be using during normal in-use operation than certification fuel. Similarly, for the CNG vehicles, locally supplied, commercially available CNG was used in the testing. A subset of the diesel vehicles was also tested on hydrogenated vegetable oil (HVO) or renewable diesel (RD).

5.3.3. Emissions Measurements and Analysis

All testing was performed at CE-CERT's heavy-duty chassis dynamometer facility, consisting of an electric AC type design chassis dynamometer that can simulate inertia loads from 10,000 lb to 80,000 lb, which covers a broad range of in-use medium and heavy-duty vehicles. Emissions measurements were obtained using CE-CERT's Mobile Emissions Laboratory (MEL) (Cocker et al., 2004). Emissions measurements included THC, CO, methane (CH_4), carbon dioxide (CO_2), and PM mass. Carbonyl compounds were sampled onto 2,4-dinitrophenylhydrazine (DNPH) coated silica cartridges from the secondary dilution tunnel with a flow rate of 1L/min through the cartridge. The DNPH cartrdges were analysis for 13 C_1-C_8 carbonyl compounds. The DNPH cartridges were eluted with 2 mL of acetonitrile (HPLC grade, EMD Millipore Corporation, Billerica, MA,

USA) and analyzed with a high-performance liquid chromatography (HPLC) system (Waters 2690 Alliance System with 996 Photodiode Array Detector) according to US EPA TO-11A method.

The gravimetric PM mass was measured with the CVS and collected on 47 mm diameter 2 μm pore Teflon filters (Whatman brand). The filters were measured for net gains using a UMX2 ultra precision microbalance with buoyancy correction in accordance with the weighing procedure guidelines set forth in the Code of Federal Regulations (CFR). The EEPS (TSI 3090, firmware version 8.0.0) was used to obtain real-time second-by-second size distributions between 5.6 to 560 nm. Elemental carbon (EC), organic carbon (OC), metals, and carbonyl compounds were measured on all vehicles. EC/OC fractions were collected on QAT Tissuquartz quartz-fiber filters that were pre-cleaned by firing for 5 h at 600 ℃ to remove carbonaceous contaminants and were quantified using a Thermal/Optical Carbon Aerosol Analyzer according to NIOSH (National Institute of Occupational Safety and Health) Method 5040. PM-bound metals and trace elements were collected on 47 mm Teflon filters and measured using the X-Ray fluorescence (XRF) method, according to EPA IO-3.3. A schematic setup of particle sampling system is shown in Figure 5.8.

5.4. **Results**

5.4.1. **Particulate Emissions**

5.4.1.1. **Particle Mass and Total Particle Number Emissions**

Figure 5.1(a)(b) show the PM mass emissions for the test vehicles by vocation/technology group for the cold start and hot start UDDS cycles on a mg/bhp-hr basis, respectively. For vehicles where the PM mass levels were at or below the background

levels, the PM emissions are reported as zero values. The PM emissions for the school bus Diesel (No SCR) #1 were not available due to an instrument issue. PM emissions were below the 10 mg/bhp-hr certification limit for the DPF-equipped diesel engines for both test cycles, which is attributed to the high reduction efficiency of the DPF. An exception was seen for the goods movement vehicle Diesel (No SCR) #2 . Although this vehicle was equipped with a DPF catalyst, PM emissions were over 15 times higher than the other DPF-equipped diesel vehicles for the cold start test and around 20 times higher for the hot start tests, indicating that this vehicle was likely equipped with a defected or poorly maintained or tampered DPF (i.e., cracked or melted substrate).

Another exception was the 0.2CNG #3 vehicle that was equipped with a model year 2011 engine with a mileage of around 400,000 miles. This vehicle was found to be equipped with a cracked TWC, as indicated by the tailpipe NOx emission levels that were close to the engine-out levels. This vehicle showed almost no NH_3 emissions in contrast to the other CNG vehicles, suggesting no catalytic activity in the TWC. In particular, ammonia typically forms over the catalyst via steam reforming of hydrocarbons or from reactions of nitrogen monoxide with hydrogen that is produced from a water-gas shift reaction with CO (Suarez-Bertoa et al., 2014; Whittington et al., 1995). Although PM reduction is not the primary function of a TWC, the elevated PM emissions, as a possible result of catalyst aging and engine deterioration, may indicate increased lubricant oil penetration into the combustion chamber as this is a source of PM emissions for CNG vehicles. Trace elements and metals originate from lubricant oil may have poisoned the active centers of the TWC leading to catalyst deactivation. Lubricant oil consumption and

infusion into the combustion chamber was more notable during cold start conditions, where PM emissions were higher than those for the hot start testing.

The very low PM mass emissions from DPF-equipped heavy-duty diesel vehicles are consistent with the results of previous chassis dynamometer studies(Jiang et al., 2018; Quiros et al., 2016), (CARB, 2015a, 2015b). For the previous CARB EMFAC2014 study, PM emission rates were below 15 mg/mi for most vehicle/cycle combinations as well, although three vehicle/cycle points did show PM emission rates ranging from 28 to 55 mg/mi (CARB, 2015a, 2015b). (Quiros et al., 2016) found PM emissions of <0.010 g/mi for a 2010+ SCR-equipped truck over a range of cycles including a UDDS, and near-dock, local, and regional drayage cycles. A more recent study (Jiang et al., 2018) shows PM mass emissions were below 15 mg/mi for all vehicles over most of cycles. There were no clear PM mass emissions reductions for RD compared to ULSD, despite the fact that RD is free of aromatics and sulfur compounds that are soot precursors (Singh et al., 2018). Natural gas has a soot-free combustion since methane has no carbon-carbon bonds. The origin of PM in natural gas engines is primarily from lubricant oil consumption that enters the combustion chamber (Karavalakis et al., 2016; Pirjola et al., 2016; Thiruvengadam et al., 2014). PM mass emissions from all CNG vehicles were comparable to those of the DPF-equipped diesel vehicles. Recent studies have shown that CNG vehicles emit comparable to or in some cases even higher PM emissions than DPF-equipped diesel vehicles (Thiruvengadam et al., 2015).

Total particle number emissions for the test vehicles by vocation/technology group are also shown for the cold start and hot start UDDS cycles on a #/bhp-hr basis in Figure 5.1(a)(b), respectively. TPN emissions for most vehicles were between $1x10^{10}$ #/bhp-hr

and $1x10^{13}$ #/bhp-hr, except for the goods movement vehicle Diesel (No SCR) #2 over both cold and hot start UDDS cycles, and 0.2CNG #2, 0.2CNG #3, and 0.02CNG #3 over the cold start UDDS cycle ranging between $8.4x10^{13}$ and $9.4x10^{14}$ #/bhp-hr. TPN emissions for the CNG vehicles were higher than those for the diesel vehicles equipped with DPFs over both cold start and hot start UDDS cycles. The TPN emissions for CNG vehicles were also comparable or higher than the current Euro 6 solid particle number emissions standard of 4.47×10^{11} #/bhp-hr (1×10^{12} #/kw-hr), noting that it is expected that TPN emissions would be naturally higher than SPN emissions. An exception was seen for the Diesel (No SCR) #2 with the damaged or tampered DPF over the hot start UDDS, which showed TPN emissions 200 times higher than the Euro 6 solid particle number standard and 7 times higher than the U.S. PM mass emission standard. The results reported here indicate that during cold start conditions CNG vehicles showed 50 to 500 times higher TPN emissions than the current Euro 6 SPN standard and within 20 times higher than the standard over the hot start UDDS.

Cold start conditions played a more important role for particle number emissions than for PM mass emissions for the CNG vehicles. The CNG vehicles over the cold start UDDS cycle showed higher TPN emissions than those over the hot start UDDS, with emissions rates ranging from 1×10^{13} to 2×10^{14} #/bhp-hr. Higher TPN emissions during cold start operation are expected due to the TWC being below its light-off temperature and the cold surfaces of the engine cylinder lines, which will cause the inefficient oxidation of the semivolatile hydrocarbon species that mostly contribute to the nucleation mode particles. Hot start emissions for CNG vehicles were generally lower than 10 times of the Euro 6 solid particle number standard. For the diesel vehicles, TPN emissions were within

5 times of the limit over both the cold start and hot start UDDS cycles, indicating less impact of cold/hot operation on TPN emissions for diesel vehicles. RD was found to be a factor that may lead to less TPN emissions due to the absence of sulfur and aromatic compounds. Studies have shown that renewable diesel can provide reductions in total and solid particle number emissions compared to ULSD (McCaffery et al., 2022). The results showed that 0.2 RD were generally lower than the 0.2 Diesel vehicles except for one 0.2 RD, with emission rates of 1.5×10^{12} #/bhp-hr for the cold start cycle and around 1×10^{12} #/bhp-hr for the hot start cycle.

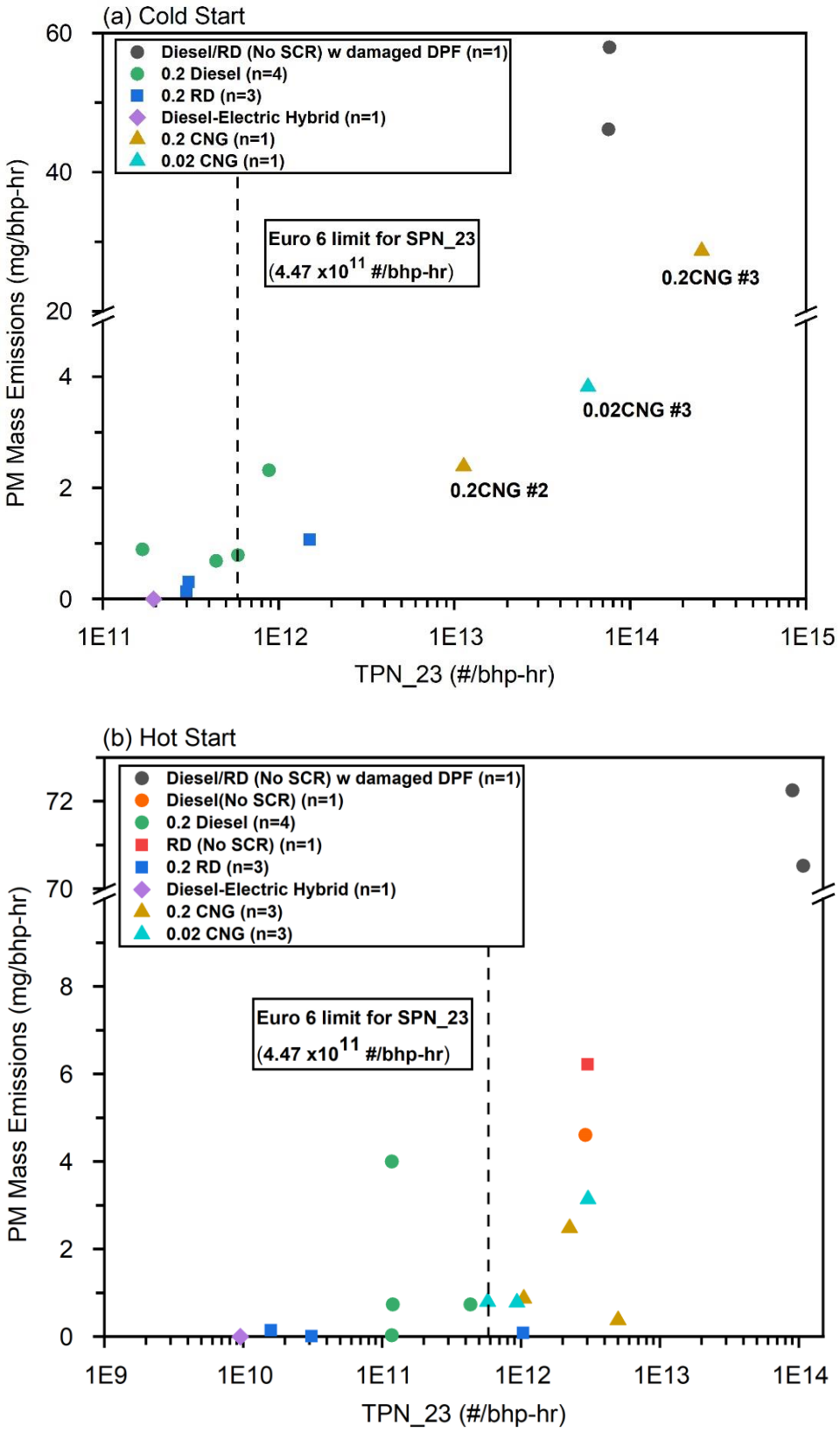

Figure 5.1(a)(b) PM emissions over cold and hot start UDDS cycles (mg/bhp-hr)

5.4.1.2. **Total Particle Number Emissions With Different Cut Sizes**

A number of studies have focused on emissions measurements for exhaust particles below 23 nm in diameter (Giechaskiel et al., 2017; Samaras et al., 2022). While the majority of these studies have been focused in light-duty applications, there is limited information for heavy-duty diesel or natural gas applications. Figure 5.2 shows the TPN emissions with a cut size of 10 nm (TPN_10) and TPN emissions with a cut size of 23 nm (TPN_23) for all the tested vehicles, based on the fuel and aftertreatment technology. Results in Figure 5.2 can be categorized into three regions: region A represents both TPN_23 and TPN_10 being below the current SPN_23 Euro 6 standard; region B represents TPN_23 emissions being below the Euro 6 limit but the TPN_10 emissions being higher than the Euro 6 limit, and region C represents both the TPN_23 and TPN_10 exceeding the Euro 6 limit.

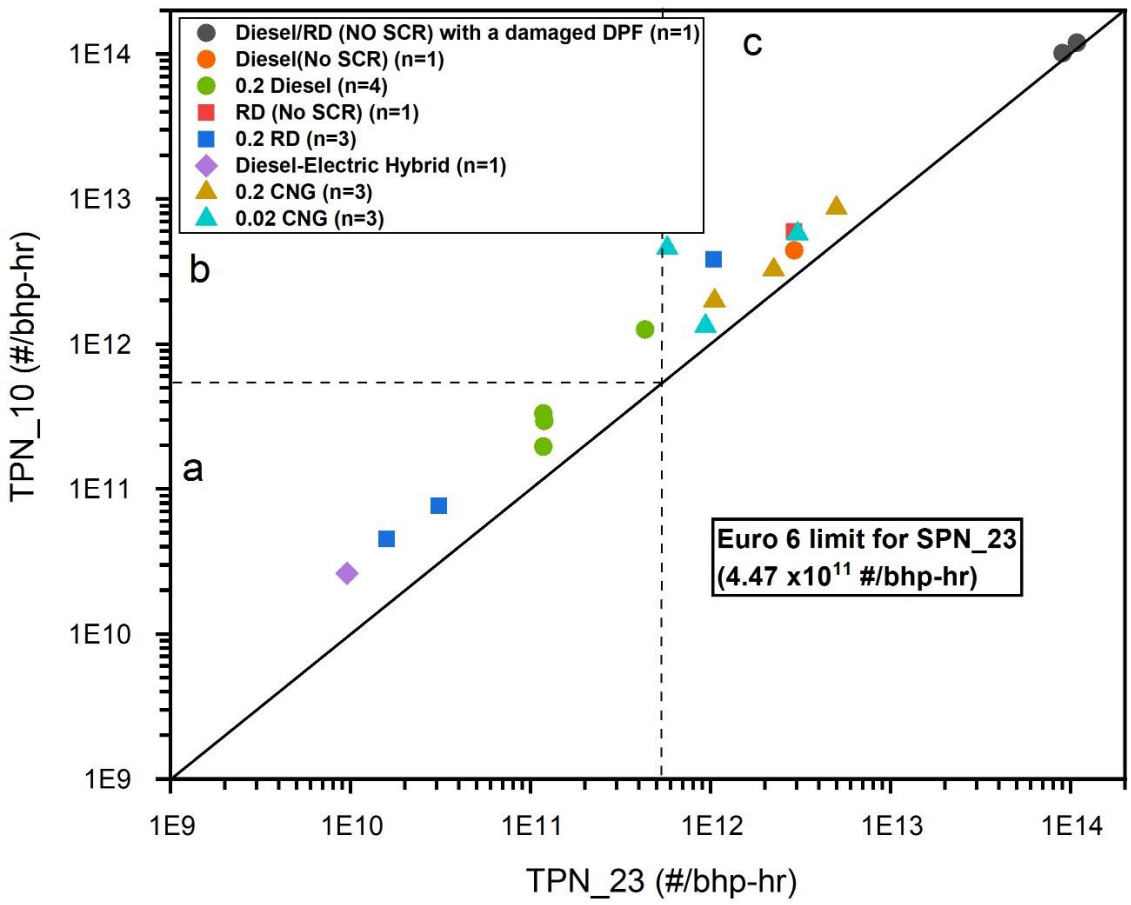

Figure 5.2 TPN_10 vs TPN_23 over hot start UDDS cycles (#/bhp-hr)

TPN_23 emissions for all 0.2diesel vehicles equipped with SCR were lower than the current Euro 6 SPN_23 limit. The 0.2RD vehicles showed lower TPN_23 and TPN_10 emissions than the 0.2Diesel vehicles except for one 0.2RD vehicle. This is consistent with the PM mass emissions being lower for the vehicles tested with renewable diesel. The diesel- hybrid electric vehicle showed the lowest TPN_23 and TPN_10 at 1.5 x 10^{12} and 1 x 10^{10} #/bhp-hr, respectively, suggesting heavy-duty hybridization could provide important benefits for particle number emissions reductions. The CNG vehicles exhibited higher TPN_23 emissions than the Euro 6 limit, with the 0.02CNG vehicles showing lower TPN_23 emissions than the 0.2CNG vehicles, indicating more advanced engine technology

and more robust TWC systems. TPN_23 and TPN_10 emissions for the Diesel (No SCR) with the damaged or tampered DPF showed TPN emissions around 1x 10^{14} #/bhp-hr.

5.4.1.3. Elevated Particle Number Emissions During Deacceleration Events

With the exception of the high emitting goods movement Diesel (No SCR) #2 vehicle, most DPF-equipped diesel vehicles showed TPN emissions comparable to or lower than those for CNG vehicles. Previous studies have shown that CNG vehicles emit more TPN emissions than DPF-equipped diesel vehicles, especially nucleation mode particles. It has been found that the smaller volatile or semi-volatile particles (i.e., with a diameter less than 23 nm) in stoichiometric CNG vehicles originate from lubricant oil metals that are part for the additive package and are emitted as metal oxides in the nucleation mode (Karavalakis et al., 2016; Thiruvengadam et al., 2014).

For the CNG vehicles tested, the elevated ultrafine particle emissions were similar to those reported in recent studies of CNG light-duty vehicles (Toumasatos et al., 2021). The results reported here suggest that a significant part of the total particle emissions reside below the 23nm size threshold. Figure 5.3 shows the real-time particle number emissions profile and particle size distribution over the hot start UDDS cycle between 740s and 820s for 0.02CNG #1. This vehicle was chosen because it was a high emitting vehicle with an emissions factor around 10 times higher than the Euro 6 PN emissions standard and this phenomenon was consistent for this vehicle across all three UDDS cycles. Particle number emissions were elevated during the deacceleration event between 775s and 800s, where the fuel to the engine was cut off. The majority of the particles reside in the nucleation mode region with an average geometric mean diameter (GMD) in the order of 10 nm. High particle concentration emission peaks were only detected during deceleration events while

no significant emissions were observed during the acceleration events or during idle operation. In particular, during the 760s to 800s timeframe, three high emission events were detected during deceleration events under motoring engine operation conditions (fuel cut-off). The current findings suggest that CNG particle emissions are mostly related to the lubricant oil escape from the oil ventilation system, from piston rings or valves. This phenomenon was more pronounced during deceleration, where a decrease of the pressure of the intake air due to the closed throttle valves favored the lubricant oil infusion into the combustion chamber (Amirante et al., 2015; Tonegawa et al., 2006).

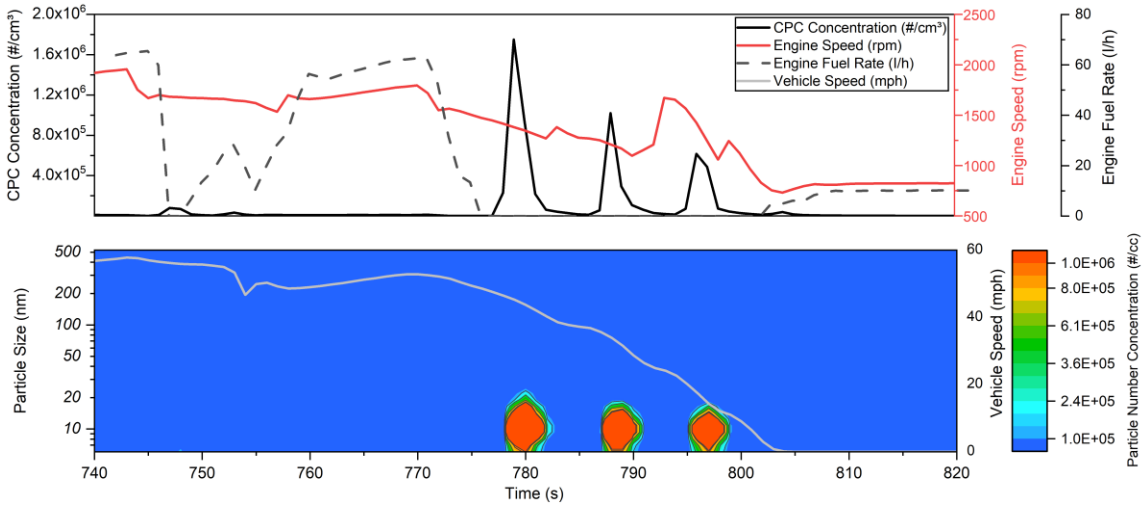

Figure 5.3 Real-time particle number emissions and particle size distribution profile with vehicle speed and engine parameters for 0.02CNG #1

Figure 5.4 shows the high-emitting goods movement Diesel (No SCR) #2 vehicle. This vehicle was selected to provide a comparison of the particles size distributions between a functioning DPF-equipped vehicle and a non-functioning DPF-equipped vehicle to better understand the characteristics of particle number emissions from diesel vehicles. The diesel vehicle with the non-functioning DPF showed elevated particle number emissions during most acceleration events. During these events. A large population of particles was detected in the area of 20 nm to 200 nm size range. The composition of these

particles was likely comprised of soot and metallic ash particles that were failed to be retained in the non-functioning DPF. Particle concentrations from the other properly functioning DPF vehicles were very low across the entire cycle, which is an indication of high collection efficiency of a properly functioning DPF. CPC-related PN emissions at 2.5nm cut-off size and particle size distributions, suggest that the majority of the diesel particle emissions coincided with vehicle acceleration, while the nature of these particles was mostly soot due to the fuel enrichments under the specific acceleration events.

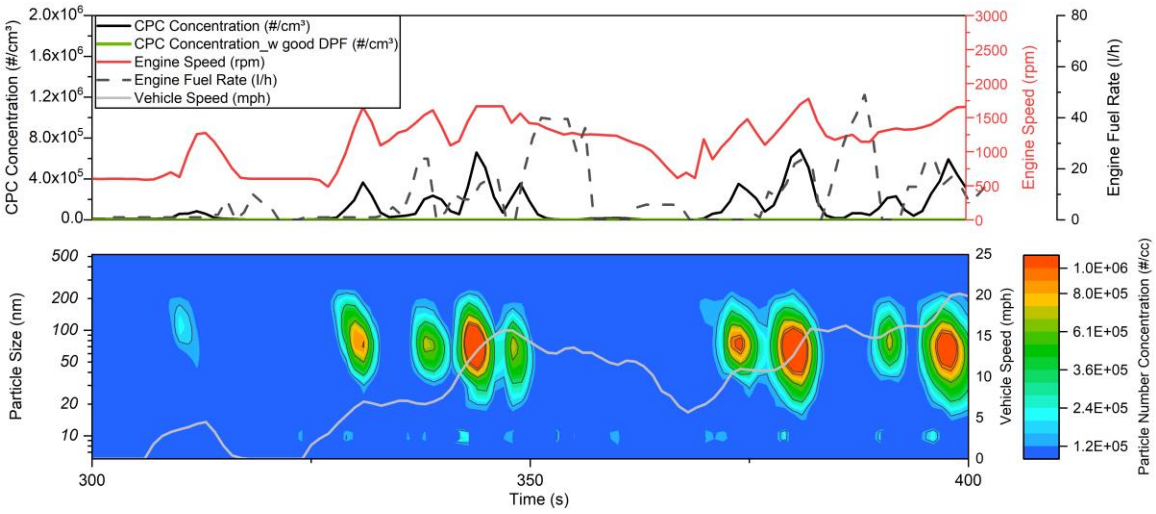

Figure 5.4 Real-time particle number emissions and particle size distribution profile with vehicle speed and engine parameters for Diesel (No SCR) #2

5.4.1.4. EC/OC and Metal Emissions

Figure 5.5(a-b) shows the EC/OC emissions on a mg/mile basis for the test vehicles by vocation/technology group over the cold and hot start UDDS cycles. Except for the Diesel/RD (No SCR) with the non-functioning DPF, EC/OC emissions for all vehicles over the cold and hot start UDDS cycles were below 15 mg/mile. EC emissions for the CNG vehicles were below 2 mg/mile, except for 0.02CNG #3 whose emissions ranging between 10 to 15 mg/mile. The low EC emissions for the CNG vehicles were expected due to that natural gas is comprised by methane and other low-molecular weight hydrocarbons that do

not contribute to soot formation. OC emissions showed some reductions for the RD when compared to regular ULSD for most diesel vehicles except for 0.2Diesel/RD#3 and 0.2Diesel/RD#4. These reductions in OC emissions ranged from 6% to 60%. OC emissions dominated the PM composition for both diesel and CNG vehicles over the hot start UDDS. The same trend was found for the cold start UDDS except for the no SCR-equipped diesel vehicles and one CNG vehicle. This particular CNG vehicle had high mileage and was equipped with a non-functional TWC. EC emissions for most diesel and CNG vehicles were below 15 mg/mile except for Diesel/RD #1. EC emissions for diesel vehicles are generally low due to the high reduction efficiency of PM from DPF. The diesel (No SCR) vehicle that was equipped with the non-functioning DPF shows high EC emissions over both cold and hot UDDS cycles.

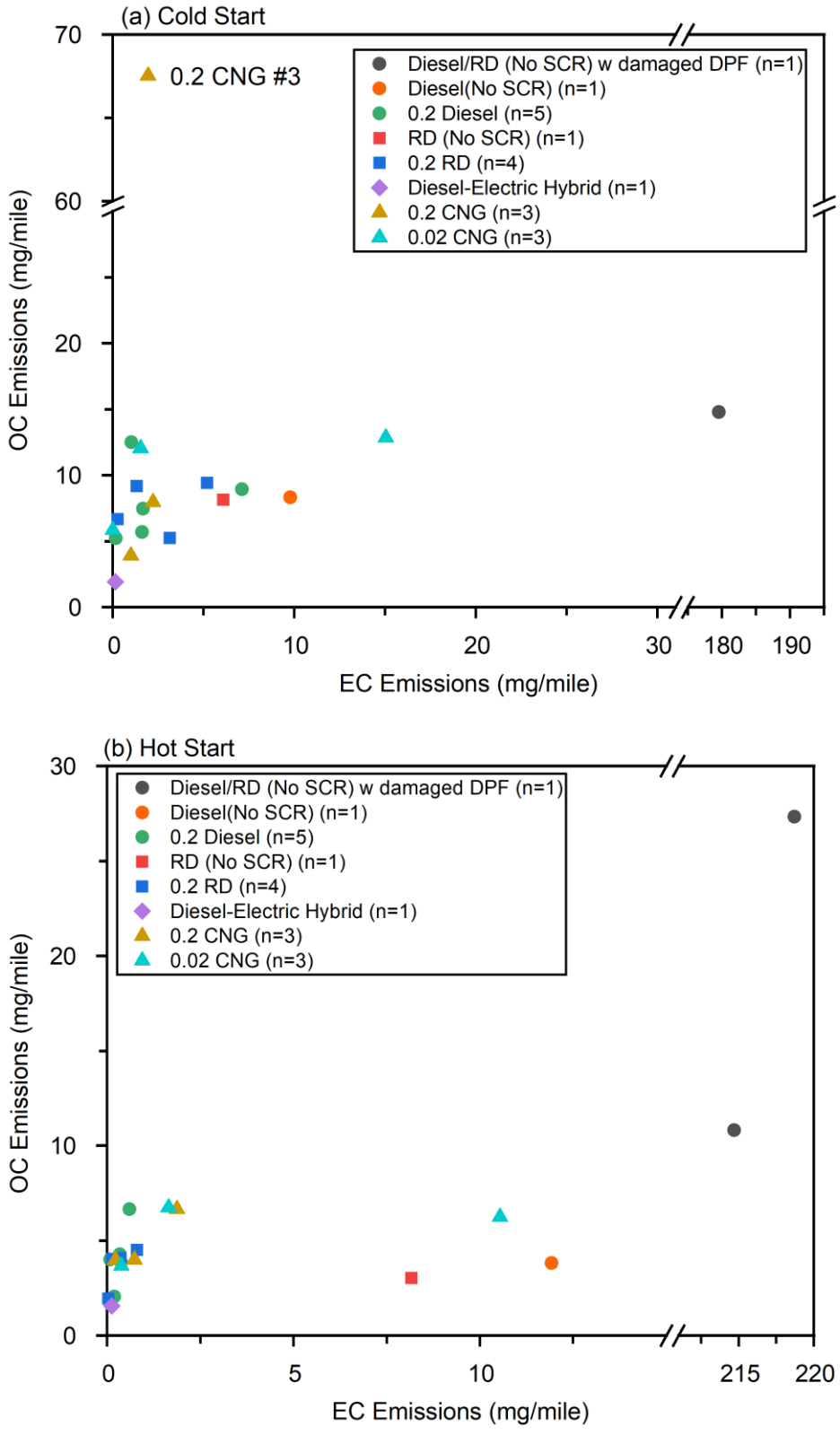

Figure 5.5(a-b) EC/OC Emissions (mg/mile)

Metal emissions for the test vehicles by vocation/technology group are shown for the cold and hot start UDDS cycles on a mg/mile basis in Table 5.2. Values below detection limits were removed. Most CNG vehicles showed higher emissions of PM-bound metals and elements compared to diesel vehicles. Phosphorus (P), sulfur (S), calcium (Ca), zinc (Zn), and iron (Fe) were the dominant metallic and non-metallic species in PM. The presence of Fe suggests that some of the PM may originate from engine wear. The presence of P, Ca, Zn confirm the hypothesis that PM from CNG engines are mostly originated from lubricant oil contribution, since these elements are typically found in the additive package. Zinc and sulfur are emitted from lubricant oil and its additives, such as zinc dithiophosphate. For diesel vehicles, the majority of metals and trace elements were close to the detection limits of the test method.

5.4.2. **Greenhouse Gas (GHG) Emissions**

Figure 5.6 shows the GHG emissions of CO_2, CH_4, and nitrous oxide (N_2O) and their global warming potential (GWP) for all vehicles over the cold and hot start UDDS cycles. For the diesel vehicles, 0.2Diesel/RD #1 showed the lowest CO_2 emissions at around 1800 g/mile and 1500 g/mile over the cold start and hot start UDDS cycles, respectively, due to smaller engine size (7.2L) of this vehicle. The other diesel vehicles showed higher CO_2 emissions ranging from 1900 g/mile to 2200 g/mile. CO_2 emissions for the diesel-hybrid electric hybrid vehicle were the lowest among all test vehicles due to the smaller engine size of this vehicle. Natural gas vehicles showed some variability in CO_2 emissions, with 0.2CNG#1 showing the lowest CO_2, followed by 0.2CNG #2, and then the 0.02CNG vehicles. CO_2 emissions for the 0.02CNG vehicles were generally higher than those from 0.2CNG vehicles with similar engine size.

Natural gas engines are generally characterized by their relatively high CH_4 emissions. Figure 5.6 showed significantly higher CH_4 emissions from a stoichiometric natural gas engine equipped with a TWC compared to conventional diesel and diesel-electric hybrid engines equipped with DPF and SCR systems. CH_4 emissions for natural gas engines mainly originate from unburned natural gas fuel. For a stoichiometric CNG engine, higher CH_4 emissions indicate lack of oxygen in the exhaust to react with unburn CH_4 emissions. From Figure 5.6, higher CH_4 emissions were observed for the 0.2CNG vehicles than the 0.02CNG vehicles, suggesting higher efficiency of TWC to oxidize the unburn CH_4 emissions. In addition, CH_4 emissions for the CNG vehicles were influenced by the cold-start cycles.

The CO_2 equivalent (CO_2eq) GWP in a unit of g/mile was derived by assuming CH_4 to be 25 times higher than CO_2 and for N_2O to be 298 times over a 100-year time horizon (Stocker, 2014). Figure 5.6 showed that CO_2 still is the dominant pollutant for GHG emissions. Interestingly, both the 0.02CNG vehicles over the cold start UDDS cycles showed the highest GWP among all vehicles. CH_4 contributes the second largest to GHG emissions for CNG vehicles over mostly the cold start UDDS cycles. N_2O was known as a product formed from the catalyst reactions for SCR-equipped diesel vehicles and for TWC equipped natural gas vehicles. N_2O also is considered to be 298 times higher than CO_2 in terms of the heat trapping ability. Therefore, N_2O contributes significantly to GWP for SCR-equipped diesel vehicles. The N_2O formation in a TWC is favored under rich burn condition and the N_2O emissions showed strong correlations to the CO emissions. Figure 5.6 shows that compared to the 0.2 CNG vehicles, the 0.02 CNG vehicles have lower N_2O

emissions suggesting better control of air-fuel ratio control to achieve a more complete combustion.

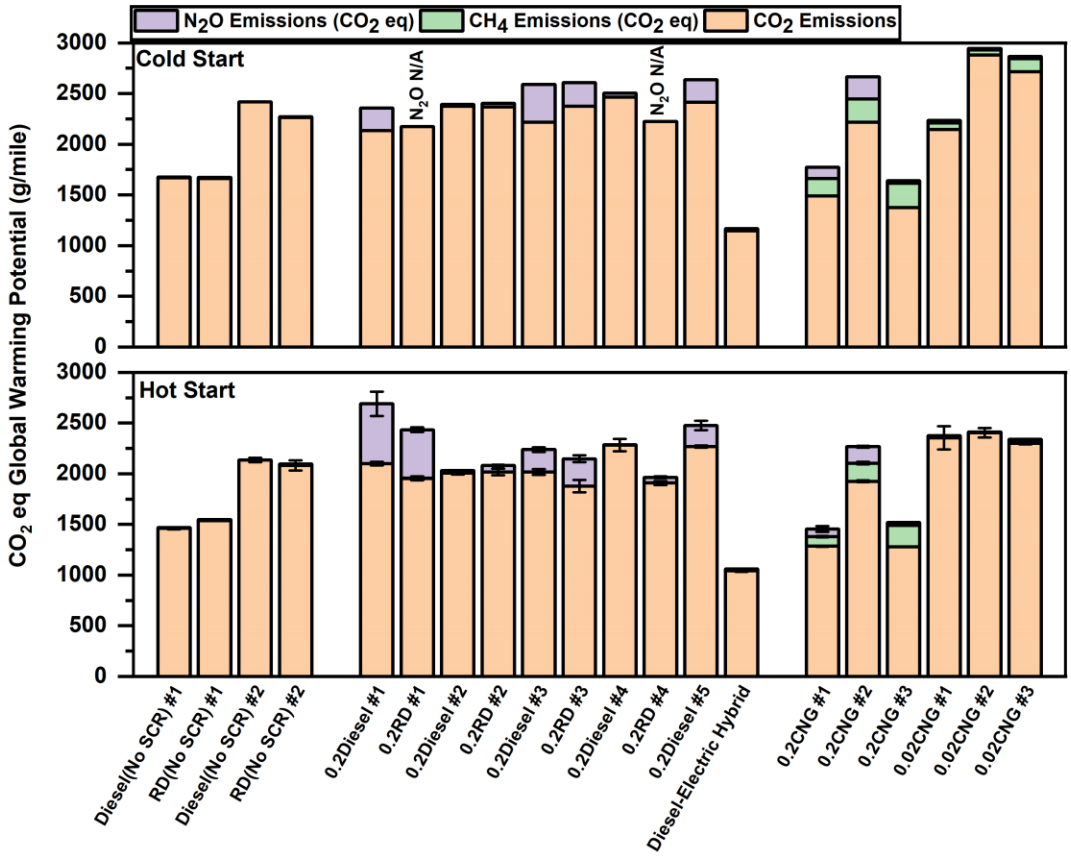

Figure 5.6 GHG Emissions and CO_2 equivalent GWP (g/mile)

5.4.3. THC and CO Emissions

THC and CO emissions for the test vehicles by vocation/technology group are shown for the cold start and hot start UDDS cycles on a g/mile basis in Figure 5.9. Both THC and CO emissions levels for diesel vehicles were at or below the background levels. CO emissions for MY 2010-compliant diesel engines that are equipped with DOC are in the relatively low level(Quiros et al., 2016). Cold start UDDS showed higher THC emissions than the hot starts for all the CNG vehicles and the 0.2CNG vehicles showed relatively higher THC emissions than the 0.02CNG vehicles. THC emissions over hot start UDDS

cycles ranged from 3.7 g/mile to 7.0 g/mile for the 0.2CNG vehicles and from 0.24 g/mile to 1.04 g/mile for the 0.02CNG vehicles. This study also found that most of the THC emissions for the CNG vehicles were CH_4 emissions.

Similar trends were observed for CO emissions over hot start UDDS cycle that the emissions rates were from 33 g/mile to 36 g/mile for the 0.2CNG vehicles and from 6.4 g/mile to 10.7 g/mile for the 0.02CNG vehicles. CNG vehicles with stochiometric-burn engines show higher CO emissions than all diesel vehicles, which is due to stochiometric burn natural gas engines. Previous studies showed CO emissions from the TWC equipped CNG vehicles ranging between 6 to 27 g/mile depending on the cycle, model year and vocation (Thiruvengadam et al., 2015; Yoon et al., 2013).

5.4.4. **Carbonyl Emissions**

Figure 5.7(a-b) shows the formaldehyde and acetaldehyde emissions for the test vehicles by vocation/technology group over the cold start and hot start UDDS cycles. Formaldehyde and acetaldehyde were the predominant aldehydes in the tailpipe, with heavier aldehydes and ketones being below the detection limits. Previous studies have also shown the abudance of low molecular weight aldehydes in diesel exhaust. Aldehydes are not present in the fuel composition, but rather combustion products from the partial oxidation of hydrocarbons (Fontaras et al., 2009; Karavalakis et al., 2017). Compared to regular diesel, RD showed some variability, with 0.2RD#1 and 0.2RD#2 higher than the vehicle 0.2Diesel #1 and 0.2Diesel #2, respectively, and with the other diesel vehicles lower than RD. Although RD is a paraffinic fuel that tend to reduce carbonyl emissions, there are studies showing higher carbonyl emissions with RD than regular diesel fuel. Additionally, cold start UDDS for most of the diesel vehicles showed higher carbonyl

emissions than hot start UDDS except for Diesel/RD (No SCR) #1 and 0.2Diesel/RD #2. Interestingly, It is noted from Figure 5.7 that cold start UDDS cycle for 0.2Diesel#3 showed the highest carbonyl emissions among all vehicles over all test cycles. The CNG vehicles showed comparable carbonyl emissions to the diesel vehicles over hot start cycles, with the formaldehyde emissions ranging from 5 mg/mile to 33 mg/mile, and with the acetaldehyde emissions ranging from 3 mg/mile to 14 mg/mile.

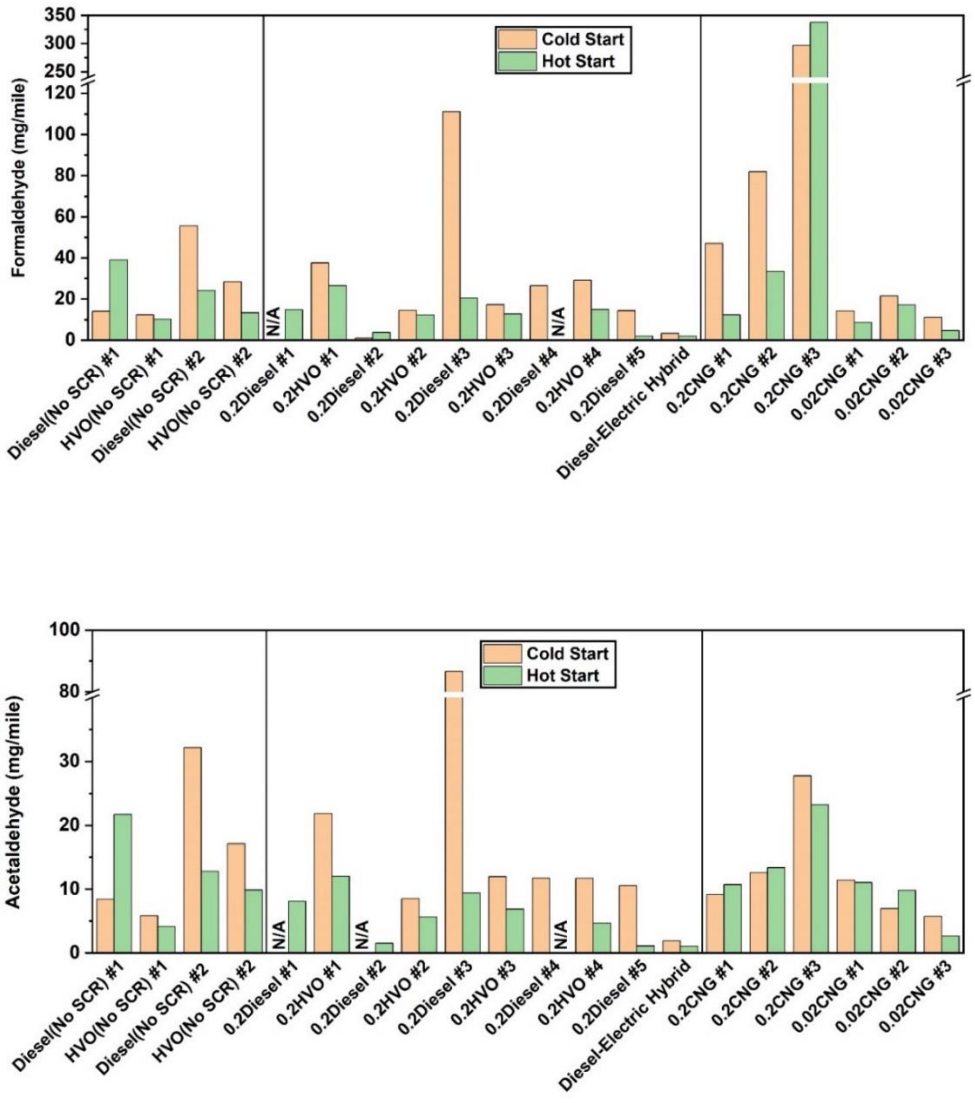

Figure 5.7 (a)(b) Formaldehyde and Acetaldehyde Emissions(g/mile); Cold start values represent a single cold-start UDDS and hot-start cycles represent three back-to-back UDDS cycles

5.5. **Conclusion**

This study provides information on particulate matter (PM), greenhouse gases (GHG), total hydrocarbon (THC), carbon monoxide (CO), and carbonly emissions from a fleet of fourteen in-use heavy-duty vehicles over Urban Dynamometer Driving Schedule (UDDS) cycles using a chassis dynamometer. Results showed PM emissions were below the 10 mg/bhp-hr certification for all vehicles over both cold and hot start cycles, with the exception for the goods movement vehicle Diesel (No SCR) #2 and one CNG vehicle with a non-functional catalyst. Total particle number emissions for most of the CNG vehicles were above the European particle number limit, although the Euro limit is only for solid particles. This indicates that more efforts need to be made to reduce particle number emissions from natural gas vehicles to the emission certification levels. Most DPF-equipped diesel vehicles showed particle number emissions below the standard. Particle number emissions were elevated during the deacceleration event, where the fuel to the engine was cut off. Furthermore, the majority of the particles reside in the nucleation mode region with an average geometric mean diameter (GMD) in the order of 10 nm. The current findings suggest that CNG particle emissions are mostly related to the lubricant oil escape from the oil ventilation system, from piston rings or valves. Phosphorus (P), sulfur (S), calcium (Ca), zinc (Zn), and iron (Fe) were the dominant metallin and non-metallic species in PM. The presence of Fe suggests that some of the PM may originate from engine wear. CO and THC emissions were found in relatively high levels, with more advanced 0.02CNG vehicles significantly lower than the 0.2CNG vehicles, indicating significant improvements in engine calibration and catalyst formulation. CO_2 emissions are the main contributor to GHG emissions for all vehicles. Natural gas engines are generally

characterized by their relatively high CH_4 emissions. CH_4 contributes the second largest to GHG emissions for CNG vehicles over mostly the UDDS cycle.

5.6. **Acknowledgements**

We acknowledge funding from the California Energy Commission (CEC), the South Coast Air Quality Management District (South Coast AQMD), Southern California Gas Company (SoCalGas), and the California Air Resources Board (CARB) under South Coast AQMD contract number 17286. The authors thank Mark Villela, Daniel Gomez, and Dan Hartnett of the University of California, Riverside for their contribution in conducting the emissions testing for this program.

5.7. **References**

Amirante R, Distaso E, Tamburrano P, Reitz RD. Measured and predicted soot particle emissions from natural gas engines. SAE Technical Paper, 2015.

EPA, Inventory of U.S. Greenhouse Gas Emissions and Sinks: 1990-2020, published 2022, https://www.epa.gov/ghgemissions/inventory-us-greenhouse-gas-emissions-and-sinks-1990-2020, Accessed Nov 2022.

EPA, Office of Transportation and Air Quality, 2011. Final Rulemaking to establish greenhouse gas emissions standards and fuel efficiency standards for medium- and heavy-duty engines and vehicles, https://www3.epa.gov/otaq/climate/documents/420r11901.pdf, Accessed Nov 2022.

EPA, 2020, Overview of Greenhouse Gases. https://www.epa.gov/ghgemissions/overview-greenhouse-gases#carbon-dioxide, Accessed Nov 2022.

Fontaras G, Karavalakis G, Kousoulidou M, Tzamkiozis T, Ntziachristos L, Bakeas E, et al. Effects of biodiesel on passenger car fuel consumption, regulated and non-regulated pollutant emissions over legislated and real-world driving cycles. Fuel 2009; 88: 1608-1617.

Giechaskiel B, Vanhanen J, Väkevä M, Martini G. Investigation of vehicle exhaust sub-23 nm particle emissions. Aerosol Science and Technology 2017; 51: 626-641.

Jiang Y, Yang J, Cocker III D, Karavalakis G, Johnson KC, Durbin TD. Characterizing emission rates of regulated pollutants from model year 2012+ heavy-duty diesel vehicles equipped with DPF and SCR systems. Science of The Total Environment 2018; 619: 765-771.

Karavalakis G, Gysel N, Schmitz DA, Cho AK, Sioutas C, Schauer JJ, et al. Impact of biodiesel on regulated and unregulated emissions, and redox and proinflammatory properties of PM emitted from heavy-duty vehicles. Science of the Total Environment 2017; 584: 1230-1238.

Karavalakis G, Hajbabaei M, Jiang Y, Yang J, Johnson KC, Cocker DR, et al. Regulated, greenhouse gas, and particulate emissions from lean-burn and stoichiometric natural gas heavy-duty vehicles on different fuel compositions. Fuel 2016; 175: 146-156.

Li Y, Xue J, Peppers J, Kado NY, Vogel CF, Alaimo CP, et al. Chemical and toxicological properties of emissions from a Light-Duty compressed natural gas vehicle fueled with renewable natural gas. Environmental science & technology 2021; 55: 2820-2830.

McCaffery C, Zhu H, Ahmed CS, Canchola A, Chen JY, Li C, et al. Effects of hydrogenated vegetable oil (HVO) and HVO/biodiesel blends on the physicochemical and toxicological properties of emissions from an off-road heavy-duty diesel engine. Fuel 2022; 323: 124283.

Murray CJ, Aravkin AY, Zheng P, Abbafati C, Abbas KM, Abbasi-Kangevari M, et al. Global burden of 87 risk factors in 204 countries and territories, 1990–2019: a systematic analysis for the Global Burden of Disease Study 2019. The Lancet 2020; 396: 1223-1249.

Pirjola L, Dittrich A, Niemi JV, Saarikoski S, Timonen H, Kuuluvainen H, et al. Physical and chemical characterization of real-world particle number and mass emissions from city buses in Finland. Environmental Science & Technology 2016; 50: 294-304.

Quiros DC, Thiruvengadam A, Pradhan S, Besch M, Thiruvengadam P, Demirgok B, et al. Real-world emissions from modern heavy-duty diesel, natural gas, and hybrid diesel trucks operating along major California freight corridors. Emission Control Science and Technology 2016; 2: 156-172.

Samaras Z, Rieker M, Papaioannou E, van Dorp W, Kousoulidou M, Ntziachristos L, et al. Perspectives for regulating 10 nm particle number emissions based on novel measurement methodologies. Journal of Aerosol Science 2022; 162: 105957.

Schraufnagel DE. The health effects of ultrafine particles. Experimental & molecular medicine 2020; 52: 311-317.

Singh D, Subramanian K, Garg M. Comprehensive review of combustion, performance and emissions characteristics of a compression ignition engine fueled with hydroprocessed renewable diesel. Renewable and Sustainable Energy Reviews 2018; 81: 2947-2954.

Stocker T. Climate change 2013: the physical science basis: Working Group I contribution to the Fifth assessment report of the Intergovernmental Panel on Climate Change: Cambridge university press, 2014.

Suarez-Bertoa R, Zardini A, Astorga C. Ammonia exhaust emissions from spark ignition vehicles over the New European Driving Cycle. Atmospheric Environment 2014; 97: 43-53.

Thiruvengadam A, Besch MC, Thiruvengadam P, Pradhan S, Carder D, Kappanna H, et al. Emission rates of regulated pollutants from current technology heavy-duty diesel and natural gas goods movement vehicles. Environmental science & technology 2015; 49: 5236-5244.

Thiruvengadam A, Besch MC, Yoon S, Collins J, Kappanna H, Carder DK, et al. Characterization of particulate matter emissions from a current technology natural gas engine. Environmental science & technology 2014; 48: 8235-8242.

Tonegawa Y, Oguchi M, Tsuchiya K, Sasaki S, Ohashi T, Goto Y. Evaluation of regulated materials and ultra fine particle emission from trial production of heavy-duty CNG engine. SAE Technical Paper, 2006.

Toumasatos Z, Kontses A, Doulgeris S, Samaras Z, Ntziachristos L. Particle emissions measurements on CNG vehicles focusing on Sub-23nm. Aerosol Science and Technology 2021; 55: 182-193.

Whittington B, Jiang C, Trimm D. Vehicle exhaust catalysis: I. The relative importance of catalytic oxidation, steam reforming and water-gas shift reactions. Catalysis today 1995; 26: 41-45.

Yoon S, Collins J, Thiruvengadam A, Gautam M, Herner J, Ayala A. Criteria pollutant and greenhouse gas emissions from CNG transit buses equipped with three-way catalysts compared to lean-burn engines and oxidation catalyst technologies. Journal of the Air & Waste Management Association 2013; 63: 926-933.

5.8. **Supplemental Materials**

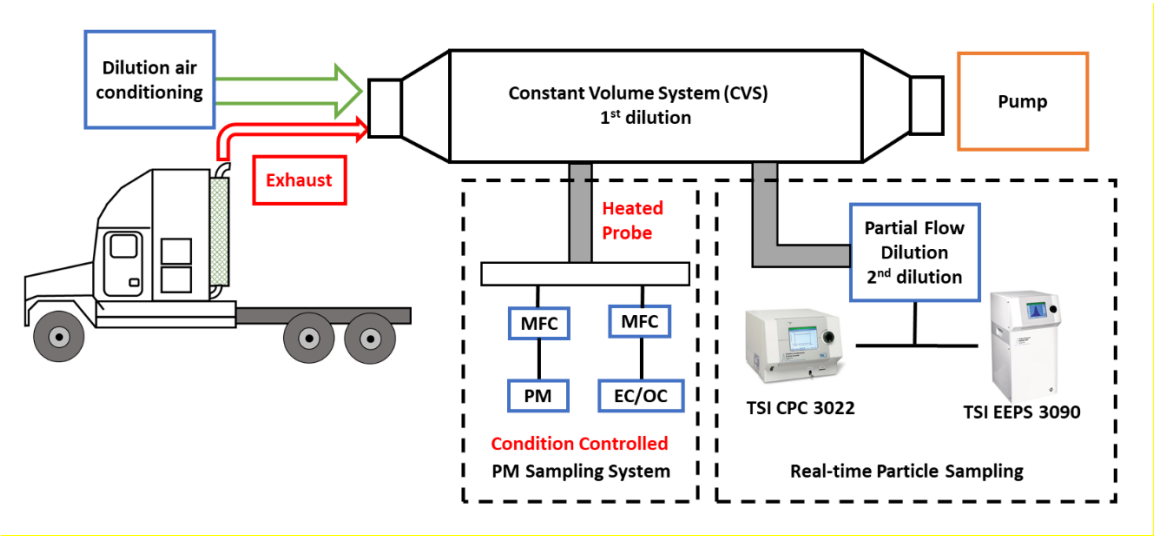

Figure 5.8 SM-1 Schematic of Particle Sampling System Setup

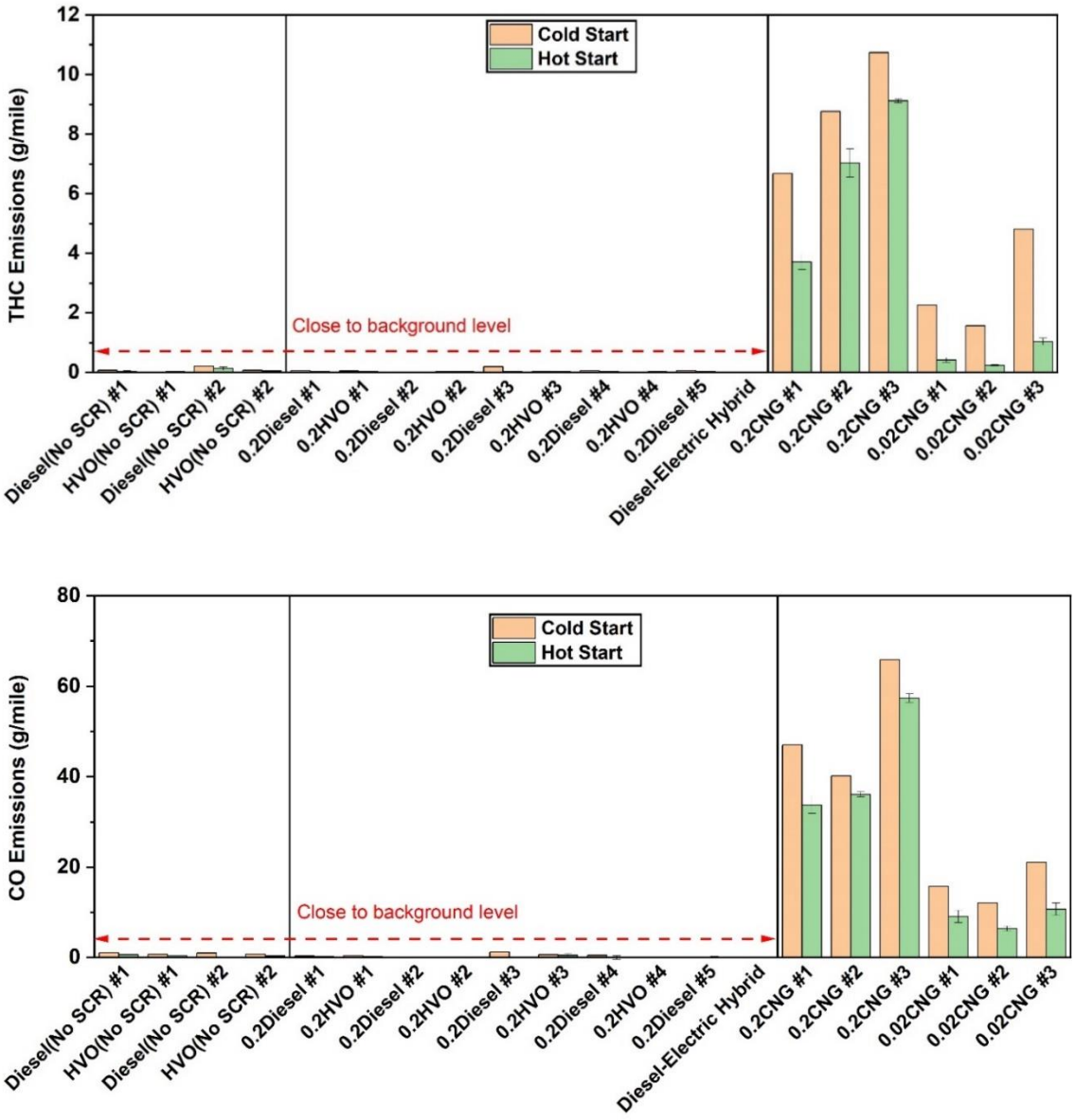

Figure 5.9 SM-2 THC and CO emissions (g/mile)

Table 5.2 SM-3 Metal emissions (µg/mile)

Fuel type	Mg (µg/mile)	Si (µg/mile)	P (µg/mile)	S (µg/mile)	Cl (µg/mile)	Ca (µg/mile)
Diesel (No SCR) #1	-	-	-	-	-	-
RD (No SCR) #1	244.7±102	66.2±14.2	-	12.2±4.5	-	-
Diesel (No SCR) #2	-	131.1±30.2	-	-	49.1±9.6	-
RD (No SCR) #2	-	372.5±29.3	9.8±9.3	-	93.1±9.3	-
0.2Diesel #1	-	-	-	-	-	-
0.2RD #1	-	-	-	-	-	-
0.2Diesel #2	-	42.5±17.8	-	-	-	-
0.2RD #2	-	70.4±17.8	-	-	-	-
0.2Diesel #3	-	-	-	-	-	-
0.2RD #3	-	-	-	-	-	-
0.2Diesel #4	-	-	-	-	-	-
0.2RD #4	-	-	-	-	-	-
0.2Diesel #5	-	-	-	-	-	36.9±32.4
Diesel-Electric	-	-	-	-	-	-
0.2CNG #1	-	-	75.6±6.0	100.0±6.0	-	280.7±20.7
0.2CNG #2	-	-	77.1±7.6	68.0±7.6	-	368.7±27.6
0.2CNG #3	-	-	-	-	-	-
0.02CNG #1	-	-	51.6±11.1	-	-	63.8±53.1
0.02CNG #2	-	-	222.0±8.0	233.8±8.0	-	729.8±28.5
0.02CNG #3	-	-	126.0±8.0	13.5±7.6	-	365.1±27.6

Table 5.2 (continued) SM-3 Metal emissions (µg/mile)

Fuel type	Cr (µg/mile)	Fe (µg/mile)	Ni (µg/mile)	Cu (µg/mile)	Zn (µg/mile)
Diesel (No SCR) #1	8.1±2.7	111.8±26.9	6.1±1.3	-	18.6±4.5
RD (No SCR) #1	10.4. ±2.7	55.6±26.7	-	-	-
Diesel (No SCR) #2	38.0±5.7	143.8±56.3	6.1±2.8	-	-
RD (No SCR) #2	13.8±5.5	134.7±54.0	11.0±2.7	-	42.3±9.2
0.2Diesel #1	-	-	22.5±2.2	10.9±4.6	-
0.2RD #1	7.7±4.5	-	-	-	-
0.2Diesel #2	-	-	-	-	-
0.2RD #2	5.7±3.4	-	-	-	-
0.2Diesel #3	-	-	10.1±2.6	-	-
0.2RD #3	-	-	-	-	-
0.2Diesel #4	8.2±4.5	77.0±44.6	-	-	30.1±7.6
0.2RD #4	6.6±4.5	-	-	-	-
0.2Diesel #5	15.5±5.4	318.1±53.3	6.4±2.6	-	-
Diesel-Electric	4.5±1.9	-	-	-	-
0.2CNG #1	5.7±3.4	190.1±33.7	3.2±1.7	100.0±6.0	121.0±5.7
0.2CNG #2	19.5±4.6	54.1±44.6	-	68.0±7.6	145.8±7.6
0.2CNG #3	-	-	-	-	-
0.02CNG #1	-	103.4±36.7	-	-	-
0.02CNG #2	14.7±4.6	129.2±44.7	-	233.8±8.0	347.6±8
0.02CNG #3	29.6±4.6	-	-	13.5±7.6	192.0±8

6. On-Road NOx Emissions Measurements From In-Use Heavy-Duty Diesel and Natural Gas Trucks

6.1. Abstract

This study characterized NOx emissions from five in-use goods movement vehicles (including one diesel vehicle without SCR, two diesel vehicles with SCR, and two ultra-low NOx CNG vehicles equipped with three-way catalysts (TWCs)) under real-world driving conditions. NOx emissions varied depending on the vehicle and the route. Diesel (NO SCR) showed the highest emissions over all the routes. The 0.2Diesel #2 vehicle showed NOx emission rates that were two times higher than those from 0.2Diesel #3, which may be attributed to catalyst deterioration. The SCR equipped diesel vehicles were within two to three times 0.2 g/bhp-hr certification standard. The 0.02CNG vehicles showed average NOx emissions around or below the optional NOx emission standard of 0.02 g/bhp-hr. The three-bin moving average window (MAW) method was utilized to show the NOx emissions across various modes of operation conditions, including idle, low load, and medium/high load, with the highest fraction of operation was found in either the low load or med/high load bins, depending on the route.

Keywords: CNG; Diesel; NOx emissions; Emissions testing; Real-world Emissions

6.2. Introduction

Nitrogen oxide (NOx) emissions are one of the most important pollutants from the transportation sector contributing to the degradation of air quality and climate (Anenberg et al., 2017). NOx emissions are a key precursor in ground-level ozone formation in the presence of volatile organic compounds (VOCs) via photochemical reactions (Simon et al.,

2015; Zhao et al., 2022). Ozone is a known respiratory irritant and has been strongly associated with respiratory diseases, such as asthma and bronchitis (Lin et al., 2008; Peel et al., 2007). Most NOx emissions in the atmosphere originate from anthropogenic sources, of which on-road vehicles account for the largest part (EPA, 2022). In California, on-road heavy-duty vehicles represent the largest single source category of NOx emissions at around 31 percent of the total emissions source inventory (CARB, 2018). California is still facing extreme challenges in meeting the federal ozone standards, and therefore reducing NOx emissions from mobile sources is critical in meeting the air quality goals.

In order to reduce emissions from on-road heavy-duty engines, the United States (U.S.) Environmental Protection Agency (EPA) introduced NOx emissions standards of 0.2 g/bhp-hr for 2010 and newer on-road heavy-duty engines (EPA, 2022). To meet these standards, selective catalyst reduction (SCR) was widely implemented in diesel engines (Piumetti et al., 2015). Although SCR provides good NOx emissions reductions under well controlled conditions during laboratory engine/chassis dynamometer testing, there are still uncertainties as to how well these systems perform under real-world driving conditions. Studies have shown that the reduction efficiencies of NOx emissions from SCR-equipped engines vary significantly under real-world conditions due to patterns of operation that are different from laboratory testing, such as more frequent stop-go driving, extended idling and more low load/speed events (Haugen and Bishop, 2018; McCaffery et al., 2021; Misra et al., 2017; Preble et al., 2019; Tan et al., 2019).

Other engine technologies and alternative fuels could also play an important role in reducing NOx emissions. Natural gas engines technology can meet the NOx emission standard of 0.2 g/bhp-hr, with recent advancements in natural gas engine technology being

capable of meeting the optional 0.02 g/bhp-hr NOx emission standard, which is 90% below the 2010 certification standard. Several recent studies have shown that late-model, stoichiometric compressed ignition engines can achieve emissions at or below the 0.02 g/bhp-hr NOx levels under various conditions during chassis dynamometer and portable emissions measurement system (PEMS) testing (Li et al., 2019; McCaffery et al., 2021; Zhu et al., 2020). However, in-use emissions data under real-world operations is still limited compared to that for diesel vehicles, so there is still uncertainty about how effective these engines are over a wide range of applications, over a variety of driving operations, and over the vehicle's full lifetime.

Controlling NOx emissions for on-road heavy-duty vehicles under real-world driving conditions is challenging. In the U.S, heavy-duty engines are typically certified using an engine dynamometer over two main test cycles, the transient Federal Test Procedure (FTP) and the Supplement Emissions Test (SET). In-use compliance testing is also conducted that covers operation during not-to exceed (NTE) events, which are characterized by operation in the NTE zone, with the engine load above 30% and SCR operational temperatures greater than 250°C, as well as other requirements, for a period 30 continuous seconds, as specified in 40 CFR 86.1370-2007. A number of studies, however, have shown that only a small fraction of in-use operation occurs under conditions meeting the conditions for an NTE event (Badshah et al., 2019; McCaffery et al., 2021; Posada et al., 2020; Tan et al., 2019). As such, the U.S. EPA and the California Air resources Board (CARB) are in the process of setting forward and implementing new methodologies for in-use compliance testing. It is still important in the near term, however, to understand how vehicles will perform under these different types of operation on a wide scale.

The objective of this study is to characterize NOx emissions from five in-use goods movement vehicles with different engine/aftertreatment technologies using a mobile emissions laboratory (MEL). Testing was performed on one diesel vehicle without SCR, two diesel vehicles with SCR, and two ultra-low NOx CNG vehicles equipped with three-way catalysts (TWCs) over for different test routes in the greater Los Angeles (L.A.) area. Both diesel vehicles with SCR were certified to 0.2 g/bhp-hr. NOx emissions standard and both CNG vehicles are certified to 0.02 g/bhp-hr NOx emissions standard. Results are discussed as a function of the impacts of engine/aftertreatment technology and driving conditions on the in-use NOx emissions. NOx emissions results were further analyzed using the 3-bin moving average window (MAW) method to evaluate the NOx emissions across different modes of operation that will be evaluated for upcoming in-use compliance testing.

6.3. **Materials and Methods**

6.3.1. **Test Vehicles and Fuels**

A total of 5 vehicles were tested in this study. All test vehicles were goods movement Class 8 trucks equipped with model year 2009 and later engines. The test matrix included one diesel vehicle without an SCR system (Diesel (NO SCR) #1), two diesel vehicles with engines certified to the 0.2 g/bhp-hr NOx level (0.2Diesel #2 and 0.2Diesel #3), and two CNG vehicles with engines certified to the 0.02 g/bhp-hr NOx level (0.02CNG#1 and 0.02CNG #2). All three diesel vehicles were equipped with diesel oxidation catalysts (DOCs) and diesel particulate filters (DPFs). Both CNG vehicles were equipped with TWCs. The main technical specifications for each vehicle are provided in Table 6.1.

The diesel vehicles were tested with commercially available grade #2, ultra-low sulfur diesel (ULSD) fuel. Similarly, for CNG vehicles, locally supplied, commercially available CNG was used. Commercially available fuel was considered to be more representative of what in-use vehicles would be using during normal in-use operation than certification fuel.

Table 6.1: Main specifications of the test vehicles

Vehicle	Manufacturer	Model Year	Model	Displacement (L)	Mileage	Aftertreatment System
Diesel (No SCR) #1	Detroit	2009	DD13	12.8	18,071	DOC/DPF
0.2Diesel #2	Detroit	2014	DD13	12.8	372,814	DOC/DPF/SCR
0.2Diesel #3	Detroit	2017	DD13	12.8	364,473	DOC/DPF/SCR
0.02CNG #1	Cummins	2019	ISX12N 400	11.9	68,873	TWC
0.02CNG #2	Cummins	2019	ISX12N 400	11.9	59,586	TWC

6.3.2. **Test Routes**

A description of the test routes is provided in Table 6.2, routes on the map are shown in Figure 6.9. Each vehicle was tested over four different routes developed by analyzing vehicle activity data collected in an earlier phase of this research. The routes were selected to represent grocery delivery operation, drayage truck operation, goods movement operation with elevation change, and highway goods movement operation in

the South Coast Air Basin (SCAB). The routes were developed by researchers at West Virginia University (WVU) with cross checks performed by the University of California, Riverside (UCR) to ensure the routes were representative of real-world driving activities for goods movement vehicles. As part of these four routes, "loading-unloading" areas were identified where the vehicles were stopped to simulate loading and unloading of goods. This simulation only represented the time of engine shutdown during the "loading-unloading" process and not any change in weight of the test vehicle.

Table 6.2 Route Statistics for On-road Testing

	Grocery Distribution	Port-Drayage	Goods Movement with Elevation Change	Highway Goods Movement
Route #	1	2	3	4
Distance (miles)	177.8	156.7	109.8	176
Time (hours)	6.74	6.56	3.12	4.63
Average speed (miles/hour)	26.4	23.9	35.2	38
Maximum speed (miles/hour)	64.8	62.9	69.6	72.1
Maximum acceleration (miles/hour/s)	10.2	5.5	6.5	5.4
Minimum acceleration (miles/hour/s)	-6.1	-10.4	-7.3	-6.1
Idle time (%)	0.7	4	2.6	2.9
Engine off time (%)	28.5	13.9	14.8	20.9

6.3.3. **Emissions Measurements**

All test vehicles were loaded with UCR's mobile emissions laboratory (MEL). The combined weight of the trailer and the MEL is typically in the range of 65,000 lbs, which is close to the national average weight of operating trucks. Detailed information of the facility and sampling setup have been discussed previously (Cocker et al., 2004). Briefly, emissions measurements included total hydrocarbons (THC) and methane (CH_4) using a flame ionization detector (FID), carbon monoxide (CO) and carbon dioxide (CO_2) using non-dispersive infrared (NDIR), and NOx using chemiluminescence technique. Tailpipe ammonia (NH_3) and nitrous oxide (N_2O) measurements were made using a Horiba MEXA-ONE-QCL-NX quantum cascade laser infrared spectrometer (QCL). This paper will only discuss NOx and NH_3 emissions results.

6.3.4. **Data Analysis**

The emissions results were calculated on a g/bhp-hr, g/mile, g/hour, and g/gallon basis. The g/gallon emission rates were calculated using fuel use rates determined using the carbon balance method. The results were also calculated based on the 3-MAW method. The 3-bin MAW method aims to cover a broader range of operating conditions compared to the previous not-to-exceed (NTE) method. The California Air Resources Board (CARB,2021) adopted this calculation methodology as part of a new regulation for NOx and PM emissions from heavy-duty diesel vehicles with model years from 2024 to 2031 on December 22nd, 2021, which included new in-use compliance procedures (CARB, 2022). The 3-bin MAW method starts with establishing a test interval for every 300 second interval after the key-on event and creates a new window starting 1 second after the start of the previous window. The mean mass rate of CO_2 over the valid window ($M_{CO2\ win}$) is

then determined for the real-world emissions. The $M_{CO2\ win}$ is then compared to the CO_2 emissions value for the engine's maximum power and its FTP Family Certification Level (FCL), which is defined as the maximum mass rate of CO_2 (M_{CO2max}). The ratio of $M_{CO2\ win}$ to M_{CO2ma} is then used to define the load level of the event as a percentage of the maximum load. The results from each 300 second window over the shift-day were separated based on their mean mass percent of CO_2 ($W_{CO2\ win}$) into one of the following three bins: Idle bin with $W_{CO2\ win} < 6\%$, Low load bin with $6\% < W_{CO2\ win} < 20\%$, and Medium/High load bin with $W_{CO2\ win} > 20\%$.

6.4. Results and Discussion

6.4.1. NOx and NH_3 Emissions

Figure 6.1 shows the NOx emissions for each vehicle and route on a g/mile and g/bhp-hr basis. Additional data is provided in Table 6.3 for NOx emissions expressed in g/hour and g/gal basis. Note that Route 4 of vehicle 0.02CNG #2 was not available due to a technical issue with the instruments. NOx emissions varied depending on the route. Diesel (no SCR) #1 showed the highest NOx emissions for all routes compared to the other diesel and CNG trucks. For Diesel (no SCR) #1, average NOx emissions ranged from 2.0 to 3.5 on a g/mile basis and from 0.6 to 1.1 on a g/bhp-hr basis, with the overall emissions for all test routes being below the engine's certification limit of 1.2 g/bhp-hr. Although the engine's certification limit is based on the results from engine dynamometer testing over the Federal Test Procedure (FTP) cycle, comparisons to the certification limit can still provide some valuable information on how real-world emissions are correlated with laboratory testing. On a g/bhp-hr, g/mile, and g/gal basis, the highest emissions for Diesel (no SCR) #1 were found over the Grocery Distribution route (Route 1), with emission rates

around 1.08 g/bhp-hr and 3.46 g/mile. The lowest emissions were generally seen for the Highway Goods Movement route (Route 4), with emission rates around 0.59 g/bhp-hr and 1.99 g/mile. The Grocery Distribution route is characterized by more extensive freeway driving in traffic in the greater Los Angeles (L.A.) area, while the Highway Goods Movement route is characterized by more steady-state open freeway driving out to Indio, CA and back to Riverside, CA. The Port-Drayage (Route 2) and Goods Movement with Elevation Change routes (Route 3) showed similar NOx emissions on a g/bhp-hr, g/mile, and g/gal basis, even though they represent considerably different driving conditions. The Port-Drayage route represents driving from the port of L.A. and port of Long Beach to inland warehousing areas, while the Goods Movement with Elevation Change route represents mountain driving conditions. The NOx emissions on a g/hour basis were the highest for the Goods Movement with Elevation Change route, which is characterized by extended operation on a steep climb, combined with an extended downhill driving on the return trip, and were lowest for the Port-Drayage route, which represents driving through the greater L.A. area.

These results can be compared to other results in literature. Emission factors from EMFAC for 2007-2009 vehicles range from 6.4 to 7.7 g/mile, which are generally lower than those measured here (CARB, 2011). McCaffery et al (2021) tested vehicles with the same engine technology over their typical daily operation using PEMS as part of a companion work to this study, with NOx emission rates ranging from 0.7 to 1.2 g/bhp-hr. For older pre-2010 non-SCR equipped diesel vehicles, Durbin et al. found considerably higher emission factors ranging between 5-30 g/mile depending on the engine model year and cycles (Durbin et al., 2008), indicating that later MY pre-2010 non-SCR vehicles show

significant advancements in engine technology and better control of post-engine NOx emissions. Although the fraction of pre-2010 non-SCR vehicles continues to decline, and particularly in California, emissions results from non-SCR equipped vehicles still provide information on potential emission reductions for other transportation sources where SCR has just started to be implemented or even for other parts of the U.S. where emissions standards are less stringent compared to those in California.

For both the SCR-equipped diesel vehicles, average NOx emissions ranged from 0.21 to 0.62 on a g/bhp-hr basis and from 0.69 to 2.24 on a g/mile basis. On a g/mile basis, the highest NOx emissions for both diesel trucks were found over the Goods Movement with Elevation Change route, with the steep climb, while the lowest emissions were generally seen for the Grocery Distribution route through the greater LA area. On a g/bhp-hr basis, the Goods Movement with Elevation Change Route (Route #3) and the Highway Goods Movement route (Route #4) showed around 50% higher emissions than the Port-Drayage route (Route #2) and the Grocery Distribution route (Route #1). For both SCR equipped diesel vehicles, all four routes were higher than the 0.2 g/bhp-hr certification limits. For 0.2Diesel #3 on a g/bhp-hr basis, the Grocery Distribution route (Route #1) and the Port-Drayage route (Route #2) showed NOx emissions around the 0.2 g/bhp-hr level which were 1.5 times higher than the limit over the other two routes. On the other hand, 0.2Diesel #2 showed emissions about twice those for 0.2Diesel #3 over all four test routes with emission rates ranging between 0.41 to 0.62 g/bhp-hr. This may indicate 0.2Diesel #2 had a greater level of deterioration. A number of studies have found that real-world deterioration of diesel vehicles emissions is highly dependent on vehicle mileage (Boveroux et al., 2021; Chen et al., 2020). In addition, real driving conditions and the

vocation of the vehicles may also impact the deterioration rate (Hao et al., 2022).On a g/hour basis, the Goods Movement with Elevation Change and Highway Goods Movement routes showed the highest NOx emissions, while the Port-Drayage and Grocery Distribution routes both showed lower emissions.

The emissions results for this study are comparable to those found in some other studies. In evaluating data from the Heavy-Duty In-Use Testing (HDIUT) program, Badshah et al. (2019) found emissions rates of 0.42 g NOx/bhp-hr when the data were averaged over all operation (Badshah et al., 2019). The results are also comparable to those obtained from similar in-use SCR-equipped vehicles when tested PEMS, with NOx emissions ranging from 0.3 to 0.6 g/bhp-hr (McCaffery et al., 2021). (Jiang et al., 2018) evaluated NOx emissions from five heavy-duty diesel trucks equipped with DPFs and SCR systems on a chassis dynamometer and showed emissions around 0.13 to 0.39 g/bhp-hr over the UDDS cycle and around 0.07 to 0.25 g/bhp-hr over the high-speed cruise cycle. The NOx emission rates are lower than those found in the 202x EMission FACtors (EMFAC) model developed by CARB. The 202x EMFAC model indicates that most of MY 2013 to 2015 heavy heavy-duty (HHD) vehicles showed emissions higher than the standard, with some low mileage vehicles showing six times higher. Furthermore, the late model year (after MY 2016) vehicles showed NOx emissions three to four times higher than the standard, ranging from 2 to 4 g/mile over a UDDS cycle (CARB, 2020). Some other studies also showed generally higher NOx emissions than this study depending on the cycles. Misra et al. also found higher NOx emissions, but in the range of the engine certification limit depending on the test cycles and cold-starts (Misra et al., 2013). A number of other investigations have indicated that engine deterioration can be caused by

higher mileage, improper dosing of urea in the SCR system, and non-functional or poorly maintained aftertreatment system that may lead to excessive NOx emissions that sometimes can be two times or even higher than the engine certification limits (Jiang et al., 2021; Misra et al., 2013; Thiruvengadam et al., 2015).

NOx emissions for both CNG vehicles were considerably lower than those for both the diesel vehicles equipped with or without SCR systems, with average NOx emissions ranging from 0.01 to 0.02 on a g/bhp-hr basis and from 0.04 to 0.07 on a g/mile basis. These emissions were all at or below the certification standard for all routes, with slightly higher emission rates for the Goods Movement with Elevation Change and Highway Goods Movement routes compared to the Port-Drayage and Grocery Distribution routes. Other studies have also indicated the potential of ultra-low NOx CNG engines of reaching NOx emissions levels at or below 0.02 g/bhp-hr (Li et al., 2019; Zhu et al., 2020). These NOx emission rates are lower than those found for similar CNG in-use vehicles tested with PEMS and ranged from 0.03 to 0.13 g/bhp-hr (McCaffery et al., 2021).

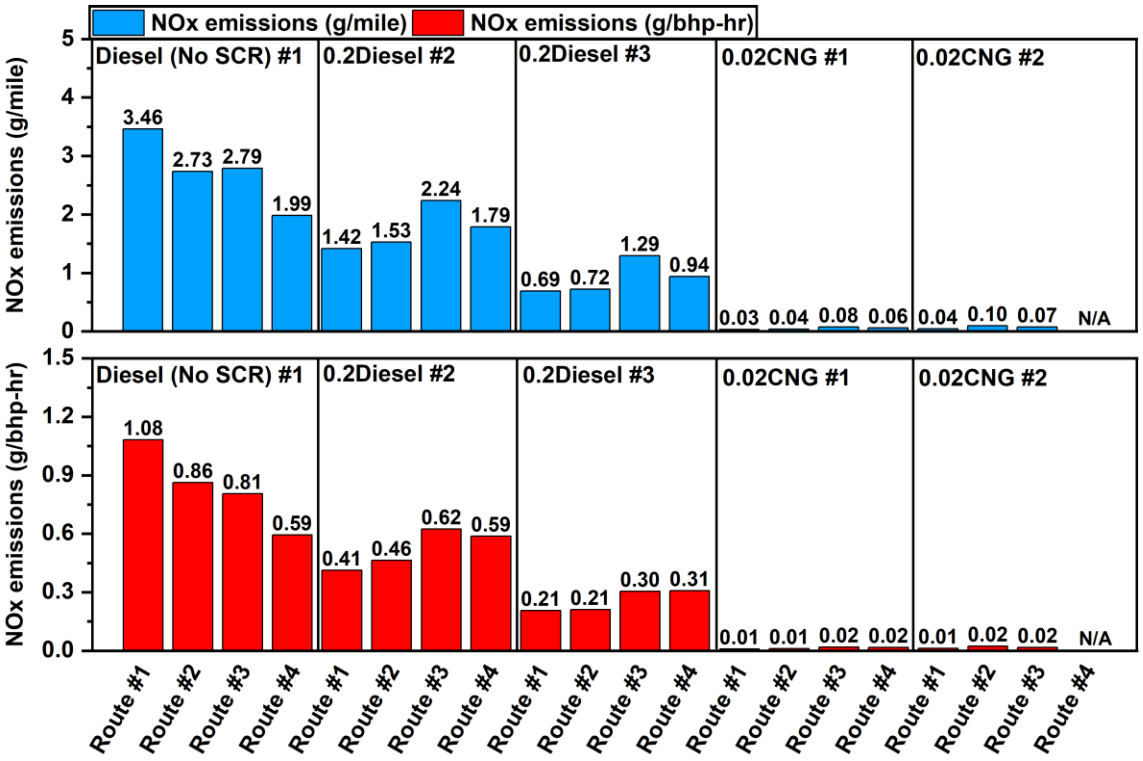

Figure 6.1 Real-World NOx Emission Results

NH_3 emissions for each vehicle and route are shown on a g/mile and g/bhp-hr basis in Figure 6.2, except for Route 4 for 0.02CNG#2. Note that Route 4 of vehicle 0.02CNG #2 was not available due to a technical issue with the measurement instruments. NH_3 emissions varied depending on the vehicle and test route. Diesel (no SCR) #1 showed almost no NH_3 emissions due to lack of SCR catalyst system. It is well known that NH_3 is not a combustion product but rather can form due to NH_3 slip through the SCR catalyst. For diesel engines, SCR systems utilize atomized urea to form NH_3 which serves as a reducing agent in converting NOx to N_2 and water (Heywood, 2018). NH_3 emissions can slip through the catalyst depending on urea dosing and other conditions (Suarez-Bertoa and Astorga, 2016), although most SCR-equipped engines are also equipped with an NH_3 slip catalyst to minimize this. Figure 6.2 shows that for both SCR-equipped diesel vehicles when operating over Route #1, Route #2, and Route #4 showed NH_3 emission rates ranging

from 0.01 to 0.03 g/bhp-hr (0.02 to 0.09 g/mile). NH_3 emissions over Route #3 were close to the measurement limits of the instrument, possibly due to better control of urea-dosing of this route.

Although CNG vehicles provide a solid potential for reducing NOx emissions in heavy-duty applications, elevated tailpipe NH_3 emissions could be a concern, due to the contribution of NH_3 to the formation of secondary fine particulate matter (PM) (Nowak et al., 2010). In the TWC, NH_3 is formed via the reduction of nitric oxide (NO) by molecular hydrogen produced from a water-gas shift reaction between CO and water or via steam reforming of hydrocarbons. The formation of hydrogen is favored under fuel rich conditions and at catalyst temperatures above 250 °C (Suarez-Bertoa and Astorga, 2016; Nevalainen et al., 2018; Whittington et al., 1995). Our results showed about 20 times higher NH_3 emissions for the CNG vehicles compared to the SCR-equipped diesel vehicles, even though the CNG vehicles exhibited over 90% NOx emissions reductions compared to the SCR-equipped vehicles. NH_3 emissions ranged from 0.1 to 0.19 g/bhp-hr (0.42 to 0.69 g/mile), with the Grocery Distribution route (Route #1) and the Port Drayage Route (Route #2) having the highest NH_3 emissions. Both these routes represented more urban driving with more transient driving patterns due to more frequent stop-and-go events. The lowest NH_3 emissions were seen for the Highway Goods Movement route (Route #4) for 0.02CNG #1, with NH_3 emissions rates of 0.19 g/bhp-hr (0.69 g/mile), which is 34% lower than those for the Grocery Distribution route.

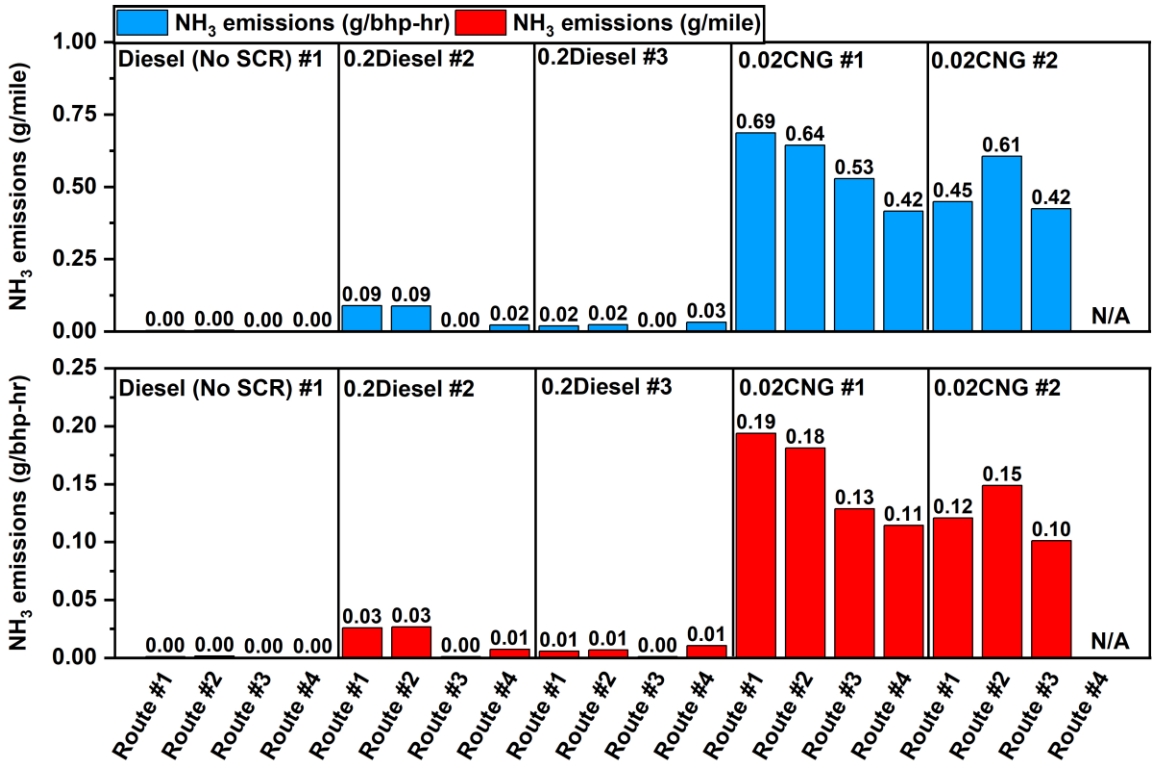

Figure 6.2 Real-World NH_3 Emission Results

6.4.2. Three Bin Moving Average Window (MAW) Method

Figure 6.3 shows the fraction of windows for each of the 3-bin MAW bins over the four routes based on the emissions and engine data from 0.2Diesel #2 and 0.2Diesel #3. The figure provides information on the fraction of vehicle operation on a time duration basis in each of the bins for each route. The bins are determined load level determined based on the ratio of M_{CO2win} to M_{CO2ma}, as discussed in section 2.4. The highest fraction of operation was found in either the low load or med/high load bins, depending on the route. The fraction of valid windows for the low load bin ranged from 33% to 52% depending on the routes. The Grocery Distribution route showed the highest fraction for the low load bins of 52%, which represents more of urban driving conditions consisting of frequent stop-and-go events. The fraction of valid windows for the med/high load bin ranged from 37% to 48%. The Highway Goods Movement route showed the highest

fraction of valid events for the medium/high load bins of 48%, which represents more freeway driving conditions consisting of high vehicle speed and engine power events.

For the idle windows, the highest fraction of valid idle windows was found for the Port-Drayage route (Route #2) and Goods Movement with Elevation Change route (Route #3), at 23% and 25%, respectively. The Port-Drayage route includes an extended idle and creep operation, which simulates port activity while the vehicle is waiting at the port terminals to load shipping containers. The Goods Movement with Elevation Change route, interestingly, also showed a large fraction of idle activity, though the vehicle was operating at a relatively high speed for most of this time. Deeper investigation of the real-time data showed that prolonged downhill driving was the main contributor to idle activity for the Goods Movement with Elevation Change route. The extended downhill driving (deceleration) is classified similarly to the idle because the the fuel is cut-off for long periods, as indicated by the CO_2 emissions. The Grocery Distribution route showed the lowest fraction of valid idle windows at 6%, followed by the Highway Goods Movement route at 11%.

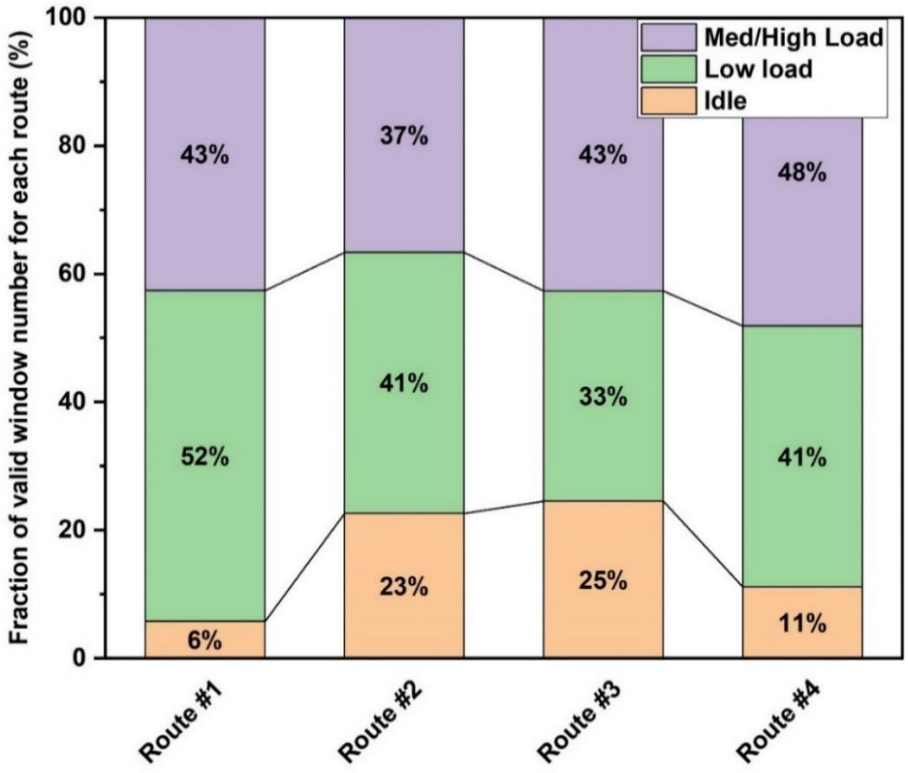

Figure 6.3 Fraction of valid window in each bin over the testing routes

Figure 6.4(a-d) shows NOx emissions results for the 3-bin MAW method for 0.2Diesel #2, 0.2Diesel #3, and 0.02CNG #1 vehicles for each route. The average NOx emissions over the full Route, including all operational modes, are also shown in Figure 6.4(d) to serve as a baseline comparison to the binning results. Average SCR/TWC inlet temperatures are also provided to show the difference in catalyst conditions between routes/engine technology types. Diesel (No SCR) #1 was excluded as non-SCR equipped diesel vehicles and are not subject to the 3-bin MAW regulation and are being phased out. CNG vehicles with spark-ignited engines are also generally not evaluated over the 3-bin MAW method, especially under low load and idle conditions, since the CO_2 mass emissions for this type of combustion engine platform do not show as much consistency compared to compression ignition engines. However, it is valuable to provide a comparison between the CNG and diesel vehicles using this method. Only one CNG

vehicle is included in the analysis since both CNG vehicles showed almost identical trends. Although vehicles manufactured prior to 2024 will not be subject to monitoring using the 3-bin MAW method, it is still useful to evaluate the current results in this context to see how current technology vehicles perform against this metric. For the 3-bin MAW window, the in-use compliance limits for the medium/high load are set to be 2 times the emissions certification value for 2024 to 2029 vehicles, and 1.5 times the emissions certification value for 2030 and beyond vehicles. The idle emissions will be compared to the idle limit, which is currently 20 g/h, but will be reduced to 10 g/hr in 2024. The 2 times limits for the medium/high load and the current 30 g/h limit are also included in the Figure 6.4 for illustrative purposes. The low load bins compliance limits for future engines will be based on 2 times the certification limit for the low load cycle that will be implemented in 2024, but this is not shown in the figures, as these engines were not certification over this cycle.

For the medium/high load bins, 0.2Diesel #3 showed emissions that were well below the in-use compliance limits over all routes, while 0.2Diesel #2 showed NOx emissions that ranged from 0.4 to 0.6 g/bhp-hr, which were between 1.3 and two times higher than the future 0.3 g/bhp-hr in-use compliance limits. The 0.2Diesel #2 vehicle showed lower NOx emission rates than 0.2Diesel#3 over all four routes despite their similar average temperature profiles, as shown in Figure 6.4(d). The average SCR inlet temperatures for the medium/high load bins were higher than those averaged over the full route, ranging between 300°C and 400°C. For the low load bins, NOx emissions for the 0.2Diesel #3 showed greater variation compared to those for 0.2Diesel #2, with Route #1 and Route #2 showing lower emissions and Route #3 and Route #4 showing higher NOx emissions. For the idle bin results, the emissions were all below the current 30 g/h limits,

except for 0.2Diesel #3 over the Goods Movement with Elevation Change route. Both vehicles showed average SCR inlet temperatures well below 200 °C for the idle periods. The idle emissions trends between different diesel vehicles are discussed in greater detail in section 3.3.2. The 0.02CNG #1 vehicle showed emissions well below those of the 0.2 SCR-equipped diesel vehicles for all three bins, with the medium/high bin emissions being well below 2 times the certification standard limits. There were some trends of slightly higher emissions for the Goods Movement with Elevation Change and Highway Goods Movement routes, which are discussed in greater detail in section 3.3.3.

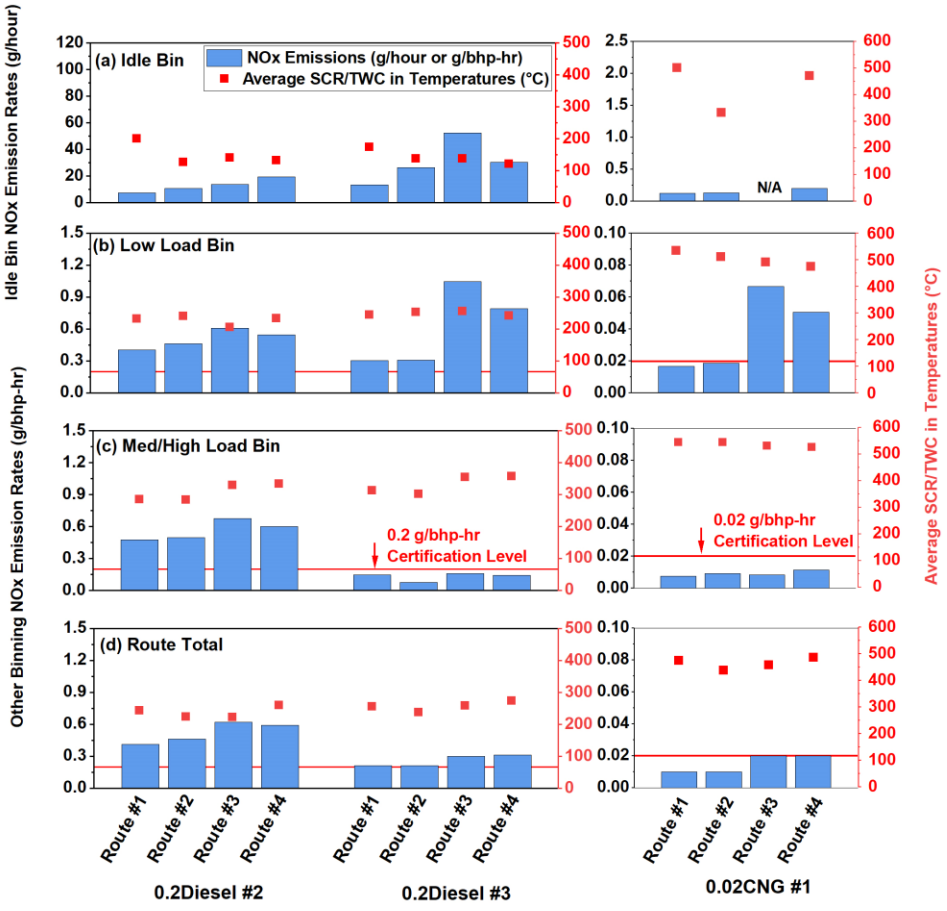

Figure 6.4(a-d) Average NOx emissions and SCR/TWC in temperatures for 0.2Diesel #2 and #3, and 0.02CNG #1 over the four testing routes at Idle bin (a), Low load bin (b), Medium/High load bin (c), and Route total (d).

6.4.3. **Real-Time Emission Profile Snapshots**

This section discusses the real-time emissions profiles for different vehicles over different routes. Real-time emissions plots are shown for both 0.2 diesel vehicles and 0.02 CNG #1 over the Grocery Distribution route and over the idle creep segment of the Port-Drayage route, and for 0.02 CNG #1 over the Goods Movement with Elevation Change route. The Grocery Distribution Route was chosen as it is the most representative route of goods movement vehicles in SCAB whose activities include a mix of urban, highway, and loading/unloading events. The idle creep segment represents traffic congestion in the port area while transferring goods, which is highlighted to help illustrate emissions under idle or low load/speed conditions. The Goods movement with elevation change route was chosen for the CNG vehicle since it is the only route that showed appreciable NOx emission event beyond the start of the route for these vehicles. The 3-bin analysis results shown previously for this route also indicate elevated NOx emissions during the low load bin, and thus more investigation on the real-time emissions plot is necessary.

6.4.3.1. **Grocery Distribution Route**

Figure 6.5 shows the real-time emissions profiles for tailpipe NOx emissions, tailpipe NH_3 emissions, the SCR inlet temperature, and vehicle speed profiles over the initial segment of the Grocery Distribution Route for the two 0.2 Diesel vehicles and one CNG vehicle. Figure 6.5 provides a clear comparison for NOx emissions between the different engine technologies over the first segment of the Grocery Distribution Route. The 0.2Diesel #2 vehicle showed almost two times higher NOx emission rates than 0.2Diesel #3, which is shown by comparing the real-time NOx emission profiles. Both diesel vehicles showed emissions during the initial cold start phase and during the first 800s, when the

SCR inlet temperatures were below around 250 °C, with emission rates reaching up to 0.1 g/s and 0.15 g/s for 0.2Diesel #2 and 0.2Diesel #3, respectively. Elevated NOx emissions were observed mostly during accelerations, where higher cylinder temperatures and combustion pressures will favor NOx formation. In contrast, 0.2Diesel #3 showed elevated NOx emissions even during periods where the SCR catalyst was above 250 °C, indicating inefficient NOx reductions from the SCR catalyst, which could be due to catalyst degradation or improper urea dosing for this vehicle. The 0.2Diesel #2 vehicle showed NH_3 emissions spikes at around 1000s, which could be due to the over-dosing of urea that results in high NH_3/NOx and thus high ammonia slip.

For 0.2Diesel #3, a DPF regeneration event occurred in segment 5 at around 28,000s, where the SCR inlet temperatures exceeded 500 °C, which is illustrated in Figure 6.8. During the regeneration event, NOx emission rates were two times higher than those under normal driving conditions, with emission rates around 0.4 g/bhp-hr. Higher NOx emissions during DPF regeneration events have been reported in previous studies and were largely attributed to the fuel-rich mode during regeneration that can increase the post injection fuel quantities, retard post injection timing, and increase the exhaust temperatures (Ko et al., 2019). Other studies have shown little influence in NOx emissions during DPF regeneration events (Huang et al., 2022; Papadopoulos et al., 2020). The 0.02CNG #1 vehicle showed elevated NOx emissions during the initial cold start phase when the TWC was below its light-off temperature. NOx emission rates during the cold start phase reached up to 0.025 g/s, which were comparable to those from the SCR-equipped diesel vehicles. NH_3 emissions, however, occurred over the course of the whole route for the 0.02CNG #1 vehicle, with emissions rate reaching up to 0.06 g/s during acceleration events.

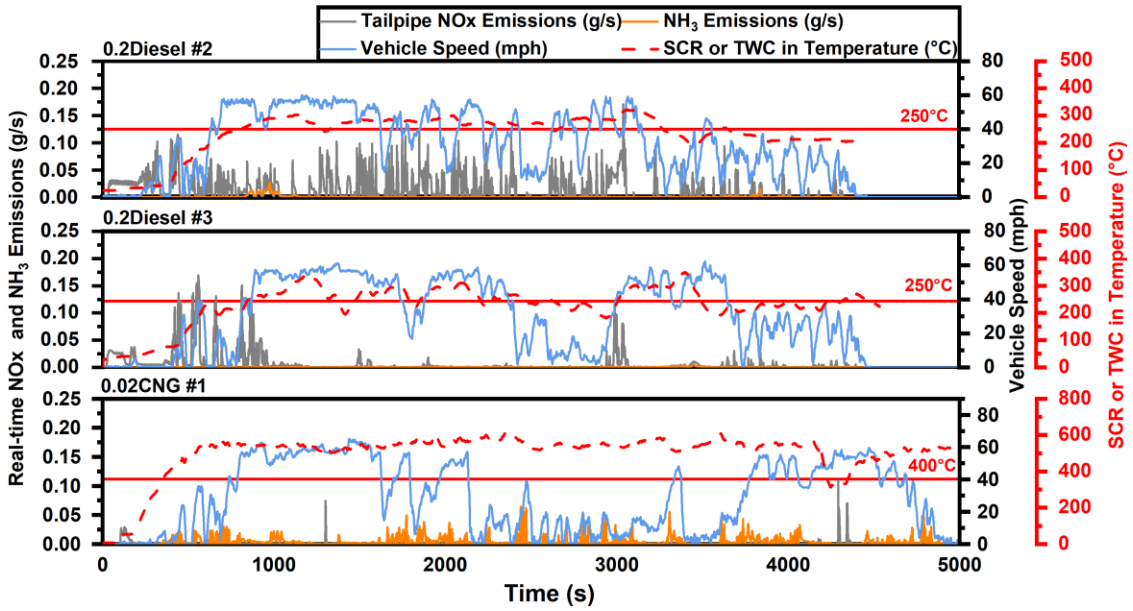

Figure 6.5 Real-time tailpipe NOx emissions (g/s), catalyst intake temperature (°C), and vehicle speed (mph) for 0.2Diesel #2, 0.2Diesel #3, and 0.02CNG #1 over the Grocery Distribution route.

6.4.3.2. Idle Creep Segment of the Port-Drayage Route

Figure 6.6 shows the real-time emissions profiles for tailpipe NOx emissions, tailpipe NH_3 emissions, the SCR inlet temperature, the EGR rate and vehicle speed profiles over a window of the idle-creep segment of the Port-Drayage Route for the two SCR-equipped vehicles and one CNG vehicle. Idle creep activity is important to understand since different factors may affect NOx emissions under this engine operating condition.

For both diesel vehicles, SCR inlet temperatures were constant during the idle period at around 100 °C, such that almost no NOx emissions reductions from the SCR catalyst was observed. For 0.2Diesel #2, the idle period showed emission rates ranging from 0.002 to 0.004 g/s (7.2 to 14.4 g/hour), with almost no engagement of EGR, except for two times at 1,200s and 2,600s, respectively. In contrast, 0.2Diesel #3 showed higher idle emission rates of around 0.006 g/s (21.6 g/hour). The EGR rate for 0.2Diesel #3 reached up to 30%, with NOx emissions spiking when the EGR rate decreased and vice

versa. This indicated that lower EGR rates contribute to higher NOx emissions. For the 0.02CNG #1 vehicle, a different phenomenon was observed where NOx emissions were mostly close to the detection limit, except for the NOx emissions between 1400s to 1600s, which was due to lower catalyst temperatures during this period. During this period, EGR rates were close to zero. NH_3 emissions spikes were observed after 1700s when the catalyst was above 400 °C, with the highest NH_3 emission rate of around 0.0016 g/s at around 1,900s. NH_3 emissions are usually seen at lower air/fuel ratios that are associated with rich combustion conditions that favor the formation of CO emissions (Suarez-Bertoa et al., 2017).

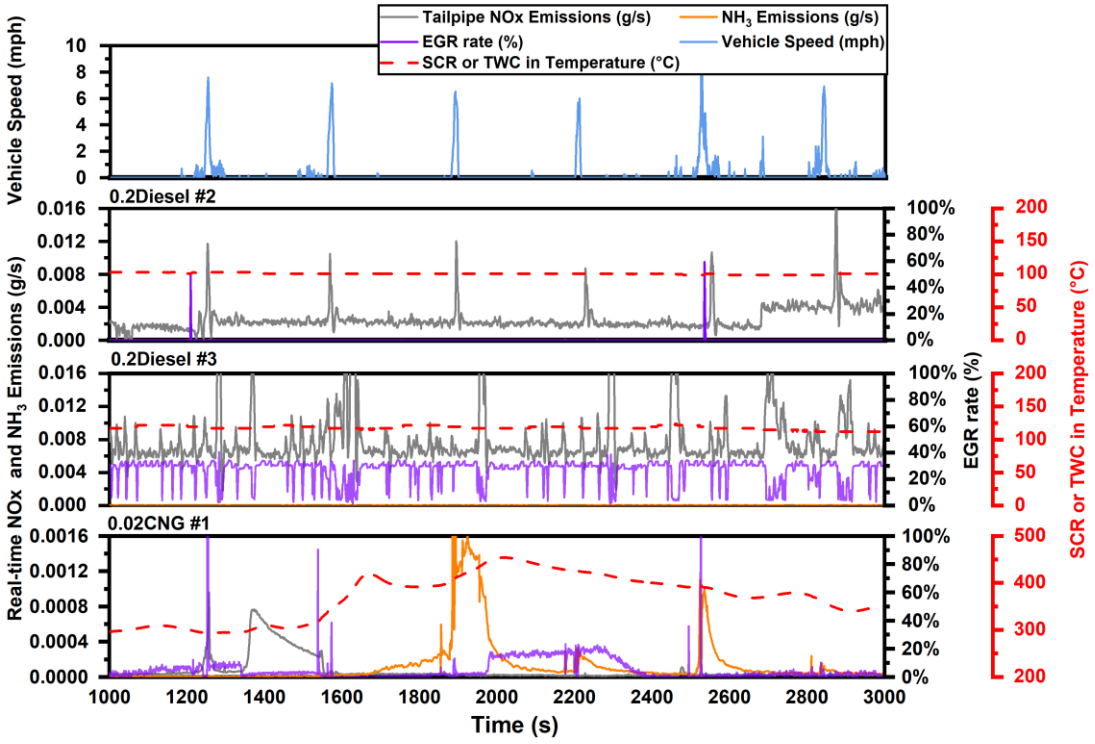

Figure 6.6 Real-time tailpipe NOx emissions (g/s), catalyst intake temperature (°C), and vehicle speed (mph) for 0.2Diesel #2, 0.2Diesel #3, and 0.02CNG #1 over idle creep segment of Port Drayage route.

6.4.3.3. **Goods Movement With Elevation Change Route (Route #3)**

Figure 6.7 shows the real-time profiles for tailpipe NOx emissions, TWC inlet temperatures, and vehicle speed for a CNG vehicles over the Goods Movement with Elevation Change route. This route was selected because the NOx emissions for the other routes were generally very low or close to the detection limit over the entire duration of the routes for the CNG vehicles, with the exception of some NOx spikes at the very beginning of each testing day, when the engine was cold and the TWC was below its light-off temperature. A fully warmed-up TWC is expected to provide high NOx reduction efficiencies, which was the case for the majority of the routes. Elevated NOx emissions were observed during downhill driving at around 4,000s and 10,000s due to the TWC temperatures being below 200 °C. NOx emissions during the downhill segment when the engine falls into the idle or low load bin accounted for about 70% of the total emissions for this route. NH_3 emissions across the entire route ranged from 0.08 g/s to close to zero during the downhill driving phase, which also indicates no catalyst reactions occurring to reduce NOx. NOx emissions during the cold-start phase accounted for about 15% of the total emissions for this route, compared to 25 % for Grocery Distribution route without significant downhill driving.

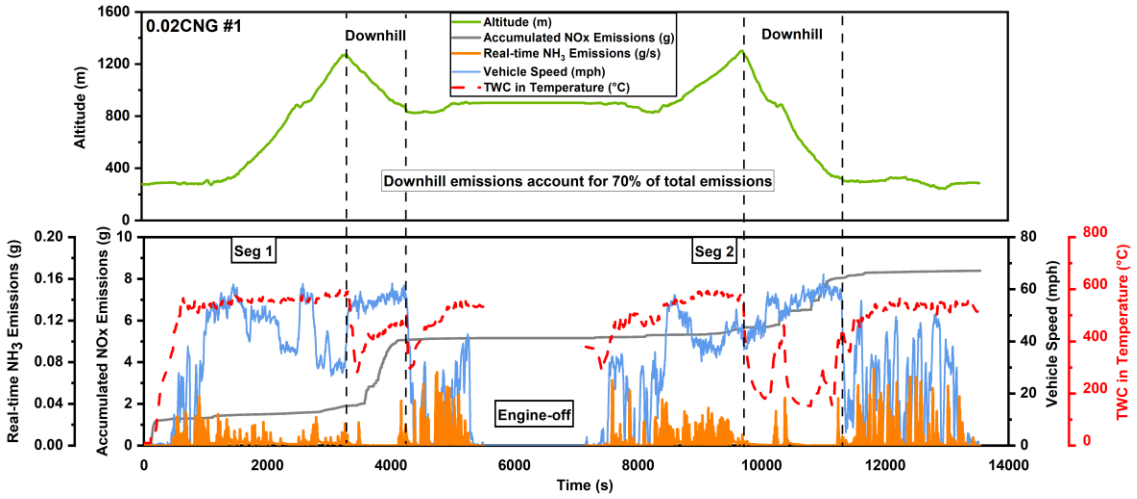

Figure 6.7 Real time tailpipe NOx emissions(g/s), catalyst intake temperature(°C) and vehicle speed (mph) for 0.02CNG #1 over Goods Movement with Elevation Change route.

6.5. Conclusions

This study measured and characterized NOx emissions from five heavy-duty diesel and natural gas goods movement vehicles with different engine technologies. All five vehicles were tested on-road under four pre-defined goods movement routes in SCAB, representing grocery distribution, port-drayage operation, and highway driving with and without elevation change. NOx emissions were measured using a mobile emissions laboratory. NOx emissions varied depending on the vehicle and the route. The diesel (no SCR) vehicle showed the highest NOx emissions over all routes, ranging from 0.6 to 1.1 g/bhp-hr. For the SCR-equipped diesel vehicles, the NOx emission rates ranged from 0.21 to 0.62 g/bhp-hr, with the NOx emissions rates for 0.2Diesel #2 being about two times higher than those from 0.2Diesel #3. This could be due to deterioration of the engines or SCR catalyst, since it showed higher NOx emissions even during section of the route where the SCR inlet temperature was at its optimal operating range. CNG vehicles showed average NOx emissions at or below the optional NOx emission standard of 0.02 g/bhp-hr.

The three-bin MAW method was utilized to show the NOx emissions across various modes of operation conditions, including idle, low load, and medium/high load. The highest fraction of operation was found in either the low load or med/high load bins, depending on the route, with the highway routes showing a greater fraction operation in the med/high load bin, and the Grocery Distribution and Port-Drayage routes showing a greater fraction operation in the low load bin. For the idle windows, the highest fraction of valid idle windows was found for the Port-Drayage route (Route #2) and Goods Movement with Elevation Change route (Route #3), at 23% and 25%, respectively.

6.6. **Acknowledgements**

We acknowledge funding from the California Energy Commission (CEC), the South Coast Air Quality Management District (South Coast AQMD), Southern California Gas Company (SoCalGas), and the California Air Resources Board (CARB) under South Coast AQMD contract number 17286. The authors thank Mark Villela, Daniel Gomez, and Dan Hartnett of the University of California, Riverside for their contribution in conducting the emissions testing for this program.

6.7. **References**

Anenberg SC, Miller J, Minjares R, Du L, Henze DK, Lacey F, et al. Impacts and mitigation of excess diesel-related NOx emissions in 11 major vehicle markets. Nature 2017; 545: 467-471.

Badshah H, Posada F, Muncrief R. Current State of NO_x Emissions from In-Use Heavy-Duty Diesel Vehicles in the United States. 2019.

Boveroux F, Cassiers S, De Meyer P, Buekenhoudt P, Bergmans B, Idczak F, et al. Impact of mileage on particle number emission factors for EURO5 and EURO6 diesel passenger cars. Atmospheric Environment 2021; 244: 117975.

California Air Resources Board, 2018. EMFAC2017 Volume III - Technical Documentation V1.0.2, July 20. https://ww3.arb.ca.gov/msei/downloads/emfac2017-volume-iii-technical-documentation.pdf

California Air Resources Board, "Heavy-Duty Omnibus Regulation," accessed January 3, 2022, https://ww2.arb.ca.gov/rulemaking/2020/hdomnibuslownox

CARB mobile emissions source inventory (MESI), updated 2011, accessed 2022. https://ww2.arb.ca.gov/our-work/programs/mobile-source-emissions-inventory/msei announcements

Chen Y, Sun R, Borken-Kleefeld J. On-Road NO x and smoke emissions of Diesel light commercial vehicles–combining remote sensing measurements from across Europe. Environmental Science & Technology 2020; 54: 11744-11752.

Cocker DR, Shah SD, Johnson K, Miller JW, Norbeck JM. Development and application of a mobile laboratory for measuring emissions from diesel engines. 1. Regulated gaseous emissions. Environmental science & technology 2004; 38: 2182-2189.

Durbin TD, Johnson K, Miller JW, Maldonado H, Chernich D. Emissions from heavy-duty vehicles under actual on-road driving conditions. Atmospheric environment 2008; 42: 4812-4821.

U.S. Environmental Protect Agency (EPA) National Emissions Inventory (NEI), April, 2022, Accessed on Nov 2022, https://www.epa.gov/air-emissions-inventories/national-emissions-inventory-nei

EPA Emission Standards for Heavy-Duty Highway Engines and Vehicles, February 2022, accessed Nov 2022 https://www.epa.gov/emission-standards-reference-guide/epa-emission-standards-heavy-dutyhighway-engines-and-vehicles

Hao L, Zhao Z, Yin H, Wang J, Li L, Lu W, et al. Study of durability of diesel vehicle emissions performance based on real driving emission measurement. Chemosphere 2022; 297: 134171.

Haugen MJ, Bishop GA. Long-term fuel-specific NO x and particle emission trends for in-use heavy-duty vehicles in california. Environmental science & technology 2018; 52: 6070-6076.

Heywood JB. Internal combustion engine fundamentals: McGraw-Hill Education, 2018.

Jiang Y, Yang J, Cocker III D, Karavalakis G, Johnson KC, Durbin TD. Characterizing emission rates of regulated pollutants from model year 2012+ heavy-duty diesel vehicles equipped with DPF and SCR systems. Science of The Total Environment 2018; 619: 765-771.

Jiang Y, Yang J, Tan Y, Yoon S, Chang H-L, Collins J, et al. Evaluation of emissions benefits of OBD-based repairs for potential application in a heavy-duty vehicle Inspection and Maintenance program. Atmospheric Environment 2021; 247: 118186.

Li C, Han Y, Jiang Y, Yang J, Karavalakis G, Durbin TD, et al. Emissions from advanced ultra-low-NOx heavy-duty natural gas vehicles. 2019.

Lin S, Bell EM, Liu W, Walker RJ, Kim NK, Hwang S-A. Ambient ozone concentration and hospital admissions due to childhood respiratory diseases in New York State, 1991–2001. Environmental Research 2008; 108: 42-47.

McCaffery C, Zhu H, Tang T, Li C, Karavalakis G, Cao S, et al. Real-world NOx emissions from heavy-duty diesel, natural gas, and diesel hybrid electric vehicles of different vocations on California roadways. Science of The Total Environment 2021; 784: 147224.

Misra C, Collins JF, Herner JD, Sax T, Krishnamurthy M, Sobieralski W, et al. In-use NO x emissions from model year 2010 and 2011 heavy-duty diesel engines equipped with aftertreatment devices. Environmental science & technology 2013; 47: 7892-7898.

Misra C, Ruehl C, Collins J, Chernich D, Herner J. In-use NOx emissions from diesel and liquefied natural gas refuse trucks equipped with SCR and TWC, respectively. Environmental science & technology 2017; 51: 6981-6989.

Peel JL, Metzger KB, Klein M, Flanders WD, Mulholland JA, Tolbert PE. Ambient air pollution and cardiovascular emergency department visits in potentially sensitive groups. American Journal of Epidemiology 2007; 165: 625-633.

Piumetti M, Bensaid S, Fino D, Russo N. Catalysis in diesel engine NO x aftertreatment: a review. Catalysis, Structure & Reactivity 2015; 1: 155-173.

Posada F, Badshah H, Rodriguez F. In-use NOx emissions and compliance evaluation for modern heavy-duty vehicles in Europe and the United States. 2020.

Preble CV, Harley RA, Kirchstetter TW. Control technology-driven changes to in-use heavy-duty diesel truck emissions of nitrogenous species and related environmental impacts. Environmental science & technology 2019; 53: 14568-14576.

Simon H, Reff A, Wells B, Xing J, Frank N. Ozone trends across the United States over a period of decreasing NOx and VOC emissions. Environmental science & technology 2015; 49: 186-195.

Tan Y, Henderick P, Yoon S, Herner J, Montes T, Boriboonsomsin K, et al. On-board sensor-based NO x emissions from heavy-duty diesel vehicles. Environmental science & technology 2019; 53: 5504-5511.

Thiruvengadam A, Besch MC, Thiruvengadam P, Pradhan S, Carder D, Kappanna H, et al. Emission rates of regulated pollutants from current technology heavy-duty diesel and natural gas goods movement vehicles. Environmental science & technology 2015; 49: 5236-5244.

Zhao Y, Tkacik DS, May AA, Donahue NM, Robinson AL. Mobile Sources Are Still an Important Source of Secondary Organic Aerosol and Fine Particulate Matter in the Los Angeles Region. Environmental Science & Technology 2022.

Zhu H, McCaffery C, Yang J, Li C, Karavalakis G, Johnson KC, et al. Characterizing emission rates of regulated and unregulated pollutants from two ultra-low NOx CNG heavy-duty vehicles. Fuel 2020; 277: 118192.

6.8. **Supplemental Materials**

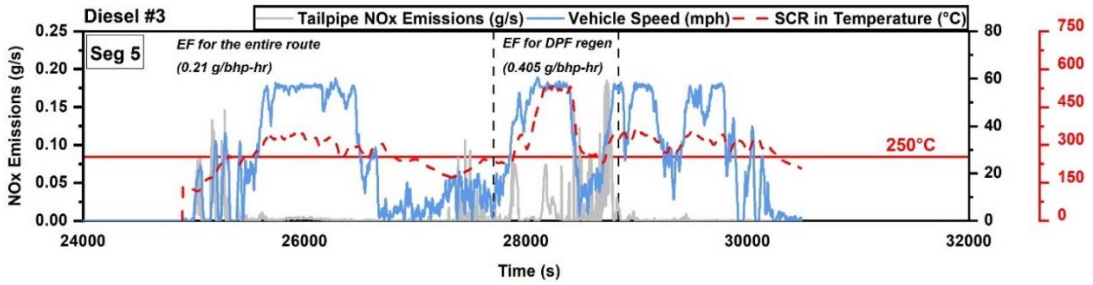

Figure 6.8 DPF regeneration event for Diesel #3

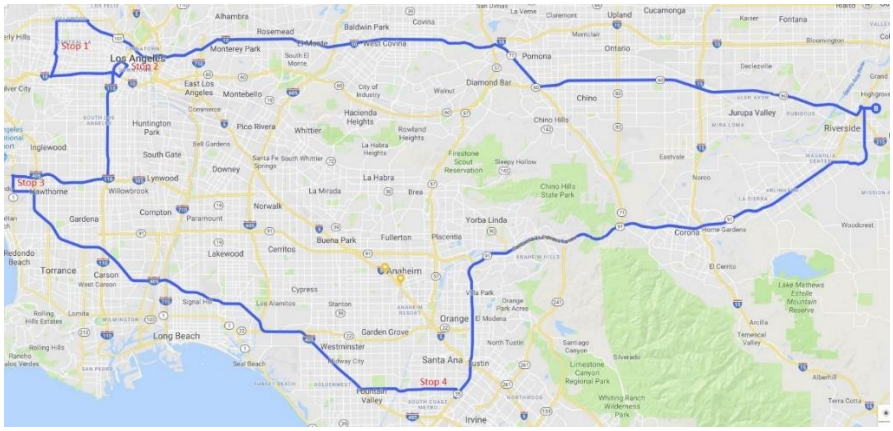

(a): Topographic map of the grocery distribution route, mix of urban, rural and highway driving including 3 or 4 stops at grocery centers with total soak time of 2.5 hours per day to simulate unloading of goods.

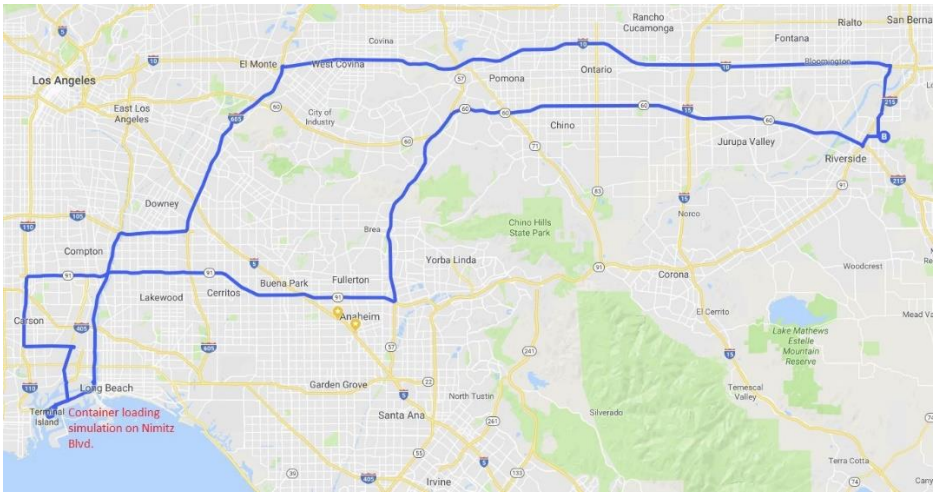

(b): Topographic map of the port-drayage route, mix port operation, and urban and highway driving including simulation of idle/creep, operation during container loading.

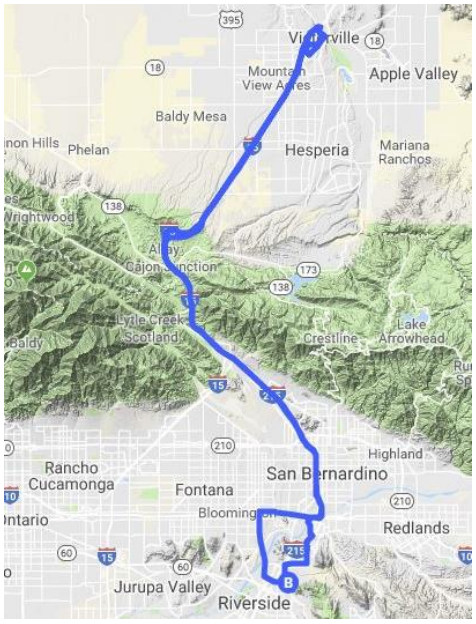

(c): Topographic map of the goods movement route with elevation change (i.e., UPS Route), extended highway driving including larger elevation changes.

(d): Topographic map of the highway goods movement route, extended highway operation with short urban links.

Figure 6.9 SM-2(a-d) Topographic maps of the test routes: (a) Grocery Distribution route (route #1), (b) Port-Drayage route (route #2), (c) Goods Movement with Elevation Change route (route #3), and (d) Highway Goods Movement route (route #4)

Table 6.3 SM-3 On-road NOx emissions for UDDS cycle

		g/hour	g/gal	g/route
Diesel (NO SCR) #1	Grocery Distribution route	91.26	23.10	615.41
	Port-Drayage route	65.37	16.48	428.57
	Goods Movement with Elevation Change route	98.29	14.83	306.32
	Highway Goods Movement route	75.51	12.56	349.46
0.2Diesel #2	Grocery Distribution route	38.59	8.34	244.75
	Port-Drayage route	39.26	11.06	245.38
	Goods Movement with Elevation Change route	74.77	13.05	235.85
	Highway Goods Movement route	72.72	11.54	304.63
0.2Diesel #3	Grocery Distribution route	20.14	4.09	112.82
	Port-Drayage route	18.83	7.99	115.63
	Goods Movement with Elevation Change route	-	12.07	-
	Highway Goods Movement route	37.68	11.65	163.72
0.02CNG #1	Grocery Distribution route	0.90	1.00	5.29
	Port-Drayage route	0.86	1.19	6.00
	Goods Movement with Elevation Change route	2.49	1.60	8.25
	Highway Goods Movement route	2.27	1.82	10.26
0.02CNG #2	Grocery Distribution route	1.24	1.53	7.48
	Port-Drayage route	2.02	1.80	7.67
	Goods Movement with Elevation Change route	2.42	1.56	7.73
	Highway Goods Movement route	-	-	-

7. Conclusions

For Chapter 2 Emission Measurements were made for 10 pieces of Tier 4 final equipment with SCR and DPF aftertreatment systems which included 3 excavators, 3 wheel loaders, 2 backhoe/loaders, and 2 crawler tractors with PEMS. This information will be useful for developing emissions inventory models, understanding the differences between certification levels and real-world emissions, and in understanding the effectiveness of advanced aftertreatment systems for off-road applications. The main conclusion in this study can be summarized as follows:

For all types of equipment, the highest NOx emissions were seen for the cold start phase due to exhaust temperatures being below the activation temperatures for the SCR system. This was followed by the travel mode operation. NOx emissions under idle ranged from 12.8 to 50 g/hour, which in many cases was higher than the NOx emissions for work modes on a time basis.

NOx emissions from all equipment categories for trench and backfill operations showed a range from 0.07 to 0.69 g/bhp-hr, and from 11.4 to 34.2 g/hour. NOx emissions for the trench and backfill modes were generally close or below the in-use compliance emission rate, except for a few pieces of equipment that had higher NOx emissions due to cooler aftertreatment systems. NOx emissions for the work modes are comparable to the OFFROAD model prediction for most of the equipment. Compared to the previous studies, the Tier 4 final equipment showed an average reduction of 91% for NOx emissions. This indicates a significant benefit could be achieved for NOx emissions by deploying Tier 4 final advanced technology, such as SCR, from an emission reduction perspective.

PM and CO emissions for all the different types of equipment were below the certification standard. PM emissions for Backhoe/Loader is higher than other equipment categories because both pieces of equipment in Backhoe/Loader category lacked a DPF to reduce PM emissions. PM emissions were generally lower than those for the OFFROAD model, suggesting PM emissions might be overestimated in categories where DPFs are more prevalent than predicted.

For Chapter 3, the work investigated the emissions impacts from two near-zero NOx emissions natural gas heavy-duty vehicles in different vocations. Both vehicles were exercised over different driving cycles on a chassis dynamometer. The results reported here showed very low NOx emissions levels for both vehicles and dramatic reductions of up to 90% compared to the 2010 certification standard. This study highlighted the potential importance of using ultra-low NOx stoichiometric natural gas platforms in captive fleets, seaport equipment, and goods movement vehicles to alleviate ground-level ozone formation in urban areas of the South Coast Air basin. The impact of the cold-start period on NOx emissions was found to be relatively small considering the real-world fraction of time natural gas heavy-duty vehicles of any vocation operate in cold mode compared to hot mode. Both vehicles showed elevated solid particle number emissions that were above the European particle number limit, indicating that significant work should be undertaken to reduce solid particle number emissions from natural gas vehicles to levels comparable to those of diesel vehicles equipped with DPFs. In addition, a significant fraction of smaller sub 23 nm particles exists in natural gas engine exhaust, which could be a major concern from regulatory and health effects perspectives. For the 12L goods movement vehicle, the profile of the particle size distribution was highly dependent on the test cycle. For some

test cycles, high particle concentrations in the nucleation mode regime were observed during acceleration events, whereas for other test cycles particles in the accumulation mode were seen during deceleration. Both driving patterns favor the infusion of lubrication oil via the piston ring into the combustion chamber, which will result in particle formation. For the 6.7L yard tractor, nucleation mode particles in the 5-10 nm diameter dominated the particle size distribution, with the higher load cycle producing greater populations of both nucleation and accumulation mode particles than the lower load cycles. CO emissions were found in relatively high levels, but lower than older technology stoichiometric natural gas engines, indicating significant improvements in engine calibration and catalyst formulation. Emissions of N_2O and NH_3 were highly dependent of the cold-start cycles showing higher concentrations for both vehicles compared to the hot-start tests. CH_4, the principal component of natural gas, showed elevated emission levels associated with the incomplete combustion of CH_4, especially during transient operation and at higher engine speeds.

For Chapter 4 and 5, NOx, N_2O, NH_3, particulate matter (PM), greenhouse gases (GHG), total hydrocarbon (THC), carbon monoxide (CO), and carbonly emissions were measured from a fleet of 14 different heavy-duty vehicles over different drive cycles using a chassis dynamometer. Chapter 4 showed that the UDDS NOx emissions varied depending on the vocation and the technology with average NOx emissions across all vehicles ranged from 0.003 to 6.16 g/bhp-hr. NOx emissions for vocational cycle and HHDDT cruise cycles showed some variances compared with the UDDS cycle but in the same range. For the 0.2 g diesel vehicles, the in-use PEMS NOx emissions were higher than those over the vocational and UDDS cycles, except for goods movement vehicles 0.2Diesel #3 and #5,

suggesting, for most of cases, that there were elements of the in-use operations that are still not necessarily captured in the vocational cycles. HVO provided significant reductions in NOx emissions for diesel (no SCR) vehicles. The 0.2 g diesel vehicles with model years newer than 2010 showed more similar emissions between diesel fuel and HVO, that were generally comparable within the experimental variability for the hot start UDDS. NH_3 and N_2O emissions are also pollutants of concern for air quality and global warming, which originates from the catalyst reaction. N_2O emissions from SCR equipped diesel vehicles originate from the catalyst reaction involving NH_3 and NOx emissions as well as the decomposition of nitrite particles. The formation of N_2O for CNG vehicles is favored at catalyst temperatures below 350°C.

Chapter 5 showed PM emissions were below the 10 mg/bhp-hr certification for all vehicles over both cold and hot start cycles, with the exception for the goods movement vehicle Diesel (No SCR) #2 and one CNG vehicle with a non-functional catalyst. Total particle number emissions for most of the CNG vehicles were above the European particle number limit, although the Euro limit is only for solid particles. This indicates that more efforts need to be made to reduce particle number emissions from natural gas vehicles to the emission certification levels. Most DPF-equipped diesel vehicles showed particle number emissions below the standard. Particle number emissions were elevated during the deacceleration event, where the fuel to the engine was cut off. Furthermore, the majority of the particles reside in the nucleation mode region with an average geometric mean diameter (GMD) in the order of 10 nm. The current findings suggest that CNG particle emissions are mostly related to the lubricant oil escape from the oil ventilation system, from piston rings or valves. Phosphorus (P), sulfur (S), calcium (Ca), zinc (Zn), and iron

(Fe) were the dominant metallic and non-metallic species in PM. The presence of Fe suggests that some of the PM may originate from engine wear. CO and THC emissions were found in relatively high levels, with more advanced 0.02CNG vehicles significantly lower than the 0.2CNG vehicles, indicating significant improvements in engine calibration and catalyst formulation. CO_2 emissions are the main contributor to GHG emissions for all vehicles. Natural gas engines are generally characterized by their relatively high CH_4 emissions. CH_4 contributes the second largest to GHG emissions for CNG vehicles over mostly the UDDS cycle.

Chapter 6 measured and characterized NOx emissions from five heavy-duty diesel and natural gas goods movement vehicles with different engine technologies. All five vehicles were tested on-road under four pre-defined goods movement routes in SCAB, representing grocery distribution, port-drayage operation, and highway driving with and without elevation change. NOx emissions were measured using a mobile emissions laboratory. NOx emissions varied depending on the vehicle and the route. The diesel (no SCR) vehicle showed the highest NOx emissions over all routes, ranging from 0.6 to 1.1 g/bhp-hr. For the SCR-equipped diesel vehicles, the NOx emission rates ranged from 0.21 to 0.62 g/bhp-hr, with the NOx emissions rates for 0.2Diesel #2 being about two times higher than those from 0.2Diesel #3. This could be due to deterioration of the engines or SCR catalyst, since it showed higher NOx emissions even during section of the route where the SCR inlet temperature was at its optimal operating range. CNG vehicles showed average NOx emissions at or below the optional NOx emission standard of 0.02 g/bhp-hr. The three-bin MAW method was utilized to show the NOx emissions across various modes of operation conditions, including idle, low load, and medium/high load. The highest

fraction of operation was found in either the low load or med/high load bins, depending on the route, with the highway routes showing a greater fraction operation in the med/high load bin, and the Grocery Distribution and Port-Drayage routes showing a greater fraction operation in the low load bin. For the idle windows, the highest fraction of valid idle windows was found for the Port-Drayage route (Route #2) and Goods Movement with Elevation Change route (Route #3), at 23% and 25%, respectively.